2006

Diffuse Brain Injury Triggers Ultra-Rapid Perisomatic Traumatic Axonal Injury, Wallerian Change, and Non-Specific Inflammatory Responses

Brian Joseph Kelley
Virginia Commonwealth University

DIFFUSE BRAIN INJURY TRIGGERS ULTRA-RAPID PERISOMATIC TRAUMATIC AXONAL INJURY, WALLERIAN CHANGE, AND NON-SPECIFIC INFLAMMATORY RESPONSES

A dissertation submitted in partial fulfillment of the requirements for the degree of Doctor of Philosophy at Virginia Commonwealth University.

by

BRIAN JOSEPH KELLEY
B.S. / B.A., University of Virginia, 1999

Director: John T. Povlishock, Ph.D.
Professor and Chairman
Department of Anatomy and Neurobiology

Virginia Commonwealth University
Richmond, Virginia
August, 2006

Acknowledgement

This dissertation represents the cumulative effort of many individuals working together. I would first like to recognize my advisor and mentor, Dr. John T. Povlishock, for his continuous guidance and remarkable ability to direct a young scientist-in-training towards a career he never thought was possible. His passion for scientific discovery and ability to educate scientists are skills I hope to emulate. I would also like to thank Drs. Ross Bullock, Anthony Marmarou, Linda Phillips, and John Bigbee for taking their time to serve on my thesis committee and for their feedback and advice on how to improve my studies. I would also like to thank the technicians in our laboratory to whom I owe an invaluable debt of gratitude: Sue Walker for her help with immunocytochemistry as well as processing and preparation of electron microscopic samples, Lynn Davis for her help with immunocytochemistry tissue processing and mounting, Tom Coburn for his help with tissue cutting, and Judy Williamson for her assistance with the electron microscope. This work was conducted in collaboration with other members of the laboratory including Drs. Jonathan Lifshitz and Orsolya Farkas whose contributions include helping me to think like a scientist and to provide more appropriate descriptive adjectives respectively. Finally, I would be remiss if I did not thank Dr. Richard Singleton who showed me the ropes when I first started working in the laboratory and contributed greatly to my desire to pursue a career in the neurosciences.

While the above individuals were instrumental in my scientific development, there are others who have contributed equally towards my personal growth during this educational experience. I am very lucky to have a very supportive family. My parents, Michael Kelley and Joan Hunter, have supported me throughout my academic life and instilled in me the desire to continuously discover what life has to offer. Upon acceptance to medical school and the combined degree program, I mentioned to my grandfather that I had moved "... from the outhouse to the penthouse." His infectious laugh and volunteering to be my first patient spoke volumes as to his support of my career choice. Additionally, my brother John has always provided valuable insight into my "dorkiness" and helped to keep my perspective balanced.

Finally, I should mention that the summer before medical school started, I took a seemingly innocuous trip to New York City to visit a friend for a change of scenery. My friend mentioned that she was throwing a birthday party for her roommate and that I could tag along if I wanted. At this party, I met her roommate... And five years later we were married. While I certainly need to thank my telephone, my car, and Amtrak, my most important acknowledgment goes to my wife Lauren Kelley. Thank you for being my best friend... I am so lucky to have you in my life and I am looking forward to our next journey together. P.S. - To everyone in the lab: The t-shirts are coming...

Table of Contents

Table of Contents

List of Figures

Figure **Page**

List of Abbreviations

α	Alpha
ABC	Avidin-biotin complex
ANOVA	Analysis of variance
APP	β-Amyloid precursor protein
atm	Atmospheres
ATP	Adenosine triphosphate
β	Beta
BBB	Blood-brain barrier
BSA	Bovine serum albumin
°C	Degrees Celsius
$CaCl_2$	Calcium chloride
CMSP	Calpain-mediated spectrin proteolysis
CNS	Central nervous system
CR3	Complement receptor three
(a)CSF	Cerebrospinal fluid (artificial)
CT	Computed tomography
cyt c	cytochrome c (cellular injury)
d	days
DAB	Diaminobenzidine
DAI	Diffuse axonal injury
DBI	Diffuse brain injury
DL	Dorsolateral
eIF2-α(P)	Serine-51 phosphorylated alpha subunit of eukaryotic translation initiator factor 2 (impaired protein translation)
EM	Electron microscopy (-e, -ic)
F-actin	Fibrous actin
(c)FPI	Fluid percussion injury (midline/central)
G-actin	Globular actin
GAP-43	43 kDa growth-associated protein
GCS	Glasgow Coma Score
GFAP	Glial fibrillary acidic protein
gm	gram
H_2O_2	Hydrogen peroxide
HRP	Horseradish peroxidase
HSD	Highly significant difference (Tukey's)

HSP-60	60 kDa heat shock protein
HSP-70	70 kDa heat shock protein
ICAM-1	Intracellular adhesion molecule - one
IL	Interleukin
KCl	Potassium chloride
kDa	Kilodalton
kg	Kilogram
LM	Light microscopy (-e, -ic)
MAP	Microtubule-associated protein
MCP-1	Monocyte chemotactive protein - one
MF	Microfilament
MIP-1	Macrophage inflammatory protein - one
$MgCl_2$	Magnesium chloride
MHC	Major histocompatibility complex
mM	Millimolar
mm	Millimeter
µm	Micrometer
mg	Milligram
µg	Microgram
mg/ml	Milligrams per milliliter
min	Minute
ml	Milliliter
µl	Microliter
mrf-1	Microglia response factor - one
MRI	Magnetic resonance image (-ing)
MT	Microtubule
MW	Molecular weight
NaCl	Sodium chloride
$NaHCO_3$	Sodium hydroxide
NaH_2PO_4	Sodium phosphate dibasic anhydrous
nm	Nanometer
N_2O	Nitrous oxide
NGS	Normal goat serum
NF	Neurofilament
NF-H	180-200 kDa, heavy neurofilament
NF-L	60-70 kDa, light neurofilament
NF-M	130-170 kDa, medium neurofilament
NHS	Normal horse serum
Nitro-Tyr	Nitrated tyrosine (cellular injury)
O_2	Oxygen

PARP	Poly(ADP-ribose) polymerase (DNA repair)
P-BAD	Serine-136 phosphorylated pro-apoptotic protein (cellular survival)
PAF	Platelet activating factor
PBS	Phosphate buffered saline
PNS	Peripheral nervous system
PSD-93	93 kDa post-synaptic density protein
PSD-95	95 kDa post-synaptic density protein
SD	Standard deviation
SEM	Smooth endoplasmic reticulum
TAI	Traumatic axonal injury
TBI	Traumatic brain injury
TGF-β	Transforming growth factor - beta
TNF-α	Tumor necrosis factor - alpha
TUNEL	Terminal deoxynucleotide transferase mediated d-UTP nick end labeling
VPL	Ventral posteriolateral
VPM	Ventral posteriomedial

Abstract

DIFFUSE BRAIN INJURY TRIGGERS ULTRA-RAPID PERISOMATIC TRAUMATIC AXONAL INJURY, WALLERIAN CHANGE, AND NON-SPECIFIC INFLAMMATORY RESPONSES

By Brian Joseph Kelley, Ph.D.

A dissertation submitted in partial fulfillment of the requirements for the degree of Doctor of Philosophy at Virginia Commonwealth University.

Virginia Commonwealth University, 2006

Major Director: John T. Povlishock, Ph.D.
Professor and Chairman
Department of Anatomy and Neurobiology

A significant component of diffuse brain injury (DBI) is diffuse axonal injury (DAI) which is responsible for the morbidity and mortality associated with this condition. DAI and its experimental counterpart traumatic axonal injury (TAI) result in scattered microscopic pathology characterized by focal impairment of axonal transport leading to progressive swelling and delayed axotomy. DBI-mediated perisomatic axotomy does not result in acute neuronal death suggesting that delayed axotomy was responsible for this unanticipated response. To evaluate this hypothesis, we examined the spatiotemporal progression of DBI-mediated perisomatic TAI. LM / TEM identified impaired axonal transport within 15 – 30 min post-injury. Perisomatic TAI revealed

somata and related proximal / distal axonal segments with normal ultrastructural detail continuous with axonal swellings. In other cases, axotomy was confirmed by loss of axonal continuity distal to the swelling. By 60 – 180 min post-injury, somatic, proximal segment, and swelling ultrastructure were comparable to earlier time points although swelling diameter increased. Distal segment ultrastructure revealed the initial stages of Wallerian degeneration. Axotomy sites did not internalize pre-injury administered dextran suggesting pathogenesis independent of altered axolemmal permeability. Given the rapidity of perisomatic axotomy, absence of axolemmal permeability may constitute the more significant finding in terms of somatic protection.

DBI-mediated neuroinflammatory reactions were then examined to see if this non-lethal neuronal pathology evoked responses comparable to those following focal injury. Microglia / macrophage responses within diffusely injured loci uncomplicated by focal pathology were explored using LM, TEM, and confocal evaluations as was albumin immunoreactivity to assess injury-induced blood-brain barrier (BBB) alterations. Initially, microglial activation was observed within injured loci while microglia within adjoining regions maintained resting phenotypes. Scattered activated microglia were observed among injured axons though no clear associations were seen. Later, activated microglia contained myelin debris while only limited microglial aggregations were recognized. Macrophages also localized to injured loci with select cells approximating somata of axotomized neurons. Immune cell observations correlated with altered BBB permeability. These data indicated rapid, yet initially uncoordinated, and persistent immune cell reactivity to DBI pathology. Taken together,

these responses suggest that histopathological evaluation following DBI may include non-lethal neuronal injury with unique neuroinflammatory findings.

Chapter 1

GENERAL INTRODUCTION

TRAUMATIC BRAIN INJURY: SOCIETAL AND ECONOMIC IMPACT

Traumatic brain injury (TBI) is a significant societal problem affecting approximately 1.4 million individuals each year. While many TBI-related events go undiagnosed and untreated due to lack of debilitating clinical symptoms associated with mild head trauma, more moderate to severe injuries account for a significant number of hospitalizations. Approximately 1.1 million people are treated and released from emergency departments annually for TBI-related symptoms while 235,000 patients are hospitalized of which 80,000 – 90,000 cases result in long-term disability and 50,000 cases result in death (Thurman et al., 1999; Langlois et al., 2004). Although these statistics are lower than those from previous years, the incidence of TBI is still approximately eight times greater than breast cancer and 34 times higher than HIV/AIDS causing one report to designate TBI the "invisible epidemic" (Traumatic Brain Injury 1999; Traumatic Brain Injury 2002). While all age groups are vulnerable to brain trauma, TBI affects primarily persons aged 0 – 14, 15 – 24 and over 75 (Thurman et al., 1999). Falls are the leading cause of TBI-related death and disability in children ages 0 – 14 and elderly people over age 75 while motor vehicle accidents are more

likely to affect adolescents and young adults ages 15 – 24. It should also be noted that the very young (ages 0 – 4) have an increased incidence of TBI when compared to the general population which is presumably a consequence of child abuse (1999). In addition to age stratification, TBI also demonstrates a gender bias with studies indicating that across all age categories, men are approximately twice as likely to suffer from brain injury than women (NIH Consensus Development Panel on Rehabilitation of Persons With Traumatic Brain Injury, 1999; Langlois et al., 2004).

While data collection and analysis of TBI-related age and gender demographics is relatively straight forward, it is more difficult to estimate the financial impact of TBI on society due to the numerous costs associated with evaluation and treatment of the injured individual as well as economic burdens placed on caregivers. Direct costs of acute care and rehabilitation for individuals suffering TBI are an estimated 9 – 10 billion dollars annually with a total economic impact of 56.3 billion dollars when supplementary factors such as long-term care, lost wages, and disability are included (NIH Consensus Development Panel on Rehabilitation of Persons With Traumatic Brain Injury, 1999; Thurman, 2001; Traumatic Brain Injury 2002).

A significant component of this estimated total expense is long-term care of the TBI patient. It is estimated that at least 5.3 million people (approximately 2% of the US population) are currently living with disabilities or require assistance to perform activities of daily living as a result of TBI (Thurman et al., 1999). Excluding mortality, TBI-related clinical outcomes range from return to normal function typically seen following mild injury to maintenance in a persistent vegetative state following severe

injury. Individuals sustaining mild TBI generally experience good outcomes with limited long-term complications although approximately 15 percent will have lingering problems including headaches, dizziness, attention deficits, and emotional liability (Alexander, 1995; Guerrero et al., 2000). Similarly, those individuals sustaining moderate injury may also have positive outcomes although the possibility of permanent disability or death increases (Levin, 1989). As one might expect, severely brain injured patients have the worst prognosis and often require full-time medical care when eventually released from the hospital. In addition to injury severity, age of the individual sustaining TBI is another important factor with respect to long-term outcome with older individuals (> 60 years) faring worse than their younger counterparts when subjected to injuries of comparable severity, presumably due to decreased brain plasticity (Katz and Alexander, 1994).

With major economic burdens coming from both acute and long-term care expenses, education and prevention remain at the clinical forefront in reducing the incidence of TBI. Ongoing efforts to increase head injury protection awareness, to prevent falls, and to improve vehicle safety have made strides in reducing the number of severely head-injured people. Similarly, improved clinical management of hospitalized TBI patients has also improved long-term outcomes. Efforts to reduce TBI morbidity and mortality are also ongoing in the basic science realm through research into the underlying cellular and molecular pathobiology associated with this condition. Study of the intricate post-injury responses and interactions between various brain cell types and molecules remain active areas of investigation. As a more complete understanding of

the pathophysiological processes involved in TBI emerges, the importance of bench-to-bedside translational research will be highlighted, especially in areas such as therapeutic interventions targeting specific pathological events.

While basic science research has advanced our understanding of TBI pathobiology, there remain many unanswered questions regarding the various mechanisms responsible for this "invisible epidemic." In that society's goal is to one day be able to intervene and prevent the devastating consequences of this debilitating condition, this dissertation was developed to provide additional insight into two major components of TBI pathogenesis. First, the spatiotemporal progression of a key component of diffuse TBI namely diffuse axonal injury (DAI), as known as traumatic axonal injury (TAI) in experimental settings, was evaluated in the perisomatic domain using a fluid percussion injury model of diffuse brain injury (DBI). Second, the neuroinflammatory responses accompanying DBI and its associated pathology were explored. To outline this dissertation, a general introduction to TBI and its components is first provided to give background on this pathology. This is followed by individual chapters devoted to perisomatic TAI pathogenesis (Chapter 2) and microglial / macrophages responses to DBI (Chapter 3). A general discussion (Chapter 4) is then offered to provide additional insight into these observations and to suggest future studies aimed at developing a more comprehensive understanding of these events. Ultimately, as our understanding of the underlying pathophysiology of TBI continues to improve, we must translate our basic science findings to the clinical arena with the hope

of offering concomitant improvements in medical care and long-term outcomes for TBI patients.

TRAUMATIC BRAIN INJURY: GENERAL OVERVIEW

The term "TBI" is used to describe a wide variety of clinical conditions ranging from concussion following closed head injury to missile injury from a gunshot wound. Although both are considered to be "TBI," their respective mechanisms of injury and consequent pathologies differ significantly. Recent basic science characterization has divided TBI into four phases of pathogenesis: the primary injury, the delayed consequences of the primary injury, secondary or additional injury, and recovery and functional outcome (Graham et al., 2002) with each of these stages affected by numerous factors. For example, the primary injury is dictated by the type, location, and size of injury produced by the causative agent while secondary injury is influenced by co-morbidities associated with brain trauma such as elevated intracranial pressure and ionic dysregulation. While the above characterization offers a synopsis of general TBI-related pathologies, a more descriptive classification outlined below utilizes injury location.

To begin to describe the pathogenesis of brain trauma, TBI may be first stratified into two major categories: focal and diffuse injury. This distinction is not arbitrary given that the need for surgical evaluation in focal injury is much greater than in diffuse injury (Graham et al., 2002). Focal brain injury, which most often occurs as a result of direct impact of the brain against the cranial vault, is characterized primarily by contusions, hemorrhages / hematomas, and/or mass lesions. These outcomes are in

contrast to the effects of diffuse injury that typically occur via rapid acceleration – deceleration of the cranium with or without impact resulting in shear forces distributed throughout the brain parenchyma (Graham, 1996). While focal injury is often visible either grossly or with clinical imaging techniques, diffuse pathology is more subtle given the injury dynamics and distribution. Diffuse brain pathology is microscopic in nature and involves cellular changes scattered throughout various anatomical loci. It is often difficult to detect using conventional imaging and therefore the diagnosis of DBI is often based on neurological deficits found during clinical examination or via post-mortem histological examination of specimens stained with antibody markers of neuronal injury. Although focal and diffuse injury may appear to be unique entities, they are often found within a single brain (Finnie et al., 2002). This observation highlights the complexity of TBI and illustrates the difficulty of studying either focal or diffuse pathology in isolation.

Focal versus Diffuse Injury

As noted, TBI may be classified as either focal or diffuse depending on the type and size of injury as well as brain localization. Focal damage includes pathologies such as contusion and/or laceration to the brain surface, intracranial hematoma, hemorrhage and infarction in the brainstem, and abscess formation (Graham et al., 2002). Distinguishing characteristics of focal brain injury include similar fates for related cell types within an injury nidus and diminishing pathological severity as the distance away from the nidus increases. For example, following a severe focal brain contusion, the

ensuing pathology consists of rapidly necrotic cell death creating a necrotic central core which is surrounded by a penumbral region of heterogeneously injured cells which may die via delayed apoptosis (Clark et al., 1999), thus expanding the core region. Within or immediately adjacent to the penumbra, cells may be only transiently affected and survive to recover normal function (Adams, 1992). Ultimately, this transiently affected area is encircled by uninjured tissue giving the overall injury location a concentric circular appearance in terms of cellular injury severity, with more severe injury at the center and little to no injury at the margins.

The focal injury force is concentrated on a local area and typically results in immediate physical damage to cells. If sufficient magnitude is applied, cells will experience direct mechanical injury to their membranes leading to loss of ionic homeostasis. Ionic dysregulation leads to loss of energy substrate production and various intracellular pathologies ultimately culminating in necrotic cell death. Those cells immediately adjacent to the central impact location experience varying degrees of force resulting in variety of pathological outcomes. Thus force magnitude is responsible for the size over which the focal injury extends into the brain parenchyma. From the standpoint of diagnosis and treatment, the location of focal injury may be determined based on neurological deficits observed during clinical examination and/or imaging techniques, depending on the patient's level of consciousness.

Conversely, diffuse injury exists in primarily four forms: diffuse axonal injury, diffuse hypoxic brain damage, diffuse brain swelling, and diffuse vascular injury. Diffuse injury results from dynamic loading via impact or impulsive forces with strain

being the proximate cause of brain tissue injury. The types of strain responsible for pathology include primarily tension and shear (Graham et al., 2002). When these strain forces exceed certain viscoelastic property thresholds for neurons and/or other cell types within the brain, damage to cell membranes and fibers occurs resulting in altered permeability and possible mechanical tearing. Although strain forces during injury may result in immediate tearing of cell membranes, forces causing transient membrane perturbation without mechanical rupture may also initiate of a number of pathological cascades resulting in delayed pathology.

During trauma, strain forces are distributed throughout the brain with varying degrees of severity exposing cells to unequal levels of perturbation (Margulies and Thibault, 1989; Margulies et al., 1990). For example, experimental studies have determined that the gray-white matter interface is selectively vulnerable to shear forces, presumably due to the differing densities of the two areas, resulting in axonal damage following rapid acceleration and deceleration (Meaney et al., 1995; Smith et al., 1997). While certain axons may be exposed to forces sufficient to cause injury, other neighboring fibers may not be damaged despite experiencing similar albeit unequal forces. This phenomenon results in heterogeneous injury of a diffuse nature. Therefore, unlike focal TBI, the extent of diffuse injury is more difficult to diagnose and treat due to more variable areas of the brain being affected as well as the microscopic nature of injury which makes diagnostic imaging difficult.

Ultimately, focal and diffuse injury may be thought of as ends of a continuum between which TBI-related conditions fall. Although focal and diffuse brain injury can

occur in isolation, in many cases aspects of both injuries can be found within an individual brain. One might envision a scenario (e.g. motor vehicle accident) during which the brain may experience supra-threshold tension and shear strains due to rapid deceleration causing altered membrane permeability and mechanical tearing followed by impact with the cranial vault causing a contusion. Therefore, in order to discern the various pathological mechanisms following focal and diffuse TBI, one must attempt to study either focal or diffuse injury in isolation with the understanding that these complex pathologies often overlap within an individual traumatically injured brain.

DIFFUSE / TRAUMATIC AXONAL INJURY: GENERAL INTRODUCTION

Although there are four primary forms of diffuse TBI, diffuse axonal injury (DAI) has received the most attention due to its association with poor prognoses following injury (Graham, 1996). As noted, the ability to diagnose DBI is hampered by the microscopic nature of injury. Conventional imaging techniques may offer signatures of DAI but lack the resolution to examine individual axons and determine their health following trauma. Often times, a final clinical diagnosis of DAI is reached by default after ruling out other possible pathologies. For example, a physical examination (e.g. an unresponsive comatose patient) that is incongruent with diagnostic radiographic findings (e.g. various imaging scans fail to show significant brain pathology) is often diagnostic for severe DAI. The histological pathology of DAI is characterized by widespread axonal damage in the brainstem, parasagittal white matter of the cerebral cortex, and corpus callosum and is a consistent feature of TBI (Adams et al., 1989;

Meythaler et al., 2001). To provide a more thorough understanding of DAI, the following sections first discuss the historical and current clinical perspectives. This is followed by a descriptive characterization of traumatic axonal injury (TAI), the experimental counterpart of DAI, and the molecular processes responsible for its pathogenesis.

Diffuse Axonal Injury: Historical Perspective

The first microscopic identification of DAI was made in 1956 when Sabina Strich examined five severely disabled individuals surviving for between five and 15 months following TBI (Strich, 1956). During post-mortem examination of brain specimens, Strich observed "diffuse degeneration" of cerebral hemisphere white matter. Otherwise, minor pathological changes were noted that were inconsistent with the overall severity of injury demonstrated during clinical examination prior to autopsy. Although the mechanical force of injury was suggested as a contributing factor, it was not until a follow-up study five years later that Strich identified 15 additional patients with similar pathologic findings and concluded that there was immediate shearing of nerve fibers at the time of injury and that this pathology was marked by the presence of "retraction balls" at the ends of these interrupted fibers (Strich, 1961). Strich discussed the implications of head movement in a variety of rotational and angular planes and concluded that "... nerve fibers running in a particular direction would be selectively damaged in one hemisphere and spared in the other, the quantity of damage being the same on the two sides" (Strich, 1961). Although her initial assessment of axonal injury

pathogenesis was partially flawed, Strich's pioneering work laid the foundation for more comprehensive analyses of axonal damage following TBI.

Comprehensive examinations into the mechanisms of axonal injury and disconnection began in the late 1970's and early 1980's with the development of TBI animal models capable of reproducing axonal injury (Sullivan et al., 1976; Gennarelli et al., 1982). Although not initially intended to examine axonal pathology, Sullivan and colleagues developed a feline model in which a swinging weight would strike a piston connected to a saline filled reservoir which, in turn, was connected to the epidural space of the animal (Sullivan et al., 1976). This fluid percussion injury device produced an elastic deformation in the brain similar to that seen in human head injury. However, it was not until several years later that Povlishock and colleagues first reported the diffuse axonal pathology generated by this model (Povlishock et al., 1983). One year prior to the observations made by Povlishock, Gennarelli and colleagues developed the first model capable of eliciting symptoms and axonal pathology consistent with that observed in severe human head injury (Gennarelli et al., 1982). Using a primate model, animals were subjected to sagittal, oblique, and lateral head motion with select animals experiencing post-injury coma in the absence of overt pathological change. Similarly, there was microscopic evidence of diffuse axonal swelling and disconnection, observations similar to those made by Strich. Gennarelli, as well as Adams whose article appeared in the same journal, termed this phenomenon "diffuse axonal injury" or DAI (Adams et al., 1982; Gennarelli et al., 1982).

As mentioned, the first study characterizing the axonal response to TBI-induced DAI was performed by Povlishock and colleagues (Povlishock et al., 1983). In this work, horseradish peroxidase (HRP) was injected into the motor cortex prior to fluid percussion injury. Capitalizing on the fact that HPR would be taken up by neurons and subsequently undergo anterograde transport down the axonal cylinder, this study was designed to show the spillage of HRP into the surrounding brain parenchyma immediately following TBI-induced axotomy based on Strich's hypothesis that axonal retraction balls were formed by extrusion of axonal contents at the injury site (Strich, 1961). However, this observation was not seen. Rather, focal HRP accumulations were observed within continuous axons at early post-injury time points. At later times, these HRP-laden swellings enlarged and eventually lost continuity and disconnected from their downstream segments while restricting HRP to the intra-axonal compartment (Povlishock et al., 1983). These novel observations led to the following conclusions: First, not all fibers undergo immediate axotomy post-injury and second, that during this process of delayed axotomy, axonal injury appears to take place without permanent loss of membrane integrity.

These initial observations provided the framework for future experiments designed to examine DAI pathobiology. Research into the spatiotemporal progression and mechanisms of DAI has provided unique insights into the development of TBI-induced axonal injury. As will be discussed in subsequent sections, our clinical and basic science comprehension of DAI over the last 30 years has grown tremendously in its breadth and sophistication.

Diffuse Axonal Injury: Clinical Perspective

The predominant pathological mechanism in most cases of TBI is DAI (Bennett et al., 1995). However, given the diffuse and microscopic nature of injury, many TBI patients with underlying DAI will have minimal changes noted on computed tomography (CT) and magnetic resonance imaging (MRI) scans during clinical evaluation (Bazarian et al., 2006). One prognostic indicator of DAI that may be seen on imaging are punctate hemorrhages that are associated with blood that extravasates from small vessels and that occur in areas of the brain contiguous with DAI (Meythaler et al., 2001). Shear forces responsible for axonal damage are also believed to create small tears in the vasculature causing small focal hemorrhages that enhance when imaged. These imaging findings along with clinical diagnoses of coma and/or low Glasgow Coma Score (e.g. GCS < 8) are strongly diagnostic for severe DAI. Mild to moderate DAI diagnoses rely primarily on neurological and/or cognitive deficits found during more routine clinical examination.

To provide clinical classification for DAI severity, Adams and colleagues developed a grading system based on post-mortem brain distribution of axonal pathology (Adams et al., 1977; Adams et al., 1989; Adams, 1992). In this classification, mild or grade 1 DAI is characterized by microscopic changes in the white matter of the cerebral cortex, corpus callosum, brainstem, and occasionally the cerebellum. Moderate (grade 2) DAI is defined by grossly evident focal lesions isolated to the corpus callosum. In severe (grade 3) DAI, there are additional focal lesions in the dorsolateral quadrants of the rostral brainstem, commonly the superior cerebellar peduncle.

Although the basis for this classification scheme is limited to post-mortem analyses, evidence of punctate hemorrhages found on imaging studies and located at the above mentioned anatomic loci may offer diagnostic insight into injury severity.

Improved scientific understanding of DAI pathogenesis has provided opportunities to develop treatment strategies aimed at prevention / attenuation of axonal pathology following TBI. From work in animal models, pathological characteristics such as delayed axonal swelling and disconnection have been elucidated. Given this delayed axotomy component, DAI offers a unique "therapeutic window" during which pharmacological and/or physiological manipulations may be employed to improve patient outcome. Although advancements in clinical intensive care management have improved patient outcomes, concomitant therapeutic treatment options have not been as forthcoming. Several pharmaceutical agents showing promise in animal studies have not achieved similar success when carried over to the clinical realm (Narayan et al., 2002). Similarly, attempts to slow TBI-induced pathological cascades by cooling patients to a hypothermic state followed by rewarming remains experimental and thus, controversial (Clifton et al., 2001; Markgraf et al., 2001). The inability of a single therapeutic intervention to fully attenuate DAI highlights the multiple pathological processes at work following trauma. These processes are the focus of the next section.

Traumatic Axonal Injury – Initiating Events

A point of clarification concerning nomenclature is necessary prior to a descriptive characterization of DAI pathobiology. The term "diffuse axonal injury" is

used to describe the human clinical condition associated with brain trauma. Given the importance of animal modeling to DAI hypothesis testing and the related difficulty in translating experimental results to the human condition, different terminology is used when discussing DAI within the context of basic science research. Rather, "traumatic axonal injury" (TAI) is reserved for pathology found in animal models of TBI and may refer to diffuse injury or injury within a single axon. Thus, "TAI" is used throughout this section to denote axonal injury within the context of experimental diffuse TBI.

Similar to the continuum of potential clinical conditions created by focal and diffuse injury, TAI also demonstrates a continuum of pathological change. TAI as a consequence of DBI may range from immediate tearing of the axonal membrane following trauma to fibers that experience shear and tensile strain forces but are not immediately severed. At one end of the continuum are strain forces sufficient to tear axons immediately following trauma resulting in what is known as "primary axotomy" or disruptive axonal injury (Maxwell et al., 1997). The remaining forces are of intermediate severity which do not cause immediate tearing but are responsible for initiating pathological mechanisms resulting in delayed / "secondary axotomy" or non-disruptive axonal injury during which axonal disconnection takes place at some point following the initial insult.

Historically, two hypotheses attempted to explain the biochemical and biophysical mechanisms occurring within axons that initiate secondary axotomy (Fitzpatrick et al., 1998). Although both implicated the axolemma as the initial site from which traumatically induced axonal pathology persists, they differed in their mechanism

of action. Adams and colleagues along with others proposed that focal perturbation of the axolemma was the crucial initiating event (Adams et al., 1982; Gennarelli et al., 1982; Adams et al., 1989; Maxwell et al., 1991). This perturbation was associated with increased permeability of the axolemma causing loss of ionic homeostasis across the axonal membrane and allowing for influx of extracellular calcium. Increased intra-axonal calcium, in turn, stimulated activation of proteolytic enzymes that caused collapse and dissolution of the axonal cytoskeleton, which disrupted axonal transport leading to organelle accumulation, axonal swelling, and progression towards secondary axotomy. On the other hand, Povlishock and colleagues proposed that the physical forces of injury directly perturbed the intra-axonal ultrastructure leading to altered cytoskeletal alignment and consequent impaired axonal transport (Povlishock, 1992; Grady et al., 1993; Christman et al., 1994).

More recent work by the Povlishock group has demonstrated that the initiating events in TAI pathogenesis are heterogeneous and complex processes thought to involve multiple and varied pathologies including the possibility of altered axolemmal permeability. To explore potential alterations in axolemmal permeability, the use of extracellular tracers, namely horseradish peroxidase (HRP; MW = 44 kDa) and high molecular weight dextrans (MW = 10 & 40 kDa) normally excluded from intact axons, was employed in separate animal models of DBI. The rationale for these studies was to show that if axonal perturbation led to altered permeability, then these extracellular tracers would enter the axon thus marking not only axonal injury but also sites of focal perturbation. Pettus and colleagues first explored this concept by flooding the extra-

axonal space within the brainstem with HRP and then demonstrated HRP movement into the intra-axonal space immediately following moderate but not mild TBI (Pettus et al., 1994). Subsequent work confirmed these observations and given the lack of specific neuronal HRP uptake, were interpreted to mean that physical injury caused a focal membrane opening (i.e. mechanoporation) allowing for HRP influx (Pettus and Povlishock, 1996). Similar work using high molecular weight dextrans intracerebroventricularly infused prior to injury to evaluate somatic permeability following DBI revealed multiple independent neuronal injury phenotypes including evidence suggesting both permeabilized and non-permeabilized axons (Singleton and Povlishock, 2004). Finally, in work presented in the next chapter, data showed that thalamic perisomatic axonal injury occurred independently of overt alterations in axonal permeability based on exclusion of pre-injury administered dextrans from injured axons. Collectively, these observations highlight the heterogeneity of initial axolemmal involvement in TAI pathogenesis.

In addition to the Povlishock group, other groups have also explored initiating mechanisms of axonal injury following DBI. Using a related *in vitro* stretch injury model which mimics the tensile loading incurred by axons during diffuse injury, Wolf and colleagues identified ion channels as a causative agent. Using ion sensitive dyes in combination with channel blockers, stretch injury did not cause mechanoporation allowing for passage of extracellular tracers into the intra-axonal space of cultured neurites. Instead, aberrant sodium channel opening was observed leading to depolarization and increased intra-axonal sodium concentrations. These elevated

sodium levels caused opening of voltage-gated calcium channels and reverse operation of the sodium-calcium exchanger, both of which led to increased intra-axonal calcium levels (Wolf et al., 2001). In addition to these observations, similar work by Smith and colleagues also illustrated axonal injury in the absence of dye uptake following stretch injury (Smith et al., 1999). More recent *in vivo* work by Stone and colleagues suggested that altered axolemmal permeability occurs only within a subset of uniquely injured axonal fibers following TBI (Stone et al., 2004).

Despite the heterogeneity surrounding the role of axolemmal perturbation as the causative agent for TAI, the unregulated entry of calcium into the axon following trauma is undoubtedly responsible for proteolytic cascade activation leading to cytoskeletal pathology. Calcium has been identified as a key mediator in a variety of neuronal pathological pathways (Young, 1996). Within the context of TAI, calcium has been identified at sites of focal injury (Maxwell et al., 1995) and has been shown to stimulate a number of proteolytic enzymes which target the axonal cytoskeleton leading to altered ultrastructural morphology (Buki et al., 1999; Buki et al., 2000). Focal cytoskeletal alterations in neurofilament, microtubule, and subaxolemmal spectrin ultrastructure lead to impairment of axonal transport at these sites. Despite axonal injury, continued anterograde transport from the soma results in organelle pooling at the site of impaired transport which causes focal axonal swelling. Axonal swelling may progresses over time ultimately leading to axotomy and disconnection although a recent study from the Povlishock group indicates that neurofilament compaction, occurring

independently of impaired axonal transport, may also be responsible for TAI pathology (Marmarou et al., 2005).

Markers of Traumatic Axonal Injury

TAI is marked by impaired axonal transport and altered cytoskeletal ultrastructure. It would therefore seem reasonable and rational to exploit these characteristics when trying to identify traumatically injured axons following DBI. However, in studies first identifying TAI, Strich utilized silver impregnation methods to identify swollen axons (Strich, 1956; Strich, 1961). Although the mechanism by which injured axons are marked with silver labeling remains poorly understood and is thought to underestimate the total number of injured fibers (Gentleman et al., 1995), this methodology is still used to identify axonal injury, primarily in white matter tracts (Hicks et al., 1996; Adelson et al., 2001; Ding et al., 2001; Gallyas et al., 2002; Hall et al., 2005a; Hall et al., 2005b). A second and better understood marker of TAI first utilized by Povlishock and colleagues is horseradish peroxidase (HRP). Following somatic uptake via endocytosis, HRP-laden vesicles move via fast anterograde axonal transport and pool at sites of axonal injury marked by impairment of axonal transport. With axonal injury and subsequent impairment of axonal transport being focal events, continued delivery of anterogradely transported molecules, such as HRP, lead to progressive swelling and immunoreactivity in initially continuous but later disconnected reactive axonal swellings (Povlishock et al., 1983). HRP was later found to have the added advantage of marking sites of traumatically-induced alterations in axolemmal

permeability via pre-injury lateral ventricle infusion and subsequent dispersion throughout the extracellular brain parenchyma (Pettus et al., 1994). More recently, antibodies to specific neurofilament subunits have been useful in marking altered cytoskeletal morphology at sites of axonal injury (Grady et al., 1993; Maxwell and Graham, 1997; Povlishock et al., 1997).

However, the current standard for detection of axonal injury following traumatic insult is visualization of β-amyloid precursor protein (APP). APP was first utilized as a marker for axonal injury by Gentleman and colleagues (Gentleman et al., 1993) after an earlier study by Shigematsu and McGeer revealed swollen APP positive axons, similar to those seen following trauma, within the periventricular white matter following the application of the microtubule stabilizing agent colchicine (Shigematsu and McGeer, 1992). APP is an integral membrane protein that undergoes vesicular-mediated fast anterograde axonal transport. Similar to the mechanism by which HRP marks sites of axonal injury, APP moves along the axon until reaching a site of focally impaired transport at which point the site of axonal injury will undergo expansion due to the continued delivery of transported organelles. Focal APP accumulation at the site of impaired axonal transport will lead to increased immunoreactivity of the injury focus as well as the related proximal axonal segment and corresponding soma. Visualization via routine antibody processing (Stone et al., 2000) allows for identification of axonal injury within white matter tracts as well as at perisomatic locations. The utility of APP antibody immunoreactivity as a specific marker for axonal injury has gained wide acceptance in studies of both basic science and forensic pathology (Blumbergs et al.,

1994; McKenzie et al., 1994; Sherriff et al., 1994a; Sherriff et al., 1994b; Blumbergs et al., 1995; Gentleman et al., 1995; Lewen et al., 1995; Li et al., 1995; Ahlgren et al., 1996; Lewis et al., 1996; McKenzie et al., 1996; Pierce et al., 1996; Abou-Hamden et al., 1997; Bramlett et al., 1997; Geddes et al., 1997; Murakami et al., 1998; Oehmichen et al., 1998; Van den Heuvel C. et al., 1998; Gleckman et al., 1999; Stone et al., 1999; Finnie et al., 2000; Masumura et al., 2000; Stone et al., 2000; Singleton et al., 2002).

Traumatic Axonal Injury – Cytoskeleton and Related Pathology

While altered axolemmal permeability and elevated intra-axonal calcium are the initiators of TAI pathogenesis, the resultant cytoskeletal pathology is responsible for the morphological change observed in injured axons following DBI. Therefore, in order to outline TAI pathogenesis, background information on axonal cytoskeletal composition is first provided. This information provides a conceptual framework on which mechanisms of TAI-related cytoskeletal pathology are discussed.

There are three distinct interacting structural proteins that comprise the neuronal cytoskeleton: microtubules (MTs), neurofilaments (NFs), and microfilaments (MFs) (Siegel et al., 1999). Together, these proteins form the dynamic structural latticework, encompassed by the axolemma, which serves as a scaffold for neuronal cytoarchitecture. Neurons are a highly polarized cell type that must transduce signals from one end of the cell to the other and thus, are highly dependent on their structural integrity to maintain their function. This polarization results in an axonal cytoskeletal composition that is distinct from that found in the somatic and dendritic compartments.

The axonal cytoskeleton is characterized by MTs arranged in small clusters along with dense arrays of NFs and a subaxolemmal network of MFs. Axonal MTs have uniform orientation (Kirkpatrick and Brady, 1999) which has implications for intracellular trafficking of membrane-bound organelles via molecular motor proteins (Brady, 1991; Vallee and Bloom, 1991). Similarly, NFs are oriented longitudinally, parallel to each other, and are inter-connected (Hirokawa, 1991). Interestingly, the composition of cytoskeletal elements within the axon dictates axonal caliber and thus controls the speed of impulse propagation (Pijak et al., 1996; Elder et al., 1998). This section offers a detailed description of each cytoskeletal protein along with their respective roles in axonal cytoarchitecture, intracellular transport, and TAI-related pathology.

Axonal Cytoskeleton

Microtubules (MTs) consist of polymers of globular tubulin subunits arranged in a cylindrical tube measuring 24 nm in diameter. Each tubulin dimer consists of two closely related polypeptides, α and β-tubulin (Schwartz and Westbrook, 2000). Head-to-tail arrays of tubulin heterodimers give protofilaments of which 13 are arranged in a tubular array around a hollow core. Tubulin heterodimer orientation imparts polarity to the MT, creating plus (fast-growing) and minus (slow-growing) ends. As noted, this polarity has intra-neuronal regional specificity with axonal MTs having minus ends oriented towards the cell body and plus ends oriented towards the nerve terminal (Heidemann SR et al., 1985). Although exhibiting "dynamic instability" during which they oscillate between growth and shortening phases (Mitchison and Kirschner, 1984),

neuronal MTs are relatively stable structures due to post-translational modification of tubulin following incorporation into the MT framework and alteration of intrinsic MT properties via binding by a class of molecules known as microtubule-associated proteins (MAPs). There are several MAPs, each of which demonstrates regional specificity, with tau being unique to axonal cytoarchitecture (Vallee et al., 1984).

In addition to structural support, MTs function as a "highway" for bidirectional organelle transport (Goldstein and Yang, 2000) to exchange structural and functional materials within the neuron. Organelle movement within the axon is either away from the soma (anterograde) or towards the soma (retrograde) (Lodish et al., 1999). This directed movement may be exploited to identify loci of axonal injury following trauma via use of antibodies targeting anterogradely transported proteins. These proteins collect at sites of impaired axonal transport thus identifying sites of axonal injury.

Neurofilaments (NFs) are stable polymers of neuron-specific intermediate filaments that do not demonstrate the dynamic properties of MTs (Schwartz and Westbrook, 2000). Grouped as "intermediate" because their diameter (10 nm) is between that of MTs and MFs (discussed shortly), NFs are assembled into rope-like filaments that twist around each other to produce coils of increasing thickness. Monomers form heterodimers which aggregate into tetrameric complexes known as protofilaments. Two protofilaments join to become a protofibril and three protofibrils twist helically to form the NF (Bershadsky and Vasiliev, 1988). In contrast to MTs and MFs which contain globular proteins and have polarity, NF monomers are highly elongated apolar fibrous proteins when assembled (Cooper, 2000). There are three

primary NF polypeptides: NF-light (NF-L), NF-medium (NF-M), and NF-heavy (NF-H), which differ in molecular weight (60-70, 130-170, and 180-200 kDa respectively). Polymer formation requires the NF-L subunit together with either the NF-M or NF-H subunit (Julien and Mushynski, 1998). Once assembled, NFs are transported to their site of incorporation into the cytoskeletal network (Nixon et al., 1989). During transport, all three NF subunits undergo a complex pattern of phosphorylation and dephosphorylation which regulates the different assembly states of the protein before and during axonal transport (Sihag and Nixon, 1989; Sihag and Nixon, 1990).

NFs differ from other intermediate filaments by their sidearms that project from the surface and cause them to be widely spaced (Lee and Cleveland, 1996; Kirkpatrick and Brady, 1999). Sidearms are the carboxy-terminal regions of the NF-M and NF-H polypeptides and contain a large number of consensus phosphorylation sites (KSP {Lys-Ser-Pro} sequence repeats) targeted by various kinases (Shaw, 1991; Julien and Mushynski, 1998). Sidearm phosphorylation alters the charge density on the NF surface, repelling adjacent NFs with similar charge (Gotow et al., 1994) and is a major determinant of axonal diameter (Brady, 1993). Sidearms are also thought to play a structural support role through binding to MTs (Lodish et al., 1999).

Microfilaments (MFs) are dynamic components of the membrane cytoskeleton, the area immediately adjacent to the plasma membrane (Hitt and Luna, 1994; Beck and Nelson, 1996). MFs are formed from globular actin monomers (G-actin) arranged like two strings of pearls intertwined into fibrils 4-6 nm in diameter (Kirkpatrick and Brady, 1999). Each actin monomer has binding sites that mediate head-to-tail interactions with

two other actin monomers to mediate polymerization (Cooper, 2000). The filamentous polymer (F-actin) is uniformly oriented and demonstrates polarity. MFs are organized into a meshwork of short oligomers near the axolemma and axonal MTs (Kirkpatrick and Brady, 1999).

In addition to actin MFs, several MF-associated proteins have been described (Vandekerckhove and Vancompernolle, 1992). These proteins provide further structural support to the membrane cytoskeleton via actin binding. One protein relevant to TAI pathology is spectrin. Spectrin is a flexible, rod-shaped molecule composed of homologous α and β subunits originally characterized in the erythrocyte membrane cytoskeleton. Spectrin heterodimers align to form tetramers which are cross-linked by short actin MFs (Kirkpatrick and Brady, 1999). This spectrin-actin network is coupled to the plasma membrane through direct binding to membrane proteins and serves to stabilize the membrane.

Cytoskeletal Pathology

To determine axonal cytoskeletal alterations at the injury site, the injured area must be first identified and visualized. TAI is associated with focally impaired axonal transport and concomitant axonal swelling. Capitalizing on the fact that post-injury axonal transport remains functional but is focally disrupted, immunohistochemistry with antibodies to β-APP, a molecule which moves via vesicular-mediated anterograde transport, is used to target the site of impaired axonal transport. APP and other intracellular organelles are anterogradely transported to a site at which they can

progress no further. The continued delivery and accumulation of APP and organelles at this site results in focal axonal swelling. APP may be visualized using routine light microscopy followed by tissue processing for electron microscopy to examine axonal ultrastructure.

Previous studies of TAI pathology have demonstrated cytoskeletal disruption at focal axonal swellings. In long tract axons of the brainstem, Pettus and Povlishock first noted NF misalignment and alterations in axolemmal permeability associated with rapid local NF compaction following moderate TBI, leading to delayed progression of reactive axonal change (Pettus et al., 1994). A subsequent study provided more complete cytoskeletal characterization including decreased inter-NF spacing associated with loss of sidearm projections, as well as increased NF packing and decreased MT density following moderate TBI (Pettus and Povlishock, 1996). These changes were hypothesized to cause focal impairment of axonal transport due to local ionic dysregulation given the passage of HRP into damaged fibers. Similar work by Maxwell and Graham showed focal reactive axonal change with loss of axonal MTs and NFs following non-disruptive optic nerve stretch injury (Maxwell and Graham, 1997) as did comprehensive morphological quantification studies by Jafari and colleagues (Jafari et al., 1997; Jafari et al., 1998). Further studies examining long tract axonal NF sidearms following TBI demonstrated focal alterations and consequent NF compaction associated with sites of traumatically-induced axolemmal permeability changes (Povlishock et al., 1997; Okonkwo et al., 1998).

While these studies focused on MT and NF pathology, observations of direct MF disruption have not been as forthcoming; however, membrane cytoskeletal pathology has been observed indirectly using routine immunohistochemistry targeting spectrin breakdown products that result from TBI-induced proteolytic degradation. A predominant group of proteases implicated in TAI pathogenesis are the calcium-activated neutral proteases known as calpains. When intra-axonal calcium levels reach sufficient concentrations, calcium binds to the inactive calpain molecule, resulting in activation of the protease (Kampfl et al., 1997). Using antibodies targeting calpain-mediated spectrin proteolysis (CMSP) products, Buki and colleagues demonstrated a spatiotemporal correlation between focal, intra-axonal CMSP and NF compaction following TBI, implicating calpain activation in TAI pathogenesis and spectrin as a target for this pathological activation (Buki et al., 1999). Another proteolytic molecule activated following TBI is the cysteine protease caspase-3 (Yakovlev et al., 1997; Raghupathi et al., 2000; Yakovlev and Faden, 2001). Caspase-3 activity has been indirectly documented in traumatically injured axons using antibodies targeting the specific caspase-3-mediated breakdown product of spectrin (Buki et al., 2000).

Taken together, TBI-induced protease activation destabilizes the axon within the central region (MTs / NFs) and at the membrane cytoskeleton (MFs / spectrin). Cytoskeletal destabilization contributes to continued axolemmal instability following the initial transient perturbation, allowing for further ionic dysregulation and increased calcium entry that stimulates ongoing pathology. This cycle of membrane instability followed by cytoskeletal degradation culminates in axonal disconnection due to collapse

of the cytoskeletal network. It is important to remember that axonal disconnection is delayed relative to the initial trauma. Delayed / secondary axotomy is caused by the time needed to activate pathological cascades ultimately leading to cytoskeletal collapse. This delayed pathological process is the focus of the next section and as will be discussed in Chapter 2, TAI within the perisomatic domain results in an ultra-rapid secondary axotomy with delay times significantly shorter than those reported in previous studies.

Traumatic Axonal Injury – The Somatic Response and Axotomy

TAI leading to axotomy and disconnection may be generated by a variety of experimental methods. Within the context of DBI, application of shear and tensile forces to the whole brain results in axonal pathology at various anatomical loci. These initiating forces may not immediately sever axons. Rather, they may stimulate the aforementioned pathological processes with evidence of axonal damage visible only after sufficient time has passed allowing for pathway activation. The time needed for pathway activation results in delayed disconnection which is the hallmark characteristic of secondary axotomy. On the other hand, axonal disconnection via direct surgical / mechanical severance is classified as primary axotomy in that the injury to the axon is the initiating pathology as opposed to a consequence of trauma.

Initial studies of axotomy and its related consequences employed direct severance of axonal tracts due to its relative ease and specificity (Cajal, 1914; Lieberman, 1971; Barron, 1983). Although this methodology is significantly different

from diffuse injury, information gathered from these studies may be used to begin to discern TAI-mediated secondary axotomy pathogenesis. Within one week following transection, axotomized facial neurons displayed swelling of the soma with peripheral displacement and deformation of the nucleus (Kreutzberg, 1995). These morphological changes are grouped under the term chromatolysis, also known as the axon reaction. In addition to altered morphology, axotomized neurons also undergo subcellular changes including peripheral nuclear displacement and loss of Nissl bodies. Nissl bodies, which are parallel arrays of rough endoplasmic reticulum, are either lost or much shorter than normal and are no longer arranged in a parallel fashion. Related extra-neuronal changes include glial profiles around somata and dendrites with concomitant loss of pre-synaptic terminals, a process known as synaptic stripping. Although the causes of these phenomena remain topics of debate, the favored explanation for this response following axotomy is the interrupted supply of trophic factors conveyed to the soma by retrograde transport.

Interestingly, axotomized neurons in the PNS are capable of regenerating axons and achieving functional reinnervation of targets given the appropriate conditions; however, it is well established that CNS neurons are not able to regenerate axons although various experimental manipulations may create permissive environments in which limited neurite outgrowth is visible. Comparative studies of central and peripheral neuronal axotomy have revealed different as well as common responses (Barron, 1983; Kreutzberg, 1995). Among the factors modifying the neuronal response to axotomy are: the species and age of the animal; nature of the lesion (crush,

transection, etc.); contact with the distal stump; the type of neuron; and the proximity of the lesion with respect to the soma. This last factor is of particular interest to the current dissertation. Primary lesions applied closer to the soma result in a more rapid reactive response and increased cell death (Egan et al., 1977; Villegas-Perez et al., 1993). For example, transection of the corticospinal tract in the thoracic (McBride et al., 1989), cervical (Barron and Dentinger, 1979), or medullary spinal cord (Merline and Kalil, 1990) results in delayed atrophy rather than cell death. However, lesions in the internal capsule, much closer to the somata, result in increased cell death relative to spinal cord lesions (Giehl and Tetzlaff, 1996; Bonatz et al., 2000). Similar studies using optic nerve and rubrospinal tract transections suggest that the distance of axotomy affects the cell death rate with lesions closer to the cell bodies resulting in increased cell death / loss (Liu et al., 2003; He et al., 2004).

While these studies examined lesion paradigms, a landmark study by Singleton and colleagues explored the affects of diffuse trauma on axonal injury within the perisomatic domain (Singleton et al., 2002). Utilizing a rat midline/central fluid percussion injury model of moderate severity, TAI and related axotomy was localized to within 40 – 60 μm of the sustaining soma. In contrast to previous transection-induced primary axotomy studies which generated neuronal atrophy and death, DBI-mediated perisomatic TAI did not result in acute neuronal death. Rather, subcellular changes associated with impaired protein synthesis were observed as well as evidence of potential somatic reorganization and repair. As early as 30 minutes following injury, perisomatic TAI was evident within the mediodorsal neocortex, hippocampal dentate

gyrus, and dorsolateral thalamus. While not the focus of the Singleton communication, select axonal swellings appeared continuous with their downstream segments while others appeared disconnected. These observations prompted the current investigation into the spatiotemporal and ultrastructural characterization of TAI and related axotomy within the perisomatic domain which is discussed in Chapter 2.

Traumatic Axonal Injury - Wallerian Degeneration

TAI-mediated axotomy results in loss of axonal continuity. While the axonal segment proximal to the site of injury and disconnection remains continuous with the soma, the distal segment now exists in isolation. Presumably, the proximal segment is sustained through its continuity with the soma; however, the distal segment degenerates due to loss of somatic trophic support. Degeneration of the distal axonal segment takes place via a process termed Wallerian degeneration, named for Augustus Waller who first described this phenomenon (Waller, 1850). Wallerian degeneration is a complex sequence of events that involves axonal degradation, reactive changes in glial cells, and phagocytic responses by macrophage-lineage cells (Griffin et al., 1995). It begins with enzymatic proteolysis of the axonal cytoskeleton and is a relatively rapid process which presumably clears the way (at least in the PNS) for potential axonal regeneration.

The events of Wallerian degeneration are sequential and may be arbitrarily divided into stages (Griffin et al., 1995) although the overall process is a continuum of change meaning different stages may be observed within a given tissue section. From observations based on an axonal transection model, Stage 1 immediately follows

transection and is characterized by the apparent survival of the distal axonal segment. There is accumulation of intra-axonal organelles at both ends of the distal segment due to continued bidirectional transport. The duration of Stage 1 varies depending on species, length of the distal stump, temperature, and the nature and location of the axon. There is some question as to whether distal segments in the PNS or CNS survive longer following disconnection although a recent study suggests that axonal resealing following transection takes longer in the CNS which has implications for distal segment stability (Ahmed et al., 2001). Studies using a mutant (Ola) mouse with slow Wallerian degeneration have also provided a wealth of information concerning this degenerative process and will allow for continued studies of Wallerian change (Lunn et al., 1989; Perry et al., 1990).

Stage 2 involves granular disintegration of the axoplasm and axonal breakdown. The conversion of axoplasm into fine particulate and amorphous debris represents cleavage products of the cytoskeleton. This change is believed to occur in an explosive fashion as suggested by the rarity of observing partial stages of this process. Although debris is the primary finding, remaining axolemma and mitochondria are also found within axons that have undergone cytoskeletal disintegration. It is thought that cytoskeletal degradation spreads distally from the site of axotomy with time (Lubinska, 1977) and is a calcium-dependent enzymatic process (see previous section).

Stage 3 closely follows axonal breakdown and is both similar and different within the peripheral and central nervous systems. During this stage, recruitment / activation of glial cells and macrophages takes place in both the PNS and CNS.

However, breakdown of the blood-nerve barrier occurs immediately following cytoskeletal degradation in the PNS while there is little blood-brain barrier breakdown in the CNS following degradation. In the PNS, Schwann cell responses include entry into the cell cycle, alteration of protein synthesis, and formation of chains of interdigitated cells called Bungner bands. Glial responses in the CNS include microglial expression of activation markers and increased glial fibrillary acidic protein (GFAP) expression by astrocytes. Macrophages in each nervous system express major histocompatibility complex (MHC) molecules. PNS macrophages are derived from the circulation via blood-nerve barrier breakdown while CNS macrophages appear to be recruited primarily from dedifferentiation of resident microglia although entry from the vasculature and/or perivascular locales may also contribute to observed populations. Macrophage origins as well as responses to DBI and its associated pathology are addressed in Chapter 3.

Stage 4 represents the clearance phase during which debris is removed via immune cell-mediated phagocytosis and replaced by regenerating axons in the PNS or by fibrillary glial processes in the CNS. While PNS axons regenerate and use molecular cues from degraded pathways to guide their progression, CNS axons make limited attempts at regrowth before ultimately terminating this process. Ultimately, glial processes replace sites of former axons and may collectively form a glial scar which is hostile towards promoting CNS axonal regeneration.

The temporal progression of Wallerian degeneration is dependent on several factors including species examined and anatomical location. Studies of neuronal injuries

in humans reveal evidence of continuing Wallerian change that persists for months to years post-injury as demonstrated by myelin breakdown products downstream of the injury site (Strich, 1968; Becerra et al., 1995; Buss et al., 2004). In lower order animals, Wallerian degeneration proceeds at a faster pace although the degenerative timeline outlined in Chapter 2 is significantly faster than those previously reported (George and Griffin, 1994; Pesini et al., 1999; Buss and Schwab, 2003). Wallerian change proceeds more quickly in the PNS than in the CNS, presumably conferring a regenerative advantage to PNS axonal regrowth by creating a pathway for potential regeneration (Griffin et al., 1995). To date, studies of Wallerian degeneration in the CNS come mainly from spinal cord injury models or *in vitro* transection of dorsal root ganglia. Evidence of Wallerian degeneration linked to TAI within the brain parenchyma is discussed in Chapter 2.

GLIAL RESPONSE TO TRAUMATIC BRAIN INJURY: GENERAL INTRODUCTION

In addition to TBI-induced neuronal damage and consequent degeneration, there is a corresponding glial response to brain trauma. For example, as mentioned in the previous section, the importance of glial cell activation in Wallerian degeneration has been well documented, especially within the context of axonal debris recognition and removal. Before addressing specific glial responses to TBI, a brief introduction of glial cells is provided to familiarize the reader with the various cell types within this

classification. This is followed by both historical and more current reviews of microglia, the specific cell type which is the focus of this dissertation. (**Note**: A point of clarification is necessary prior to beginning this section. Microglia are often discussed in the literature together with macrophages in that following activation by an appropriate stimulus, microglia adopt macrophage-like qualities and for all intents and purposes, transform themselves into macrophages or at least, macrophage-like cells. It is important to distinguish these endogenous brain macrophages from peripheral blood monocyte-derived macrophages. Thus, in an attempt to provide clarity, this dissertation may refer to "microglia / macrophages" when referencing endogenous brain cells and to distinguish these cells from those macrophages derived from the peripheral blood.)

Glial cells within the CNS are classified as either macroglia (e.g. oligodendrocytes, astrocytes, and ependymal cells) or microglia, with each cell type having unique form and functions. Oligodendrocytes produce myelin sheaths that insulate CNS axons, astrocytes have multiple functions including cytoskeletal support, repair following injury, and transport mechanisms while ependymal cells line the brain ventricles and the spinal cord central canal. While macroglia provide primarily neuronal support functions, microglia are responsible for CNS surveillance and subsequent inflammation, phagocytosis, and removal of extrinsic CNS content via activation and conversion to a macrophage-like phenotype. Glia differ from neurons in that they possess no synaptic contacts and retain the ability to divide throughout life, particularly in response to injury (Raine, 1999). The term "reactive gliosis" is used to describe the response of glial cells to neuronal tissue damage and implies, at the cellular level, that

glial cells react to signals that arise from injured neurons (Streit et al., 1999). While the glial response to traumatic injury relies on both neuronal signaling as well as intergliotic communication, one must focus on specific cell types to begin to discern this complex process. In that oligodendrocytes typically do not show reactive changes after CNS injury (Ludwin, 1997) and given the highly variable astrocytic responses to trauma, this dissertation focuses on the neuroinflammatory responses of microglia / macrophages to DBI and its related TAI pathogenesis. Therefore, discussion is limited to microglial / macrophage responses with the recognition that no glial response occurs in isolation.

Microglia: Historical and Current Knowledge

It is important to first provide some historical context concerning microglia / macrophages before discussing their responses to DBI and its related pathological sequelae. Microglia were first identified in the late 1890's and early 1900's by a variety of scientists including Nissl (1899), Robertson (1900), and Alzheimer (1904) although their true identity was not elucidated until del Rio Hortega introduced his silver carbonate staining method in 1932 which allowed microglia to be distinguished from oligodendrocytes based on their respective structures (del Rio Hortega, 1932). Del Rio Hortega observed that microglial distribution throughout the brain parenchyma was uniform although cells were preferentially located near neurons and blood vessels. (It was later determined that microglia at perivascular locales were in fact macrophages which had entered from the peripheral blood.)

It was not until the 1970's that microglia were determined to have a mesodermal origin and invade the CNS when the vascular supply is developing during embryogenesis. Cammermeyer's observation of microglia within the CNS of germ-free rats proved that microglia were normal CNS components and not induced by brain injury (Cammermeyer, 1970). Since these initial observations, it has been determined that microglia: 1.) are derived from circulating monocytes or precursor cells to the monocyte-macrophage lineage that originate in bone marrow; 2.) constitute ~ 10 – 20 percent of the neuroglial population being less numerous in white than in grey matter; 3.) share many marker antigens with circulating monocytes, down-regulating them in the resting state with up-regulation of their expression following an appropriate stimulus; 4.) are dynamic cells which display phenotypic heterogeneity ranging from highly ramified, small cell body resting morphology to ameboid, enlarged cell body activated morphology; 5.) are not the only source of brain macrophages depending on the nature and severity of brain injury which may allow for peripheral blood-derived monocytes / macrophages to enter the parenchyma (Barron, 1995). Unlike neurons, microglia are capable of proliferation. Thus, resident microglia remain within the brain throughout life and are the first line of defense following trauma. In response to CNS injury, microglia may undergo enhanced proliferation and localize to an injury site if presented with appropriate mitogenic and chemotactic stimuli.

Microglia are the ubiquitous resident population of immune cells within the CNS parenchyma (Raivich et al., 1999). Long thought to be quiescent until stimulated

by an appropriate signaling molecule(s) and therefore given "resting" versus "active" phenotype designations, more recent studies suggest that "resting" microglia actively survey their extracellular environment via small projections from their cell surface irrespective of brain pathology (Davalos et al., 2005; Nimmerjahn et al., 2005). As such, resting microglia morphology is characterized by a small cell body with long, ramified processes: in white matter, processes are oriented parallel to the nerve fibers while in grey matter, they display a stellate morphology (Compston et al., 1997). In this resting state, microglia typically occupy non-overlapping territories approximately 30 – 40 μm in diameter and are found evenly distributed throughout the entire parenchyma although subtle regional differences exist. From an ultrastructural standpoint, microglia typically have either an oval or elongate shaped nucleus with clumps of chromatin beneath the nuclear envelope and throughout the nucleoplasm. Its granular endoplasmic reticulum reveals cisternae which are long and narrow and often wind tortuously through the cytoplasm. Dense laminar bodies, homogeneous droplets, lysosomes, and lipofuscin are commonly encountered in the cytoplasm (Peters et al., 1991).

The role of microglia in the CNS immune response is to recognize and remove pathogens as well as cellular debris, thus facilitating healing within damaged areas of the brain parenchyma although they also have other related functions (Kreutzberg, 1996). In response to various types of brain pathology including neuronal damage, microglial activation involves stereotyped changes which include increased cell body size, thickened proximal processes, decreased distal branch ramification, and differentiation towards a more macrophage-like phenotype (Raivich et al., 1999). For

example, if neurons die, microglia will transform into brain macrophages and remove the dead cells. However, if neurons recover, active microglia may revert back to the resting phenotype (Streit et al., 1999). Following activation, the distinction between microglia and macrophage-like cell phenotype is subtle and is typically made by morphological appearance and expression of cell surface molecules. Resting microglia have a down-regulated immunophenotype adapted to the acute sensitivity of the CNS microenvironment (Kreutzberg, 1996); however, upon appropriate stimulation, microglia are actively transformed to a macrophage phenotype and express molecules such as major histocompatibility complex (MHC) and CD45 (leukocyte common antigen) on their cell surface (Berry et al., 2002). The microglial reaction to brain injury is graded, with more severe injury resulting in greater activation and dedifferentiation to macrophages.

In studies using a facial nerve axotomy model which involves a primary lesion but lacks blood-brain barrier disruption, Kreutzberg and colleagues demonstrated microglial proliferation and ensheathment of the lesioned nerve with interposing processes between afferent synaptic terminals and the neuronal surface (Kreutzberg, 1995). This phenomenon, known as synaptic stripping, is believed to confer an adaptive advantage in terms of neuronal reorganization following injury by allowing the injured neuron to recover without the additional burden of constant synaptic input. In addition to deafferentation of the injured neuron, ensheathment also places microglia within close proximity to the injured cells. This proximity may be essential for facilitating specific microglia – neuron interactions, such as the delivery of microglial-derived

trophic factors that promote neuronal survival or toxic factors leading to expedited cell death (Streit et al., 1999).

There is strong evidence to support microglial – neuron interactions within the context of neuronal injury. It is conceivable that microglia may have dual responses to trauma with the nature of injury dictating the manner in which microglia interact with injured neurons. In a model proposed by Streit and colleagues, microglia may take a perineuronal position based on chemotactic signals released by injured neurons. If the nature of injury is reversible, signals released by the neuron may induce production of trophic factors by perineuronal microglia. In the event of irreversible injury, neuron-derived signals may cause microglia to produce neurotoxic factors that may speed neuronal cell death thus facilitating phagocytosis by the prepositioned microglial cell (Streit et al., 1999). Although close approximation between microglia and neurons is found in the normal CNS (Palacios, 1990; Peters et al., 1991), this proximity is highlighted following reactive microgliosis in response to neuronal injury.

Microglial Responses to Traumatic Brain Injury

Immune cell responses to focal TBI have received considerably more attention than those related to diffuse TBI. Focal brain injury involves related contusion and/or hemorrhagic-mediated tissue damage stemming from alterations of blood-brain barrier (BBB) permeability and/or integrity. To date, various brain trauma models with focal injury components, such as stab lesion, cortical contusion injury, and lateral / parasagittal fluid percussion injury, have been used to elicit neuroinflammatory

responses. In 1976, Persson performed small stab wounds in the rat frontal lobe by insertion of a glass capillary or steel needle and observed neurotrophilic leukocytes, monocytes, and pericytes within the first post-operative week with subsequent phagocytosis of necrotic debris during the first two weeks (Persson, 1976). Interestingly, certain cells within the cavity were of intermediate morphology between astrocytes and oligodendrocytes, similar to the "third type of neuroglial cell" recognized by del Rio Hortega in 1932 and suggestive of microglia. Profound reactivity was observed in both invading hematogenous phagocytes (i.e. leukocytes and monocytes) and neuroglial cells suggesting microglial cell activation. Using similar injury methodology, Giulian and colleagues later observed activated microglia / macrophages within and immediately adjacent to the stab lesion within hours post-injury via phagocytic uptake of fluorescently labeled microspheres from the lesion (Giulian et al., 1989). More comprehensive analyses of immune cell responses to cortical cryolesion injury revealed immunoreactive microglia at 1 – 3 d post-injury within the lesion rim, the border zone between cerebral cortex and underlying white matter, and thalamic nuclei (Hermann et al., 2000), indicating microglial responsiveness at the injury site as well as within areas remote from the primary pathology. Based on these and other related studies, progressive axonal / Wallerian degeneration and neuronal / glial cell death have been recognized as primary stimulants of immune cell activation and consequent phagocytic removal of debris (Streit et al., 1999).

In terms of microglial responses to DBI, Carbonell and Grady provided regional and temporal characterization following severe lateral FPI in the mouse (Carbonell and

Grady, 1999). Microglial activation was consistently observed within regions of neuronal injury including the ipsilateral cortex, hippocampus, and thalamus by 24 hrs post-injury. Interestingly, the level of injury severity led to subdural hematoma formation in all injured animals, indicated that a significant focal injury accompanied the observed diffuse pathology. Other studies have demonstrated microglia / macrophage activation and clustering within various axonal injury loci following diffuse TBI although cellular interactions at these sites were not characterized (Oehmichen et al., 1999; Csuka et al., 2000). Microglial clustering was observed infrequently while macrophage immunoreactivity was relegated to vascular and perivascular locales.

Irrespective of the mechanism of injury, microglia undergo activation and adhesion to damaged neuronal structures ultimately transforming into macrophage-like phagocytic cells that remove debris. Phagocytosis is observed during the later stages of Wallerian degeneration via the removal of disconnected axons and myelin as well as in the removal of dead neurons, frequently leading to the formation of microglial nodules consisting of 3 – 20 microglial phagocytes (Raivich et al., 1999).

Given the lack of information on DBI-mediated neuroinflammatory responses, this dissertation focuses on the microglial / macrophage responses to DBI within loci marked by TAI and uncomplicated by focal pathology such as acute neuronal cell death, overt contusion, and hemorrhagic-mediated tissue damage. These observations and subsequent discussion provided in Chapter 3 illustrate the differences between

neuroinflammatory responses to focal and diffuse injury and suggest that indicators of TBI may inadvertently overlook and thus underestimate the extent of diffuse pathology.

STATEMENT OF PURPOSE

In the preceding chapter, we have attempted to provide a detailed analysis of our current understanding of the pathobiology of TBI, particularly in the context of DAI which, as stated previously, is a major player in the morbidity and mortality associated with TBI. Our understanding of the pathogenesis of TAI has improved vastly, as has our understanding of its anterograde and retrograde consequences in terms of the ensuing neuronal somatic and Wallerian responses. Yet, many questions remain in relation to these anterograde and retrograde responses. For example, it appears counterintuitive that the perisomatic axotomy described in the diffusely injured brain does not result in rapid neuronal cell death that would have been anticipated based upon the use of experimental axonal transection paradigms. Such a fundamental difference suggests that the pathobiology of perisomatic axotomy versus physical transection is dissimilar, potentially explaining the unanticipated finding of neuronal perturbation without lethality. This dissertation seeks to explore this issue in the context of diffuse TBI. Through the use of multiple structural and tracer approaches, Chapter 2 seeks to explore if the rapidity of disconnection associated with perisomatic axotomy is the critical variable or alternatively, is it the integrity of the axolemma as it progresses through various phases of modification, resulting in axonal disconnection. Further, in that the preservation of these perisomatically injured neuronal soma would suggest a

non-lethal /non-widespread immune response, Chapter 3 also directly investigates this issue in the context of diffuse TBI. Here, we attempt to compare and contrast the nature of the subsequent neuroinflammatory response triggered by diffuse injury to more destructive tissue tearing involved with focal injury-mediated transection. Collectively, the conduct of these studies seeks to provide further insight into the complex pathobiology associated with DAI, explaining the precise nature of perisomatic axonal failure, its anterograde and retrograde responses, as well as the neuroimmunological sequelae associated with these events. It is hoped that these findings, together with others emerging in the field, will help improve our understanding of patients sustaining DAI and their ultimate therapeutic management.

Chapter 2

TRAUMATIC AXONAL INJURY IN THE PERISOMATIC DOMAIN TRIGGERS ULTRARAPID SECONDARY AXOTOMY AND WALLERIAN DEGENERATION

Introduction

Traumatic brain injury (TBI) remains a leading cause of death and disability, especially in children and young adults (Sosin et al., 1995; Kraus et al., 1996; Langlois et al., 2004). Within this context, diffuse brain injury (DBI) occurs via rapid cranial acceleration-deceleration with or without impact and generates little overt pathology in comparison to focal lesions (Adams, 1992; Meythaler et al., 2001; Hardman and Manoukian, 2002). A significant component of DBI is diffuse axonal injury (DAI) which contributes to the associated morbidity and mortality (Christman et al., 1994; Graham et al., 2002). Traumatic axonal injury (TAI), the experimental counterpart of DAI, is characterized microscopically by focal impairment of axonal transport leading to progressive axonal swelling and disconnection over several hours post-injury (secondary axotomy) due to cytoskeletal misalignment and collapse via neurofilament compaction, microtubule loss, and disruption of the subaxolemmal spectrin network (Povlishock, 1992; Pettus and Povlishock, 1996; Povlishock and Pettus, 1996; Okonkwo et al., 1998). Proposed mechanisms of moderate to severe TAI pathogenesis

include traumatically induced transient perturbation of the axonal membrane allowing for massive calcium influx which stimulates pathological cascades targeting the axonal cytoskeleton for degradation (Povlishock and Pettus, 1996; Buki et al., 1999; Buki et al., 2000).

Although considerable information has been generated concerning TAI and its pathogenesis, particularly in long tract axons of the brainstem, it has been difficult to evaluate the consequences of TAI in terms of the related neuronal somatic fate that also must contribute to any ensuing traumatically induced morbidity. To better explore this issue, our laboratory recently utilized a midline/central fluid percussion injury (cFPI) model to study the neuronal somatic response to DBI-mediated axotomy that occurred in the perisomatic domain (Singleton et al., 2002). Using this model, perisomatic axotomized fibers were localized to within 40 - 60 μm of the sustaining somata and were found within distinct anatomical loci, namely the neocortex, hippocampus, and thalamus. Contrary to expectations based on the existing literature of experimental transection-induced primary axotomy (Barron, 1983; Kreutzberg, 1995), perisomatic traumatic axotomy did not result in acute neuronal cell death. Rather the related somata revealed impaired protein synthesis followed by neuronal cell reorganization and repair (Singleton et al., 2002). Based on these unanticipated, non-lethal neuronal responses, we questioned whether the structural and related subcellular changes associated with perisomatic TAI significantly differed from those TAI changes previously described within brainstem fiber tracts. To this end, we followed the course of this perisomatic axotomy, focusing on its occurrence in discrete nuclei within the thalamus.

Recognizing that axotomy within the long tract axons of the brainstem is typically associated with impaired axonal transport and altered axolemmal permeability (Pettus et al., 1994; Stone et al., 2004), we used immunocytochemical light and electron microscopy as well as confocal microscopy with antibodies to β-amyloid precursor protein (APP), a marker of impaired axonal transport, as well as extracellular tracers (fluorescently-conjugated 10 kDa dextrans) normally excluded from intact axons to critically evaluate the spatiotemporal and ultrastructural features of perisomatic TAI following moderate cFPI. Routine LM analysis offered insight into the temporal course of perisomatic axonal injury progression while EM semi-serial image reconstruction permitted the characterization of the axonal subcellular responses at the site of injury in addition to those proximal - distal changes ongoing in the axon cylinder. Parallel confocal microscopy was used to explore post-injury alterations of axolemmal permeability and its relation to focal APP accumulation at the axotomy site. Contrary to expectations, these approaches demonstrated that the thalamic perisomatic TAI was associated with an ultra-rapid axotomy followed by rapid initiation of Wallerian degeneration. Further, despite the rapidity of this axotomy, this event was not accompanied by overt alterations in axolemmal permeability.

Materials and Methods

Animal preparation and injury

To follow the pathogenesis of thalamic perisomatic TAI, animals were subjected to moderate cFPI consistent with methods described previously (Dixon et al., 1987;

Singleton et al., 2002). Adult male Sprague Dawley rats (375 - 400 gm) were anesthetized with 4% isoflurane in 70% N_2O and 30% O_2, intubated, and maintained on a ventilator with 1-2% isoflurane for injury preparation. Intubated animals were placed on a heating pad connected to a thermostat controlled by a rectal probe (Harvard Apparatus, Holliston, MA) to maintain 37°C body temperature. To prepare the animal for cFPI, the top portion of a Leur-Loc syringe hub of a 20 gauge needle, two fixation screws, and dental acrylic were fixed to a midline craniotomy in the skull over the intact dura and then connected to the injury device. Briefly, a 4.8mm circular craniotomy along the sagittal suture midway between bregma and lambda was generated taking care not to disrupt the underlying dura and superior sagittal sinus. The top portion of the Leur-Loc hub (Becton Dickinson, Franklin Lakes, NJ) was cut away from the 20 gauge needle, beveled, scored, and affixed over the craniotomy site using cyanoacrylate. After confirming the integrity of the seal between the hub and the skull, fixation screws were inserted into 1mm holes drilled into the right frontal and occipital bones. Dental acrylic (Hygenic Corp., Akron, OH) was applied around the hub and over the screws and allowed to harden to provide stability during the injury induction. After the dental acrylic hardened, the skin was closed over the hub with sutures, topical Lidocaine ointment was applied, and the animal was removed from anesthesia and monitored in a warmed cage until fully recovered (~ 1 hr).

Prior to injury, the animal was again anesthetized with isoflurane. The incision was quickly opened and the male end of a spacing tube was inserted into the Leur-Loc hub. The female end of the spacer-hub assembly, filled with normal saline, was then

inserted onto the male end of the fluid percussion device, ensuring that no air bubbles were introduced into the system. A ~ 2.1 atmosphere (1.9 – 2.3 atm) injury was administered, consistent with brain injury of moderate severity (Dixon et al., 1987). Injury preparation and induction were completed prior to the animal's recovery from anesthesia. Following injury, the spacer-hub assembly was immediately removed *en bloc*, bleeding was controlled with Gelfoam (Parmacia, Kalamazoo, MI), and the incision was closed with sutures. Animals were monitored for spontaneous respiration and, if necessary, ventilated with room air to ensure adequate post-injury oxygenation. Post-injury recovery times for the following reflexes were recorded: toe pinch, tail pinch, corneal blink, pinnal, and righting. Following recovery of the righting reflex, animals were placed in a holding cage with a heating pad to ensure maintenance of normothermia and monitored until the appropriate perfusion time. For sham-injured control animals, the above steps were followed without injury induction. All injured animals had righting reflex recovery times greater than 6 min compared to less than 2 min for sham-injured animals (data not shown). Experiments were conducted in accordance with NIH and institutional guidelines concerning the care and use of laboratory animals (IACUC).

Tissue preparation

Animals (n = 5 / injury group and 2 / sham-injury group) were euthanized at t = 15, 30, 60, 180 min post-injury via an overdose of sodium pentobarbital IP (150 mg/kg) and transcardially perfused with 4% paraformaldehyde / 0.1% glutaraldehyde in

Millonig's buffer for immunocytochemistry. Following perfusion, brains were removed and blocked in a coronal blocking device to include the thalamus with overlying neocortex and hippocampus. The blocked region was then re-immersed in the same fixative for 24 hours. Following postfixation, the blocked region was flat-mounted on a metal plate with cyanoacrylate, embedded in agar, and sectioned in 0.1M phosphate buffer at a thickness of 40 μm using a vibrotome (Leica Microsystems, Bannockburn, IL). Serial coronal sections (n = 60 sections at 40 μm / section) were collected starting from 1600 μm caudal to the anterior commissure. Additionally, select blocked brains were bisected along the midline, flat-mounted, and sectioned through the sagittal plane. These sampling strategies allowed for a comprehensive examination of the thalamus based on stereotactic coordinates relative to the anterior commissure (Paxinos and Watson, 1986). Systematic uniform random sampling of coronal sections was employed with every fifth section collected for a total of twelve sections per animal. Additional tissue was stored in Millonig's buffer in 12-well culture plates (Falcon, Newark, DE).

Immunocytochemistry for light microscopy

Sections were processed with APP antibody to permit visualization of thalamic perisomatic TAI and its spatiotemporal and ultrastructural characterization. Intra-axonal APP moves via anterograde transport and pools at sites of impaired axonal transport, thus serving as a marker of TAI (Stone et al., 2000). Sections were processed for APP immunoreactivity using an established protocol including modified microwave antigen retrieval described previously (Stone et al., 1999).(Stone et al., 2000) Briefly,

endogenous peroxidase activity within the tissue was first blocked with 0.3% H_2O_2 in PBS for 30 min. Sections were then processed using the temperature-controlled microwave antigen retrieval approach, preincubated for 60 min in 10% normal goat serum (NGS) with 0.2% Triton X-100 in PBS, and incubated overnight with C-terminus specific APP (1:1500; rabbit anti-C-APP; Zymed, San Francisco, CA) primary antibody in 1% NGS in PBS. Sections were then incubated for 1 hr with biotinylated rat-absorbed goat anti-rabbit IgG secondary antibody (1:200 Vector, Burlington, CA) diluted in 1% NGS in PBS. Sections were visualized via incubation in avidin-horseradish peroxidase complex (Vectastain ABC Standard Elite Kit; Vector) for 1 hr followed by 0.05% diaminobenzidine, 0.01% H_2O_2, and 0.3% imidazole in 0.1M phosphate buffer for 10-20 min. Sections for light microscopic analysis were mounted on gelatin-coated slides, dehydrated, and coverslipped while additional sections underwent continued processing for EM. As an internal control, additional sections were processed as described above; however, primary antibody was omitted from the procedure. Images were captured using an Eclipse 800 microscope (Nikon, Tokyo, Japan) fitted with a Spot-RT digital camera (Diagnostic Instruments, Sterling Heights, MI).

Immunoelectron microscopy

Following LM processing, select sections were further processed for EM analysis to ascertain related ultrastructural pathology. Following processing for APP antibody, tissue was osmicated in 1% OsO_4 and then placed in graded alcohols and

propylene oxide prior to placement in epoxy resin (Ted Pella, Redding, CA). Sections were then embedded between plastic slides (Thomas Scientific Co., Swedesboro, NJ), placed in 55°C oven for 3 days, and then scanned to identify immunoreactive axonal swellings in continuity with their sustaining somata. Once identified, these sites were removed, mounted onto plastic studs, and thick sectioned to the depth of interest using an ultramicrotome (Leica Ultracut R; Wien, Austria). Semithin sections (1 μm) stained with 1% Toluidine Blue were screened for evidence of perisomatic TAI and Wallerian degeneration. Serial thin sections (70 nm) were then cut, picked up onto Formvar-coated slotted grids, and stained in 5% uranyl acetate in 50% methanol for 2 min. and 0.5% lead citrate for 1 min. The length and non-linear path taken by many thalamic axons required reconstruction of semi-serial sections in order to examine the complete axonal cylinder including the swelling site and proximal - distal axonal segments. Images were captured using a JOEL 1230 electron microscope using either negative film (Kodak, Rochester, NY) or digital camera (Gatan Digital Micrograph, Pleasanton, CA) and were imported into Adobe Photoshop (Adobe Systems, San Jose, CA) prior to publication to allow for thin section reconstruction.

Tracer studies and double-label immunofluorescence for confocal microscopy

To determine the potential for focal alterations of axolemmal permeability reminiscent of those described in the brainstem following injury as well as the potential co-localization of altered permeability with impaired axonal transport and APP accumulation, another population of animals (n = 3 / injury group and 2 / sham-injured

group) received stereotactic injections of Alexa 488-conjugated 10kDa dextran (80 μl at 20 mg/ml) into the lateral ventricle prior to injury. Dextran was infused (Microinjection Pump; Bioanalytical Systems, West Lafayette, IN) at a rate (2 μl/min) previously recognized in our laboratory to maintain normal intracranial pressure. Tracer circulated within the brain parenchyma for 3 hrs prior to injury induction. At t = 15, 30, 60, and 180 min post-injury, animals were perfused with 4% paraformaldehyde and sections were processed for APP immunocytochemistry as described previously. However, goat anti-rabbit Alexa 594 secondary antibody (1:1000; Molecular Probes, Eugene, OR) was used to allow for simultaneous visualization of dextran and APP immunofluorescence. Sections were mounted with an anti-fade aqueous mounting media (ProLong; Molecular Probes, Eugene, OR) onto glass slides, coverslipped, and sealed with nail polish. Images were captured using a confocal microscope (Leica TCS-SP2 AOBS; Leica Microsystems, Bannockburn, IL) with appropriate excitation lasers, detectors, and analysis software.

Axonal swelling measurements and statistical analysis

Axonal swelling diameter at each post-injury time point was quantified using systematic random sampling within the thalamus. Using computer-assisted counting software (CAST; Olympus, Copenhagen, Denmark) the thalamus was first outlined bilaterally at low power (2X) after which a high power (100X with oil) objective was used to count axonal swelling diameters at randomly assigned locations within the defined thalamic region. Counts (n = 35) were obtained from a single animal at each

time point using coronal tissue sections taken from comparable stereotactic coordinates (approximately -3.60 mm relative to bregma) (Paxinos and Watson, 1986). Perisomatic swellings or swellings in isolation were identified by APP immunoreactivity and diameters were quantified at the maximal distance across the swelling by first focusing through the z axis and then measuring the distance using a calibrated measuring tool. Data were reported as mean ± standard deviation and were analyzed using Welch ANOVA and Tukey's HSD post-hoc. In addition to swelling diameter quantification, swelling frequency versus diameter for the 15, 30, and 60 min post-injury time points were plotted to provide additional insight into the temporal pattern of swelling development.

Results

Sham-injury - General findings

Macroscopically, sham-injured brains showed no evidence of compression, contusion, or tissue loss. Tissue sections from sham-injured animals processed with APP antibody and examined at the LM level demonstrated limited background staining with the finding of only isolated immunoreactive somata. However, there was no evidence of immunoreactive axons or swellings adjacent to these somata (data not shown).

Injury - LM findings

The injured brains shared identical macroscopic features with sham-injured brains with the exception of limited subarachnoid hemorrhage underlying the craniotomy site and petechial hemorrhages within the corpus callosum. In tissue sections, APP immunoreactive perisomatic thalamic axonal swellings were visible at all post-injury time points. In addition to thalamic swellings, comparable perisomatic axonal changes were found in the lateral neocortex and hippocampus, with other swellings found scattered in the corpus callosum, subcortical white matter, and brainstem. These findings were consistent with previous observations (Singleton et al., 2002); however, they were not the focus of the current communication that centered exclusively on thalamic change. Fifteen minutes post-injury, APP immunoreactive axons were visible within thalamic nuclei, with most concentrated in the dorsolateral (DL) quadrant. These axons revealed focal swellings reflected in the localized increase of their relative axonal diameter. The swellings were within 40 - 60 μm of their somata of origin and many were continuous with axonal immunoreactivity in both proximal and distal directions, consistent with the maintenance of axonal continuity (Figs. 2-1A&B). In contrast to these continuous immunoreactive axonal profiles, other immunoreactive perisomatic axonal swellings demonstrated no association with any immunoreactivity distal to the swelling, suggesting axonal disconnection. Swelling diameter at 15 min post-injury was 1.96 ± 0.36 μm (mean ± SD). By 30 min post-injury, immunoreactive axonal swellings were now observed in the ventral posteriomedial (VPM) and posteriolateral (VPL) nuclei together with the DL quadrant. These swellings were

Fig. 2-1. The low magnification microphotograph is provided only to orient the reader to the dorsolateral thalamic locus (rectangle) in which perisomatic TAI is found. Higher magnifications of this region at sequential post-injury time points demonstrate the progression of perisomatic TAI via APP immunoreactivity. At 15 min post-injury (A&B), immunoreactive axonal segments proximal and distal to swellings (arrowheads) suggest axonal continuity despite focal impairment of axonal transport. Note that the proximal segment immunoreactivity can be traced back to the corresponding soma of origin. At 30 min post-injury (C), the focal axonal diameter at swelling sites (arrowheads) is increased. The upper neuronal profile shows immunoreactivity distal to the swelling while the lower profile lacks distal immunoreactivity, suggestive of axonal disconnection. Note that by 60 min post-injury (D), most immunoreactive swellings have lost distal immunoreactivity and that the focal axonal swellings (arrowheads) now take on a rounded appearance. (Scale bar = 10 μm)

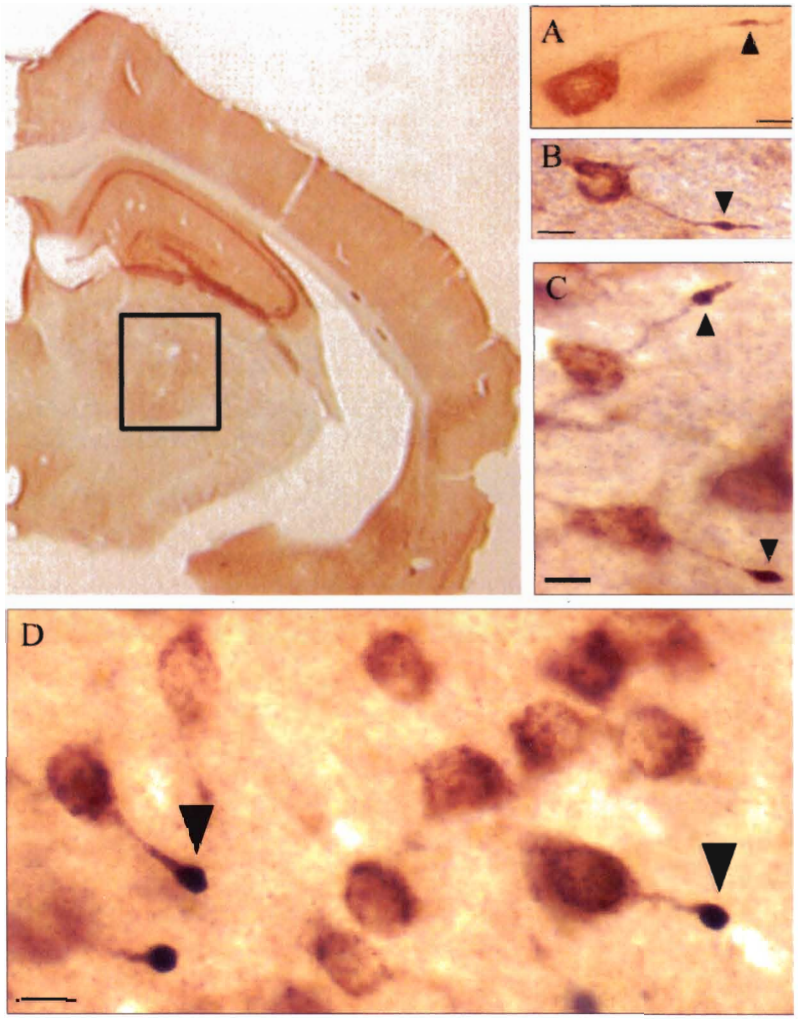

Figure 2-1

similar to those seen at 15 min; however, they were increased in diameter (2.63 ± 0.41 μm) and as such, were more intensely immunoreactive, consistent with continued delivery of APP via anterograde transport. Although quantitative assessments were not performed, there appeared to be increased numbers of these reactive swellings compared to 15 min post-injury. Isolated immunoreactive axonal swellings revealed continuity between the proximal and distal immunoreactive axonal segments; however, the majority of immunoreactive axonal swellings at this time point demonstrated continuity only with their proximal segments, without any evidence of downstream axonal immunoreactivity (Fig. 2-1C). This observation was consistent with the premise that these axonal swellings had become detached from their downstream segments. At 60 - 180 min, the above described thalamic nuclei continued to demonstrate axonal swellings that had expanded in diameter from 4.41 ± 0.87 μm at 60 min to 4.20 ± 0.78 μm at 180 min. In this time interval, most axons with reactive swellings showed no evidence of distal immunoreactivity consistent with complete axotomy and disconnection (Fig. 2-1D).

Statistical analysis and progression of axonal swelling diameter

Statistical analysis of swelling diameter within each group showed a normal distribution with unequal variances. Therefore, axonal swelling diameter measurements from comparable thalamic regions for each of the four survival groups (15, 30, 60, and 180 min post-injury) were compared using Welch ANOVA and found to be significantly different ($F(3,74) = 139.4$, p value < 0.0001). Using Tukey's HSD post-

hoc analysis, a progressive increase in swelling diameter over time post-injury was confirmed. At 60 - 180 min post-injury, swelling diameter (4.41 ± 0.87 μm and 4.20 ± 0.78 μm respectively) was greater than at 30 min (2.63 ± 0.41 μm) which, in turn, was greater than at 15 min (1.96 ± 0.36 μm). There was no significant difference between swelling diameters at 60 and 180 min. The rapidity of axonal swelling was highlighted by an approximate doubling in diameter when 15 and 60 min mean swelling diameters were compared: 1.96 versus 4.41 μm respectively. To examine axonal swelling progression, swelling frequency versus diameter was plotted as a function of time post-injury (Fig. 2-2). Swelling diameter showed a tendency to cluster at all time points and increased as time post-injury increased. Similarly, axonal swellings appeared to expand to a maximal diameter given the comparable mean diameter values at 60 and 180 min post-injury.

EM findings

EM observations confirmed and supplemented those findings described at the LM level. Specifically, as early as 15 - 30 min post-injury, a similar progression of change was seen in all thalamic nuclei assessed. At these time points, focal axonal swellings in continuity with their proximal and distal segments were seen, consistent with LM observations. These swellings showed an intact yet expanded axolemma that encompassed an organelle-laden mass composed primarily of mitochondria along with smooth endoplasmic reticulum (SER) and vesicles, both containing immunoreactive / electron-dense APP. Proximal to the swelling, the axonal cylinder appeared

Fig. 2-2. Graph of swelling frequency versus swelling diameter (μm) as a function of time post-injury. Trend lines indicate swelling clustering by diameter as a function of time post-injury. Mean diameter values demonstrate a statistically significant increase over time. Note the relatively modest number of small swellings at 60 min post-injury indicating minimal *de novo* swelling development in the later phases of injury. This data suggests that perisomatic TAI occurs in the acute post-injury timeframe and that there is an approximate doubling in swelling diameter within the first hour for those fibers injured during the acute timeframe. (Note: 180 min data has been omitted for simplicity)

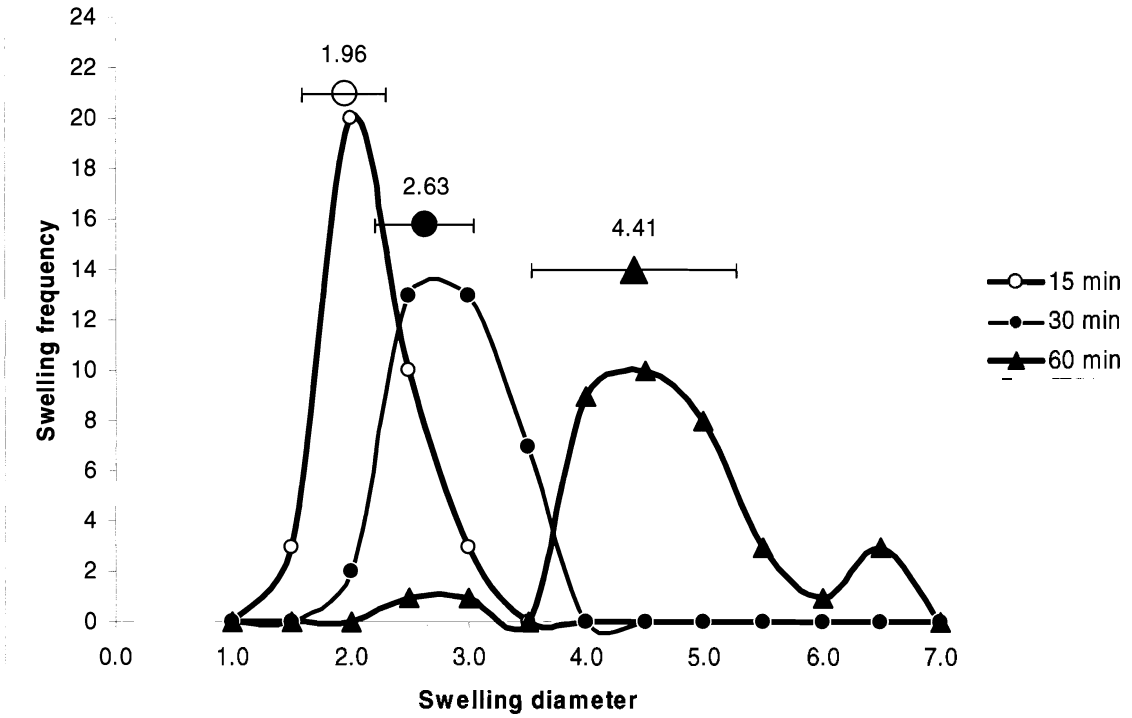
24
22
20
18
16
14
12
10
8
6
4
2
0
Swelling frequency
1.96
2.63
4.41
0.0
1.0
2.0
3.0
4.0
5.0
6.0
7.0
Swelling diameter
15 min
30 min
60 min

Figure 2-2

unremarkable showing normal axonal detail, while the related soma revealed no overt subcellular changes. Similarly, the related distal axonal segment also appeared morphologically normal. Of note was the fact that these perisomatic swellings typically occurred just prior to the initiation of the myelin sheath although infrequently a myelin investment was identified, consistent with involvement of the first internodal segment. In contrast to these isolated continuous / non-axotomized fibers, many of the axonal swellings seen at these time points demonstrated frank disconnection (Figs. 2-3 – 2-4). This axonal disconnection, suggested at the LM level by the loss of immunoreactivity distal to the swelling, was confirmed at the EM level via the loss of axonal continuity distal to the site of axonal swelling. Consistent with LM findings, perisomatic swellings were expanded containing numerous APP-laden vesicular profiles and abundant mitochondria consistent with their continued delivery via anterograde axonal transport. The related somata again appeared unremarkable. Although the proximal segment between the soma and the swelling appeared structurally intact, some evidence of initial change was reflected in the finding that many of the mitochondria within this axonal segment were dilated. This was particularly so for those mitochondria approximating the axonal segment immediately adjacent to the swelling (Fig. 2-3A). The swellings themselves were surrounded by a continuous axolemma that encompassed a pool of immunoreactive vesicles as well as mitochondria capping aggregated and disorientated neurofilaments and microtubules (Fig. 2-4B). Immediately distal to the swelling, no axonal continuity could be observed even when the sections were followed in semi-serial order. Typically when downstream segments were identified via semi-serial

Fig. 2-3. This micrograph reveals a reactive axonal swelling with corresponding proximal and distal segments 30 min post-injury (Bar = 5 μm). In rectangle A of Fig. 3, separation of myelin lamellae can be seen within the proximal segment. Note that the myelin sheath remains intact until just prior to the swelling. This segment, enlarged in panel 3A, contains mitochondria demonstrating normal structural detail (single arrowheads) as well as pathological swelling (double arrowheads). Linear neurofilaments and microtubules are observed until the area of mitochondrial pathology at which point their orientation becomes disorganized. Swelling characteristics include edema and loss of myelin / axonal ultrastructure. Granular electron-dense precipitate at the site of the swelling is consistent with the pooling of APP immunoreactive vesicles via impaired axonal transport. Axotomy is confirmed via loss of axonal ultrastructure immediately distal to the swelling. Note that despite axonal disconnection, the distal segment, seen in rectangle B of Fig. 2-3 and enlarged in panel 3B, remains ultrastructurally intact with normal-appearing axonal morphology. (Bar = 2 μm)

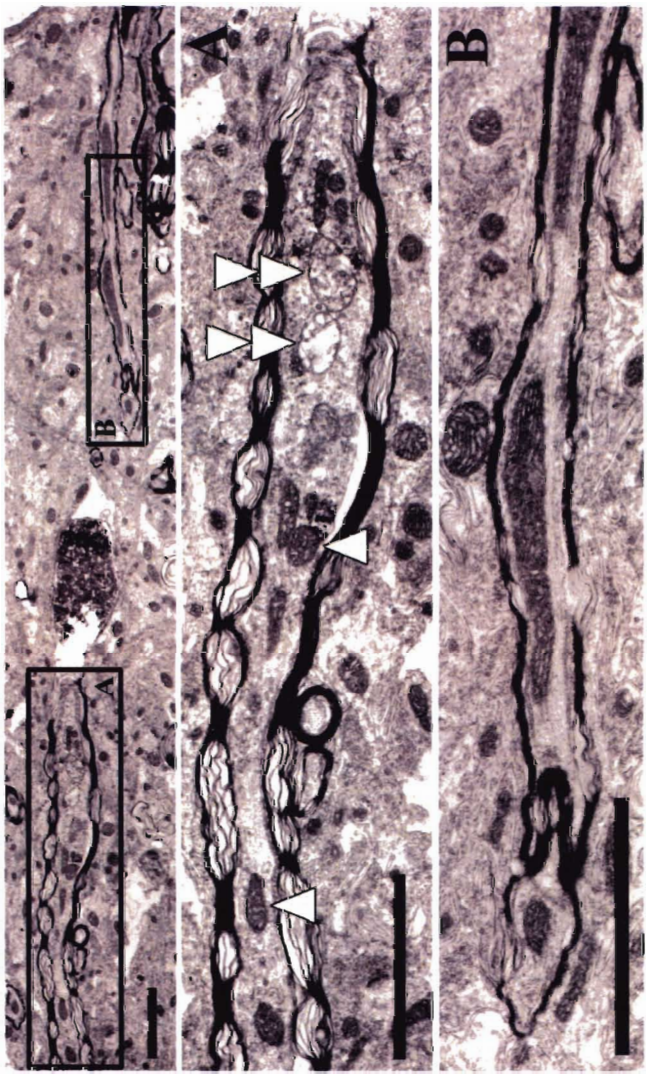

Figure 2-3

Fig. 2-4. This micrograph illustrates a reactive axonal swelling and proximal segment ultrastructure 15 min post-injury (Bar = 2 μm). Proximal segment ultrastructure, shown in panel 4A corresponding to rectangle A in Fig. 2-4, appears morphologically normal with linear neurofilaments along the longitudinal axis, together with microtubules and compact, elongated mitochondria within an intact unmyelinated axolemma. Within this segment, electron-dense APP immunoreactivity (arrowhead) can be seen within scattered vesicles. In panel 4B corresponding to rectangle B in Fig. 2-4, swelling ultrastructure is characterized by neurofilamentous disorganization (asterisks), microtubule loss, and pooling of mitochondria. Within the swelling, the pooling of APP immunoreactive vesicles (arrowheads) is consistent with an impairment of axonal transport at this site. (Bar = 1 μm)

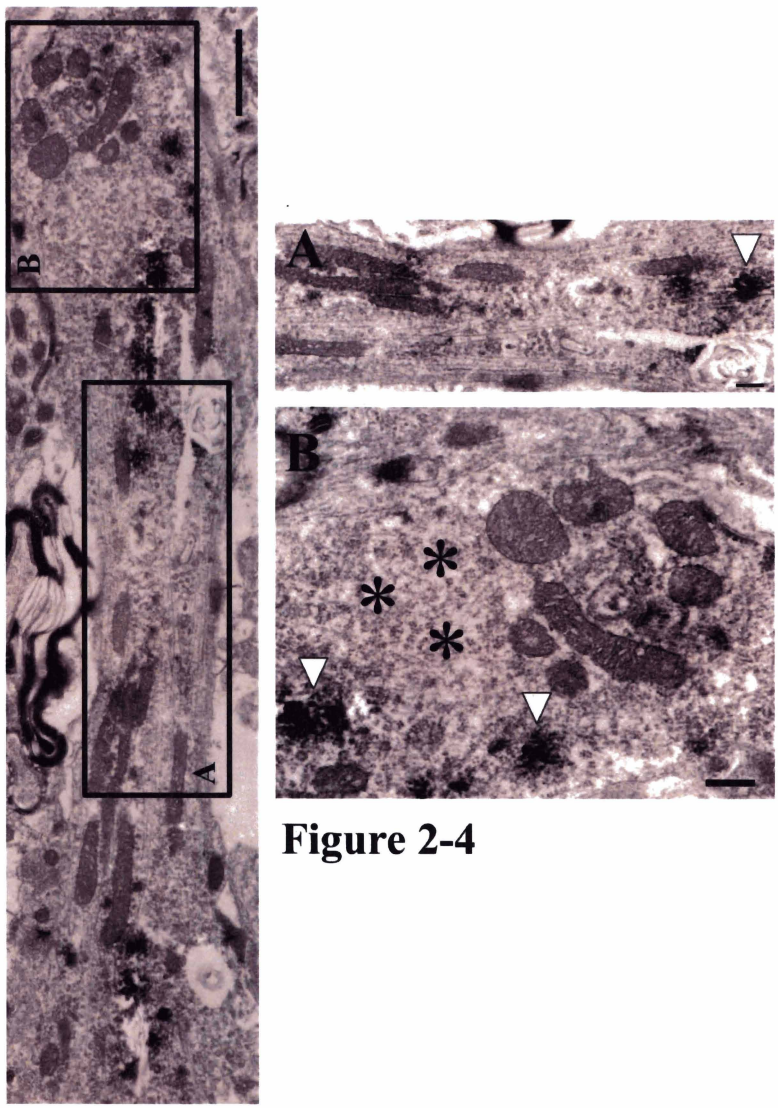

Figure 2-4

section analysis, they were found up to 5 μm beyond the site of axotomy and axonal swelling. Despite disconnection from their proximal segments, the tips of these distal axonal segments were sealed by a continuous axolemma, with no evidence of structural change. The distal segments appeared morphologically normal and contained an intact cytoskeleton and organelles that included linear arrays of neurofilaments, microtubules, and compact mitochondria within a well-defined axolemma (Fig. 2-3B). Axonal swellings were seen at initial segments (Fig. 2-4), prior to initiation of the myelin sheath, as well as within internodal segments (Fig. 2-3) approximating the somata of origin as identified by myelin investment. Although quantitative studies were not performed, swollen profiles were more commonly observed at the initial segment as compared to the internodal segment. Remarkably, despite these processes of axonal injury, swelling, and disconnection, the related brain parenchyma appeared unaltered. The reactive changes occurring in the perisomatic axonal swelling and its disconnected segment were not associated with local tissue tearing, overt structural damage, or intrinsic vasculature disruption (Figs. 2-3 – 2-4).

By 60 - 180 min post-injury, the proximal axonal segment and related soma remained morphologically intact, while axonal swellings demonstrated continued cytoskeletal pathology, organelle accumulation, and axolemmal expansion (Fig. 2-5 – 2-7). The majority of axonal swellings now visualized were encompassed by a continuous axolemma, with no evidence of downstream axonal continuity. Only isolated swellings were found continuous with their distal segments which now were devoid of organelles and contained amorphous debris suggestive of the initial stages of

Fig. 2-5. Evidence of axonal disconnection and anterograde / Wallerian degeneration is seen at 60 min post-injury (Bar = 2 μm). In Fig. 2-5, the myelinated proximal segment, seen in rectangle A, demonstrates normal morphology similar to injured axons at earlier post-injury time points. The swelling, enlarged in panel 5A from rectangle A in Fig. 2-5, reveals edema and loss of axonal constituents although the overlying myelin sheath remains intact and continuous with the proximal portion of the myelin sheath. Note that local glial swelling and perivascular edema within the adjacent parenchyma can be seen. Axonal disconnection is confirmed by the finding of myelinated, APP immunoreactive, edematous debris immediately distal to the swelling as seen in rectangles B&C. The debris, enlarged in panels 5B&C, reveal axonal fragmentation and vacuolization. Note the amorphous precipitate in an axoplasm devoid of organelles that is bounded by a continuous axolemma. The more distal segment, enlarged in panel 5D from rectangle D, reveals return of normal axonal ultrastructural detail including linear neurofilaments and compact mitochondria within an intact axolemma. (Bar = 1 μm)

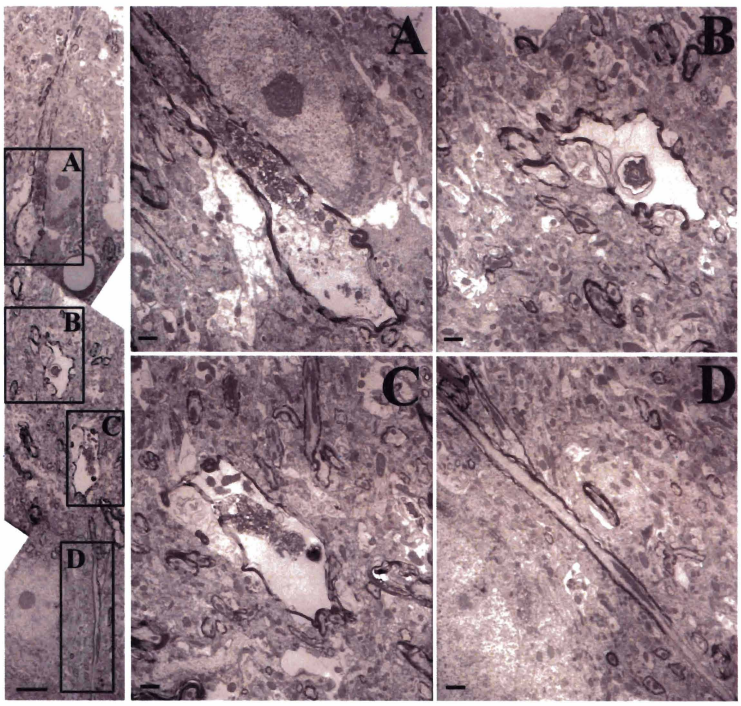

Figure 2-5

Fig. 2-6. The atypical finding of maintained axonal continuity at 180 min post-injury is shown in this micrograph (Bar = 5 μm) which also reveals an example of internodal involvement in the process of axonal injury. Note the presence of a swelling (asterisk) that is continuous with both the proximal and distal axonal segments, encompassed by a thinned, yet continuous, myelin sheath. Also note that the myelinated, proximal axonal segment ultrastructure remains normal until immediately prior to the swelling. At the intersection of the proximal segment and related swelling enlarged in panel 6A from rectangle A in Fig. 2-6, linear neurofilaments and microtubules enter the swelling at which point their orientation becomes disorganized. Further progression into the swelling, enlarged in panel B from rectangle B, reveals neurofilament disorganization (box within panel B) encompassing both normal and pathologically swollen (arrowhead) mitochondria. Pooling of axoplasmic organelles and electron-dense APP immunoreactive vesicles (double arrowhead) is consistent with impaired axonal transport. The distal (although not disconnected) segment shows loss of axoplasmic constituents and amorphous precipitate although portions of the myelin sheath remain intact. These changes appear consistent with the onset of Wallerian degeneration. (Bar = 1 μm)

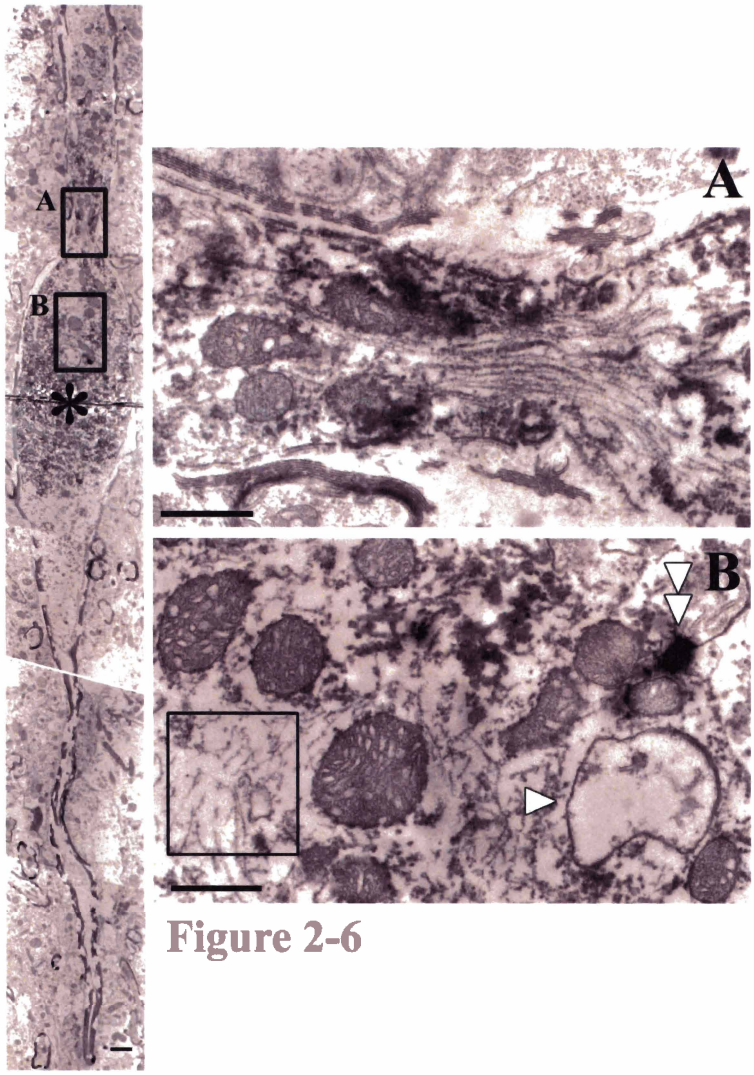

Figure 2-6

Fig. 2-7. In contrast to Fig. 2-6, Fig. 2-7 shows evidence of disconnection. Note that in Fig. 2-7, the sustaining soma (N) can be seen in continuity with the proximal axonal segment which is enlarged in panel 7A from rectangle A. The axonal swelling and disconnection enlarged in panel 7B from rectangle B shows evidence of downstream Wallerian change seen in panel 7C enlarged from rectangle C (Bar = 5 μm). Note that the initial segment (panel 7A) ultrastructure seen in continuity with its sustaining soma appears morphologically normal although periaxonal edema is present. Within this segment, electron-dense APP immunoreactive vesicles are evident (arrowheads). At the swelling (panel 7B), impaired axonal transport is marked by loss of neurofilament linearity and microtubules along with pooling of immunoreactive vesicles (arrowheads). Immediately distal to the site of swelling and disconnection, myelinated axonal debris (panel 7C) is seen. Within this disconnected segment, granular amorphous content is seen within the myelinated axonal cylinder. (Panel A&B Bar = 1 μm; Panel C Bar = 2 μm)

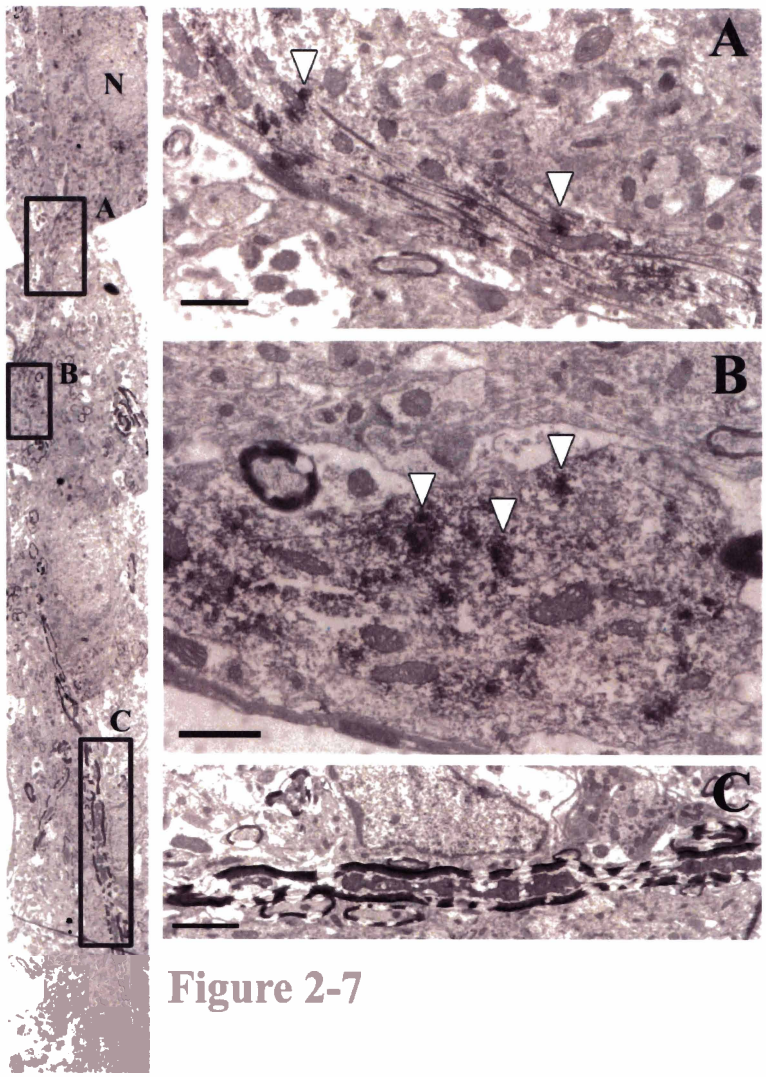

Figure 2-7

Wallerian change (Fig. 2-6). In contrast to earlier time points, all distal disconnected axonal segments now displayed evidence of pathological change that included axonal fragmentation and vacuolization together with myelin disruption and separation, pathologies consistent with Wallerian degeneration (Fig. 2-5B&C). The most distal portions that could be identified revealed the loss of their intra-axonal components with electron-dense amorphous precipitate observed within intact axonal cylinders (Fig. 2-7C). These events again occurred at the initial axonal segment although infrequent internodal involvement was also recognized. As in earlier time points, these processes occurred without evidence of tissue tearing; however, these perisomatic axonal changes were now associated with local glial swelling and perivascular edema (Fig. 2-5).

Tracer studies

As noted, an extracellular tracer was used to assess the potential for traumatically induced axolemmal failure as a prelude to swelling development and axotomy. Additionally, following axonal disconnection, the tracer also provided the added advantage of offering insight into the process of axonal disconnection and potential membrane resealing. To explore these issues, confocal microscopy was employed to examine fluorescently-conjugated 10 kDa dextran co-localized with APP immunofluorescence.

In sham-injured tissue, APP immunofluorescence was identical to that described by routine enzyme-linked LM immunohistochemistry. Limited somatic immunofluorescence was observed with no evidence of immunoreactive axonal

swellings. Following tracer administration, its diffusion throughout the parenchyma and perivascular sleeves of the thalamus was apparent; however, there were no signs of local axonal or neuronal uptake (Fig. 2-8A). In injured tissue, APP immunofluorescence was consistent with characteristics of perisomatic TAI. As with our previous observations, select swellings were found within continuous axons while others appeared disconnected from their distal segments. Despite the dispersion of tracer throughout the thalamic parenchyma prior to injury, no axonal tracer uptake was observed at any post-injury time point. Further, there was no co-localization of tracer and APP immunofluorescence at sites of axotomy identified by APP positive axonal swellings lacking distal immunofluorescence (Fig. 2-8B). These findings suggested that perisomatic TAI pathogenesis occurred not only independent of overt alterations of axolemmal permeability but also that rapid axolemmal resealing or disconnection with membrane closure occurred with axotomy. Consistent with previous reports from our laboratory (Singleton and Povlishock, 2004), isolated somatic flooding was observed following injury; however, this somatic flooding was consistently independent of perisomatic TAI pathology with the caveat that the tracer entered these neuronal somata via defects in their plasmalemmae.

Discussion

The results of this communication reveal, for the first time, the pathogenesis of DBI-mediated perisomatic TAI with concomitant secondary axotomy and Wallerian degeneration following moderate cFPI. Using a well-documented antibody marker of

Fig. 2-8. This confocal microscopic image illustrates that thalamic perisomatic TAI occurs independently of overt alterations in axolemmal permeability. At 180 min post-injury, panel 8A is from a sham-injured animal receiving pre-injury extracellular tracer. Note that the 10 kDa dextran (green) can be seen within the perivascular sleeves (arrowheads) and surrounding parenchyma, while the APP immunoreactivity (red) is limited to neuronal somata. In panel 8B, a perisomatic axonal swelling (double arrowhead) can be traced to its sustaining soma. Swellings (double and triple arrowheads) are surrounded by, but independent of, somatic flooding (single arrowheads). Lack of dextran - APP co-localization at the site of swelling and disconnection suggests either axolemmal sealing prior to disconnection or ultra-rapid membrane resealing following axotomy. (Bar = 40 μm)

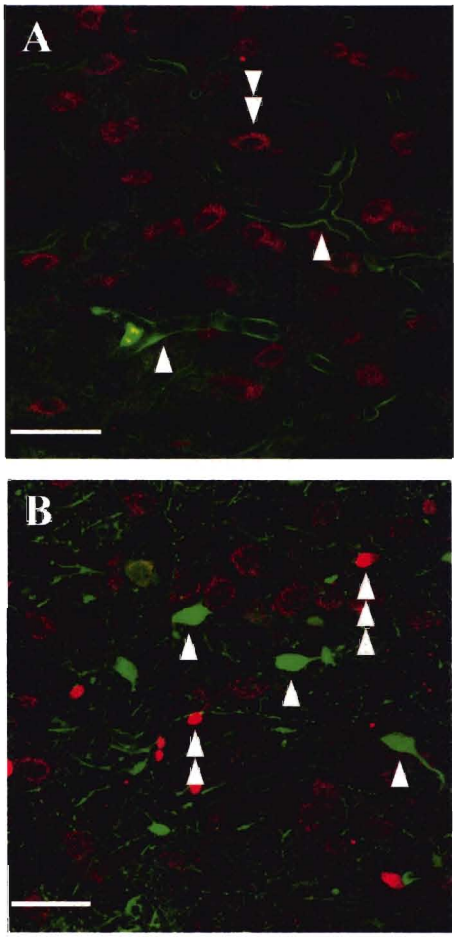

Figure 2-8

impaired axonal transport (Stone et al., 2000), secondary axotomy and disconnection at the site of injury were seen within the thalamus as early as 15 min post-injury, without evidence of axonal tearing or related parenchymal disruption. Wallerian change associated with the loss of axoplasmic constituents and ultrastructural integrity occurred within the axonal segment distal to the site of disconnection by 60 - 180 min and was accompanied by evidence of local edema and reactive glial change. The parallel exclusion of 10 kDa dextrans from the site of this progressive axonal response to injury demonstrated that perisomatic TAI was not accompanied by overt alterations in axolemmal permeability. Analysis of the temporal progression of perisomatic TAI revealed an increase in axonal swelling diameter over time with the suggestion of a maximal swelling diameter at 60 - 180 min post-injury. Additionally, the finding of modest numbers of small swellings at 60 min post-injury indicated that few *de novo* axonal swellings occurred in the later phases of injury. Taken together, these findings indicate that axonal injury, swelling, and detachment occur rapidly following traumatic insult and that this progressive change occurs only within those fibers injured at the moment of traumatic injury without delayed recruitment via secondary injury mechanisms.

While others have explored TAI within the thalamus following parasagittal FPI, these evaluations were initiated at 24 hrs post-injury in contrast to the much earlier evaluations reported here (Bramlett et al., 1997). Further, previous studies from our laboratory also demonstrated the occurrence of bilateral perisomatic TAI in the thalamus following cFPI (Singleton et al., 2002). Yet, these studies neither evaluated

the spatiotemporal progression of the TAI nor examined the related axonal ultrastructural responses and/or any related axolemmal permeability change. It was assumed that the repertoire of injury-induced change occurring within these perisomatic axonal domains paralleled that previously described in the brainstem wherein focal altered axolemmal permeability, neurofilament misalignment and compaction, microtubule loss, mitochondrial swelling, and secondary axotomy typically took place over several hours post-injury (Pettus et al., 1994; Pettus and Povlishock, 1996). While components of perisomatic TAI pathobiology parallel brainstem TAI in terms of neurofilament / microtubule pathology and focal impairment of axonal transport reflected in organelle and mitochondrial pooling, several aspects of perisomatic TAI pathogenesis appear unique.

While the initiating processes of TAI-related pathology have been documented as early as 5 - 30 min following injury, its progression to disconnection in brainstem axons has been typically described over a several hour period (Pettus et al., 1994; Povlishock et al., 1997; Maxwell and Graham, 1997; Maxwell et al., 1999). However, this timeframe within brainstem axons was not comparable to that seen within thalamic perisomatic TAI wherein the ultra-rapid progression of axonal swelling and disconnection represent an unexpected and novel finding. The reason for these differences between perisomatic and long tract brainstem fibers is unclear; however, it may be related to multiple factors. In contrast to brainstem TAI that is found primarily within the major ascending and descending white matter tracts remote from their cell bodies of origin, perisomatic TAI is found at the gray-white matter interface within the

neocortex and thalamus, areas subjected to increased shearing during trauma, rendering this locus selectively vulnerable to axonal injury (Smith et al., 1997; Meythaler et al., 2001). Of additional relevance, the perisomatic injury typically occurred at or near the initial segment of the axon prior to the initiation of the myelin sheath (Conradi, 1969). Here the axon would be exposed to the forces of injury which could act on the unprotected axolemma causing transient membrane perturbation with calcium influx and the precipitation of calcium-mediated proteolytic pathways (Singleton et al., 2002). Although 10 kDa dextran passage was not observed at this site, this does not preclude the possibility of a more subtle membrane perturbation, allowing for calcium ion influx with the exclusion of higher molecular weight species. Alternatively, an alteration of sodium channels at the initial segment could also allow for traumatically-induced abnormal sodium influx, triggering voltage-gated calcium channel opening and a reversal of sodium-calcium exchange, leading to pathologically elevated intra-axonal calcium concentrations (LoPachin and Lehning, 1997; Wolf et al., 2001).

In the current study, it is of note that no focal axolemmal permeability alterations to the extracellularly applied 10 kDa dextrans occurred following perisomatic axotomy. These observations contrast with previous findings in the brainstem where focal axonal flooding with a relatively large molecular weight species (horseradish peroxidase; 44 kDa) has been described as early as 5 min post-injury (Pettus et al., 1994). In this regard, our observations are more consistent with Smith et al. who, using *in vitro* dynamic stretch injury, demonstrated that axonal injury occurred independent of 570 Da dye uptake (Smith et al., 1999). Complicating this issue is the *in*

vivo work of Stone et al. who suggested that impaired axonal transport and altered axolemmal permeability occurred within different populations of axons following TBI (Stone et al., 2004) suggesting that not all injured axons demonstrate axolemmal permeability change, at least to the relatively large molecular weight tracers used. Conceivably, the axonal tracer flooding previously described within the brainstem may delineate the more severe forms of TAI. Perhaps, the perisomatically injured axons assessed in this study undergo more subtle pathological alterations of their axolemmae allowing for focal ion (e.g. calcium, sodium) influx, resulting in localized cytoskeletal pathology and impaired axonal transport.

Not only did this study fail to demonstrate any acute axolemmal permeability changes to the tracer used but also, there was no evidence of tracer influx even in the face of focal axonal swelling and disconnection. To date, virtually no information exists concerning axolemmal resealing / repair following DBI-mediated axotomy. A recent study examining transection-mediated CNS axon resealing, a paradigm quite dissimilar from DBI, suggested delayed resealing (Ahmed et al., 2001). Work in non-neuronal cells has demonstrated that the membrane resealing following injury involves calcium-mediated vesicular fusion, with the observation that membrane integrity can be reestablished within seconds following injury (Terasaki et al., 1997; McNeil and Baker, 2001). In the current study, despite tracer dispersion within the thalamic parenchyma prior to injury, there was no co-localization of dextran and APP immunofluoresence within the swellings, suggesting that either axolemmal sealing occurred prior to disconnection or that ultra-rapid membrane closure followed axotomy. The fact that we

observed disconnected axonal swellings consistently enclosed by an intact axolemma supports both possibilities. Thus, further studies targeting the axolemmal components involved in membrane resealing / repair following secondary axotomy are needed to decipher these complex biological issues.

In addition to the above described rapid progression of axonal swelling and disconnection, the current study also provided unique information into the precise sequence of Wallerian change triggered by this observed axonal pathology. Like the processes of swelling and disconnection, the onset of Wallerian change was also rapid in contrast to that described in the existing literature. Classic descriptions of Wallerian change in the CNS of humans and higher order animals describe a process that is slow to evolve and persists for months to years post-injury (Strich, 1968; Becerra et al., 1995; Buss et al., 2004). Even in lower order animals and rodent models of TAI, this process is much more delayed than described in the current communication. Maxwell et al. provided the first ultrastructural evidence of Wallerian degeneration in the post-acute (> 1 day) timeframe using an optic nerve stretch injury model of TAI (Maxwell et al., 2003). Similar to our findings, they reported altered ultrastructural morphologies including lucent, abnormal mitochondria within injured axons, the separation of the myelin lamellae, as well as amorphous content, flocculent precipitate, and lack of axoplasmic organelles within the axonal segment distal to the swelling. However, the timeframe during which these findings were described was different from the current communication. Maxwell reported initial evidence of Wallerian change at 24 hrs post-injury; yet, our data suggests the onset of Wallerian change by 60 - 180 min. While

different injury models may account for this time discrepancy, this issue requires continued investigation.

Finally, an important question remains regarding the implications of the above findings to our previous observations that the occurrence of perisomatic axotomy did not elicit rapid neuronal death (Singleton et al., 2002) as had been suggested by previous transection paradigms (Barron, 1983; Kreutzberg, 1995). We had assumed that this finding was related to the likelihood that, similar to the long tract axons within the brainstem, a slowly progressive axotomy within the perisomatic domain would shield the related soma from rapid exposure to the ionic dysregulation and its adverse consequences typically associated with physical transection models. In this context, our finding of rapid disconnection was unanticipated and initially suggested that our previous beliefs regarding subsequent cell death or survival were incorrect. However, despite the rapidity of the detachment observed in the current communication, the fact that detachment did not translate into rapid cell death suggests that cell death may not be directly related to the actual speed of disconnection. Rather, the fact that this disconnection occurred without related overt alterations in axolemmal permeability may constitute the more significant finding. As such, it indirectly suggests that the maintenance of membrane integrity may be pivotal to attenuating the onset of rapid neuronal death as seen with transection wherein the axon cylinder itself remains transiently yet fully exposed to the extracellular environment and its different ionic milieu.

In sum, the current communication builds on previous TAI studies and expands TAI characterization to include thalamic perisomatic TAI with ultra-rapid secondary axotomy and Wallerian degeneration within the context of DBI. Importantly, these findings have implications for preclinical studies of therapeutic interventions attempting to target pathological mechanisms during the delay prior to axonal swelling and disconnection, a goal that may ultimately prove unattainable in the perisomatic domain. This study again illustrates the complexity of TAI pathobiology and provides the impetus for future studies of neuronal membrane repair mechanisms and potential recovery following traumatic brain injury.

ADDENDUM TO CHAPTER TWO

Having evaluated the acute phase of perisomatic TAI pathogenesis, additional studies were undertaken to examine the long-term fate of these injured neurons. A previous study by Singleton and colleagues demonstrated that neurons injured within the perisomatic domain did not progress to acute cell death (Singleton et al., 2002). Therefore, we extended our observations to 28 d post-injury and utilized stereological assessments of neuronal somatic volume as well as employed additional antibody markers of neuronal health to determine what becomes of this uniquely injured neuronal population. Neuronal measurements were taken from sham-injured tissue sections and compared to measurements taken at 1, 7, and 28 d post-injury. Our findings revealed a statistically significant decrease in tissue region and neuronal nuclear volume at each

post-injury time point when compared to sham control (article in preparation). These findings suggest neuronal atrophic changes in response to DBI.

To further clarify mechanisms related to this observation, antibodies to neuronal deafferentation / remodeling (e.g. PSD-93, PSD-95, GAP-43, synaptotagmin, synaptophysin), intracellular protein synthesis (e.g. eif-2α(P), HSP-60, HSP-70), and cell death / survival (e.g. TUNEL, Nitro-Tyr, activated caspase-3, P-Bad, cyt c, PARP) were employed. While certain antibodies demonstrated immunoreactivity with regions of TAI pathology (e.g. eif-2α(P), HSP-70) that were consistent with previous communications from our laboratory (Singleton et al., 2002), the remaining antibodies failed to demonstrate compelling evidence linking perisomatic TAI to their respective mechanisms of action.

Given the atrophic but apparently non-lethal neuronal response to perisomatic TAI, we then examined the corresponding microglia / macrophage responses within diffuse injured brain regions to provide a more comprehensive study of DBI and its related pathological sequelae as well as to compare / contrast this response to the inflammatory response following focal TBI. Chapter 3 will outline the neuroinflammatory response within specific anatomical loci known to elicit DBI-mediated TAI and uncomplicated by focal pathology. The relationship between inflammatory cells and injured neurons will be discussed as will implications for the use of neuroinflammatory responses as markers for DBI-mediated axonal pathology.

Chapter 3

NEUROINFLAMMATORY RESPONSES TO DIFFUSE TRAUMATIC BRAIN INJURY

Introduction

The immune response to traumatic brain injury (TBI) involves microglia as well as leukocytes recruited from the surrounding vasculature. To date, this immunological response has been studied most extensively in the context of focal TBI despite the fact that diffuse TBI remains the most significant component of the morbidity associated with traumatic injury. Focal injuries, often associated with blunt force trauma, are associated with cerebral contusions and hematomas while diffuse injuries, a common result of motor vehicle accidents, depend on inertial forces and result in more subtle scattered microscopic pathology. To date, the immune cell responses to experimental focal brain injury have been studied extensively (Persson, 1976; Giulian et al., 1989; Clark et al., 1994; Mathew et al., 1994; Hermann et al., 2000; Chen et al., 2003). Additionally, limited studies have documented generalized immune cell responses to diffuse brain injury (DBI) (Oehmichen et al., 1999; Csuka et al., 2000), yet both clinical and experimental studies have been typically complicated by focal brain contusion and related hemorrhagic components

(Aihara et al., 1995; Soares et al., 1995; Carbonell and Grady, 1999) thereby allowing leukocytes to enter the injured brain parenchyma via the overt disruption of the blood-brain barrier (BBB). This contusion-related BBB disruption also permitted the unregulated passage of stimulatory molecules from the vasculature complicating the evaluation of glial activation.

Fortunately, in the experimental setting other animal models have been developed to minimize the potential for contusion and/or hemorrhage while maintaining many of the important features of diffuse TBI, including diffuse axonal injury (DAI) and its subsequent anterograde and retrograde consequences. Specifically, the use of midline/central fluid percussion injury (cFPI) in the rat allows for the generation of traumatic axonal injury (TAI), the experimental counterpart of DAI, characterized by the focal impairment of axonal transport leading to progressive axonal swelling and secondary axotomy (Povlishock, 1992; Pettus and Povlishock, 1996; Povlishock and Pettus, 1996; Okonkwo et al., 1998). Moderately severe cFPI can induce perisomatic TAI (i.e. within 40-60 μm of the sustaining soma) allowing for the critical assessment of both the retrograde neuronal somatic responses to injury as well as specific anterograde / Wallerian responses as outlined in Chapter 2 (Singleton et al., 2002). Using this model, TAI has been observed scattered within various anatomical loci, including the mediodorsal neocortex, hippocampal dentate gyrus, and dorsolateral thalamus without any associated contusions and/or hemorrhagic-mediated tissue damage. These factors provided the opportunity to explore microglial / macrophage

responses within diffusely injured brain regions uncomplicated by focal brain pathology.

The present study provides immunocytochemical light, electron, and confocal microscopic characterization of the immune responses to DBI in the absence of focal tissue damage. Microglia within brain loci revealing TAI responded rapidly, albeit in an initially uncoordinated fashion, via changes in their cellular morphology. This was followed by their persistent activation and phagocytic activity. In contrast, the microglia observed in non-TAI containing regions maintained a resting phenotype. Macrophages displayed similar spatiotemporal responses to DBI and its associated TAI. Select macrophages approximated scattered somata of traumatically injured neurons showing evidence of somatic bouton disruption and loss. Taken together, these findings suggest that neuroinflammatory responses to DBI with TAI may be distinct from those related to more focal TBI pathology. These findings may have implications for post-mortem histopathological evaluation of TBI and its characterization based upon specific microglial / macrophage responses.

Materials and Methods

Animal preparation and injury

To explore microglial / macrophage responses to DBI, animals were subjected to moderate cFPI consistent with methods described previously (Dixon et al., 1987; Singleton et al., 2002). Adult male Sprague Dawley rats (375 - 400 gm) were anesthetized with 4% isoflurane in 70% N_2O and 30% O_2, intubated, and maintained on

a ventilator with 1-2% isoflurane for injury preparation. Intubated animals were placed on a heating pad connected to a thermostat controlled by a rectal probe (Harvard Apparatus, Holliston, MA) to maintain 37°C body temperature. To prepare the animal for cFPI, the top portion of a Leur-Loc syringe hub of a 20 gauge needle, two fixation screws, and dental acrylic were fixed to a midline craniotomy in the skull over the intact dura and then connected to the injury device. Briefly, a 4.8mm circular craniotomy along the sagittal suture midway between bregma and lambda was generated taking care not to disrupt the underlying dura and superior sagittal sinus. The top portion of the Leur-Loc hub (Becton Dickinson, Franklin Lakes, NJ) was cut away from the 20 gauge needle, beveled, scored, and affixed over the craniotomy site using cyanoacrylate. After confirming the integrity of the seal between the hub and the skull, fixation screws were inserted into 1mm holes drilled into the right frontal and occipital bones. Dental acrylic (Hygenic Corp., Akron, OH) was applied around the hub and over the screws and allowed to harden to provide stability during the injury induction. After the dental acrylic hardened, the skin was closed over the hub with sutures, topical Lidocaine ointment was applied, and the animal was removed from anesthesia and monitored in a warmed cage until fully recovered (~ 1 hr).

Prior to injury, each animal was again anesthetized with isoflurane. The incision was quickly opened and the male end of a spacing tube was inserted into the Leur-Loc hub. The female end of the spacer-hub assembly, filled with normal saline, was then inserted onto the male end of the fluid percussion device, ensuring that no air bubbles were introduced into the system. A ~ 2.1 atmosphere (1.9 – 2.3 atm) injury was

administered, consistent with brain injury of moderate severity (Dixon et al., 1987). Injury preparation and induction were completed prior to the animal's recovery from anesthesia. Following injury, the spacer-hub assembly was immediately removed *en bloc*, bleeding was controlled with Gelfoam (Parmacia, Kalamazoo, MI), and the incision was closed with sutures. Animals were monitored for spontaneous respiration and, if necessary, ventilated with room air to ensure adequate post-injury oxygenation. Post-injury recovery times for the following reflexes were recorded: toe pinch, tail pinch, corneal blink, pinnal, and righting. Following recovery of the righting reflex, animals were placed in a holding cage with a heating pad to ensure maintenance of normothermia and monitored until the appropriate perfusion time. For sham-injured control animals, the above steps were followed without injury induction. All injured animals had righting reflex recovery times greater than 6 min compared to less than 2 min for sham-injured animals (data not shown). Experiments were conducted in accordance with NIH and institutional guidelines concerning the care and use of laboratory animals (IACUC).

Tissue Preparation

Animals (n = 6 / injury group, 2 / sham-injury group, and 2 naive) were euthanized at t = 6 and 24 hrs as well as 2, 7, 14, 21, and 28 days post-injury via an overdose of sodium pentobarbital IP (150 mg/kg) and transcardially perfused with 4% paraformaldehyde in Millonig's buffer for immunocytochemistry. Following perfusion, brains were removed and blocked in a coronal blocking device to include the thalamus

with overlying neocortex and hippocampus (Fig. 3-1). A previous study, as well as observations from Chapter 2, has identified TAI scattered throughout these regions, consistent with the occurrence of diffuse injury (Singleton et al., 2002). The tissue block was flat-mounted on a metal plate with cyanoacrylate, embedded in agar, and sectioned in 0.1M phosphate buffer at a thickness of 40 μm using a vibrotome (Leica Microsystems, Bannockburn, IL). Serial coronal sections (n = 60 sections at 40 μm / section) were collected starting from 1600 μm caudal to the anterior commissure. This sampling strategy allowed for a comprehensive examination of the neocortex, hippocampus, and thalamus (Paxinos and Watson, 1986). Systematic uniform sampling of coronal sections was employed with every fifth section collected for a total of twelve sections per animal. Additional tissue was stored in Millonig's buffer in 12-well culture plates (Falcon, Newark, DE).

Immunocytochemistry for confocal microscopy

Double-labeling strategies were employed to permit simultaneous visualization of microglia / macrophages and TAI, a key feature of diffuse TBI. To label microglia, tissue sections were incubated overnight with lectin (Alexa 488 conjugated isolectin B4 from *Griffonia simplicifolia* (5 μg/ml); Molecular Probes, Eugene, OR) in 20% normal horse serum (NHS) in artificial cerebrospinal fluid (aCSF: 126 mM NaCl, 3 mM KCl, 1.25 mM NaH_2PO_4, 2 mM $MgCl_2$, 2 mM $CaCl_2$, 10 mM glucose buffered with 26 mM $NaHCO_3$) consistent with previously described methods (Dailey and Waite, 1999; Stence et al., 2001; Grossmann et al., 2002; Carbonell et al., 2005). TAI was then

Fig. 3-1. The low-magnification microphotograph is provided to orient the reader to the diffusely injured brain loci revealing significant TAI that is uncomplicated by focal pathology; A: mediodorsal neocortex, B: hippocampal dentate gyrus, C: dorsolateral thalamus. Activated microglia and macrophages were localized to these areas following diffuse brain injury. In contrast, asterisks delineate related regions also sampled in the current investigation that did not contain significant TAI or other forms of overt pathology.

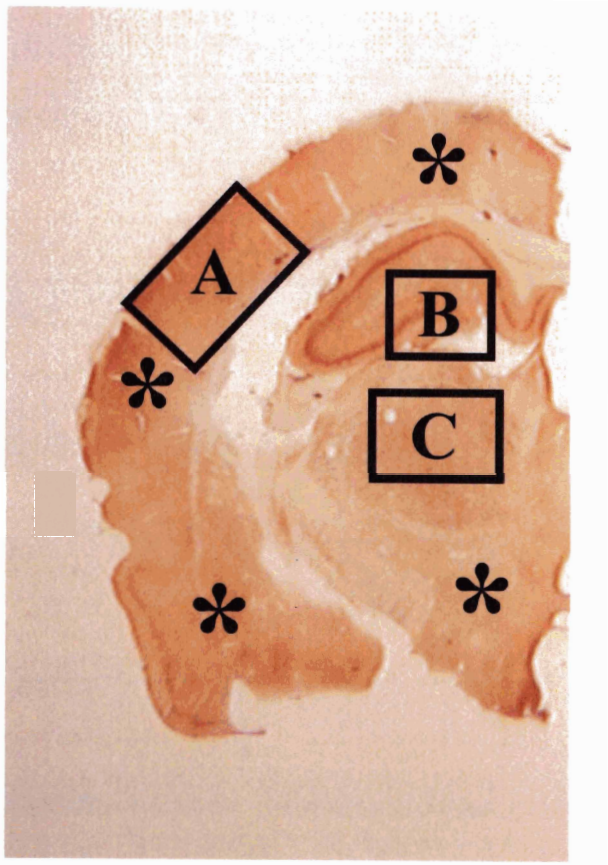

Figure 3-1

visualized using antibody to the amyloid precursor protein (APP) as described below. APP moves via anterograde transport and pools at sites of impaired axonal transport thus serving as a marker of TAI (Stone et al., 2000). To ensure maintenance of lectin binding, all steps of the lectin - APP double-labeling procedure were conducted in aCSF.

To label macrophages, sections were first preincubated for 60 min in 10% NHS with 0.2% Triton X-100 in phosphate buffered saline (PBS) and then incubated overnight with macrophage (1:2000; mouse anti-rat CD68 (ED1); Serotec, Oxford, England) primary antibody in 1% NHS in PBS / 2% bovine serum albumin (BSA). After removal of the antibody solution, sections were rinsed and incubated for 2 hrs in Alexa 488 goat anti-mouse IgG (1:1000; Molecular Probes) with 1% NHS in PBS / 2% BSA prior to processing for TAI.

For labeling TAI, sections were rinsed and incubated with 10% normal goat serum (NGS) in PBS (except for lectin – APP processing which used aCSF) for 45 min followed by an overnight incubation in C-terminus specific APP primary antibody (1:1000; rabbit anti-C-APP; Zymed, San Francisco, CA) with 1% NGS in PBS. Sections were then rinsed and incubated for 2 hrs with Alexa 594 goat anti-rabbit IgG (1:1000; Molecular Probes) in 1% NGS in PBS. Sections were rinsed six times in PBS for 5 min and twice in 0.1M phosphate buffer for 10 min. Following these rinses, sections were mounted on gelatin-coated slides. Sections were mounted with an anti-fade mounting media (ProLong; Molecular Probes), coverslipped, and sealed with nail polish. As an internal control, additional sections were processed as described above;

however, primary antibodies were omitted from the procedure. Images were captured using a confocal microscope (Leica TCS-SP2 AOBS; Leica Microsystems, Bannockburn, IL) with appropriate excitation lasers, detectors, and analysis software.

Immunocytochemistry for routine light and electron microscopy

In these protocols, sections were processed with antibodies to either CD11b/c (microglia) or CD68 (macrophages) alone or together with antibodies to APP to detect diffusely injured axons. CD11b/c antibody recognizes the microglia-specific complement type 3 receptor thus serving as a complementary marker to lectin. In addition to these approaches, adjacent brain sections were processed with antibodies to endogenous rat albumin. This was done to assess the potential for injury-induced BBB disruption. Animals for LM and EM evaluation (n = 3 / injury group, 1 / sham-injury group, 1 naive) were perfused with 4% paraformaldehyde / 0.1% glutaraldehyde in Millonig's buffer. Sections were then processed for either CD 11b/c, CD 68, and albumin or CD11b/c – APP and CD68 – APP dual immunoreactivity.(Stone et al., 2000) Briefly, endogenous peroxidase activity was blocked using 0.3% H_2O_2 in PBS for 30 min followed by temperature-controlled modified microwave antigen retrieval (Stone et al., 1999) and preincubation in 10% NGS with 0.2% Triton X-100. Sections were incubated overnight with either CD11b/c (1:700; mouse anti-rat CD11b/c; BD Pharmingen, San Diego, CA) or CD68 (1:700) primary antibody. Sections were then incubated for 1 hr with biotinylated rat-absorbed goat anti-mouse IgG (1:200 Vector, Burlington, CA) secondary antibody. Select sections for dual-labeling underwent

additional processing beginning with preincubation in 10% NGS followed by C-terminus specific APP (1:1000) primary antibody. At this time, sections for single-label albumin (1:40,000; rabbit anti-rat albumin antiserum; Bethyl Laboratories, Montgomery, TX) primary antibodies were also processed in 1% NGS in PBS. Sections processed with APP or albumin antibodies were then incubated for 1 hr with biotinylated rat-absorbed goat anti-rabbit IgG (1:200 Vector). All sections were then visualized via incubation in avidin-horseradish peroxidase complex (Vectastain ABC Standard Elite Kit; Vector) for 1 hr followed by 0.05% diaminobenzidine (DAB), 0.01% H_2O_2, and 0.3% imidazole in 0.1M phosphate buffer for 10-20 min. The common chromogen DAB was used for convenience in that structural correlates of BBB disruption, axonal injury, and microglial / macrophage change were so discreet as to create no problem in morphological recognition. Sections processed for either CD 11b/c, CD 68, or albumin as well as select sections processed for CD 11b/c – APP and CD 68 – APP were mounted on gelatin-coated slides, dehydrated, and coverslipped for routine LM evaluation while the remaining dual-labeled sections underwent continued processing for EM. As an internal control, additional sections were processed as described above; however, primary antibodies were omitted from the procedure. LM images were captured using an Eclipse 800 microscope (Nikon, Tokyo, Japan) fitted with a Spot-RT digital camera (Diagnostic Instruments, Sterling Heights, MI).

As noted, dual-labeled sections were processed for EM to ascertain ultrastructural detail relevant to those changes observed via confocal microscopy. Following antibody processing, the tissue was osmicated in 1% OsO_4 and then placed in

graded alcohols and propylene oxide prior to placement in epoxy resin (Ted Pella, Redding, CA). Sections were then embedded between plastic slides (Thomas Scientific Co., Swedesboro, NJ), placed in 55°C oven for 3 days, and then scanned to identify immunoreactive axonal swellings along with microglia / macrophages. Once identified, these sites were removed, mounted onto plastic studs, and thick sectioned to the depth of interest using an ultramicrotome (Leica Ultracut R; Wien, Austria). Semithin sections (1 μm) stained with 1% Toluidine Blue were again screened for evidence of microglial activation / macrophage localization with TAI. Serial thin sections (70 nm) were then cut, picked up onto Formvar-coated slotted grids, and stained in 5% uranyl acetate in 50% methanol for 2 min. and 0.5% lead citrate for 1 min. Images were captured using a JOEL 1230 electron microscope using a digital camera (Gatan Digital Micrograph, Pleasanton, CA).

Results

Naive and Sham-injury – General findings and cellular phenotypes

Macroscopically, sham-injured brains showed no evidence of compression, contusion, or tissue loss. Tissue sections from naive and sham-injured animals processed for the visualization of APP and examined by light and confocal microscopy demonstrated limited background staining with the finding of only isolated immunoreactive somata. There was no evidence, however, of immunoreactive axons or swellings adjacent to these somata. Markers of microglia (isolectin B4 and CD 11b/c) demonstrated conventional resting morphology in that microglia exhibited a small cell

body with highly ramified processes and were distributed evenly throughout the brain parenchyma (Fig. 3-2A-C). Sections processed for macrophage immunoreactivity (CD 68) demonstrated a limited number of immunoreactive cells primarily in perivascular locations (Fig. 3-3A-C). Sham-injured tissue sections processed for the visualization of albumin revealed only limited immunoreactivity underlying the craniotomy site together with minimal immunoreactivity within the subcortical white matter. Otherwise, albumin immunoreactivity was confined to the vascular lumen and walls with no extension into the brain parenchyma (Fig. 3-4A).

Diffuse Injury – Light, electron, and confocal microscopic findings

Injured brains shared identical macroscopic features with sham-injured brains with the exception of limited subarachnoid hemorrhage found under the craniotomy site. Additionally, scattered petechial hemorrhages could be observed within the corpus callosum.

APP Immunoreactivity

APP immunoreactive axonal swellings, a signature of diffuse TBI, were visible at 6 and 24 hrs post-injury. Consistent with previous descriptions of experimental DBI in this animal model as outlined in Chapter 2, axonal swellings were most prominent within the mediodorsal neocortex, hippocampal dentate gyrus, and dorsolateral thalamus with additional swellings found scattered in the corpus callosum, subcortical white matter, and brainstem (Singleton et al., 2002). Select swellings could be traced

Fig. 3-2. Spatiotemporal evaluation of microglia activation within DBI loci. Using antibodies to CD 11b/c, that recognize the microglia-specific complement type 3 receptor, microglial morphology was visualized within loci known to elicit DBI-mediated TAI. Note that sham-injury (A-C) reveals microglia with resting morphology characterized by a small cell body with highly ramified processes. Between 6 – 24 hrs post-injury (D-F), most microglia demonstrate the initial signs of activation including increased cell body size, with a concomitant reduction in process ramification leading to an increased immunoreactive ameboid-like morphology. However, others maintain a resting phenotype. Within DBI loci, activated morphology predominates and persists at 7 (G-I), 14 (J-L), and 28 (M-O) d post-injury. (scale bar = 100 μm)

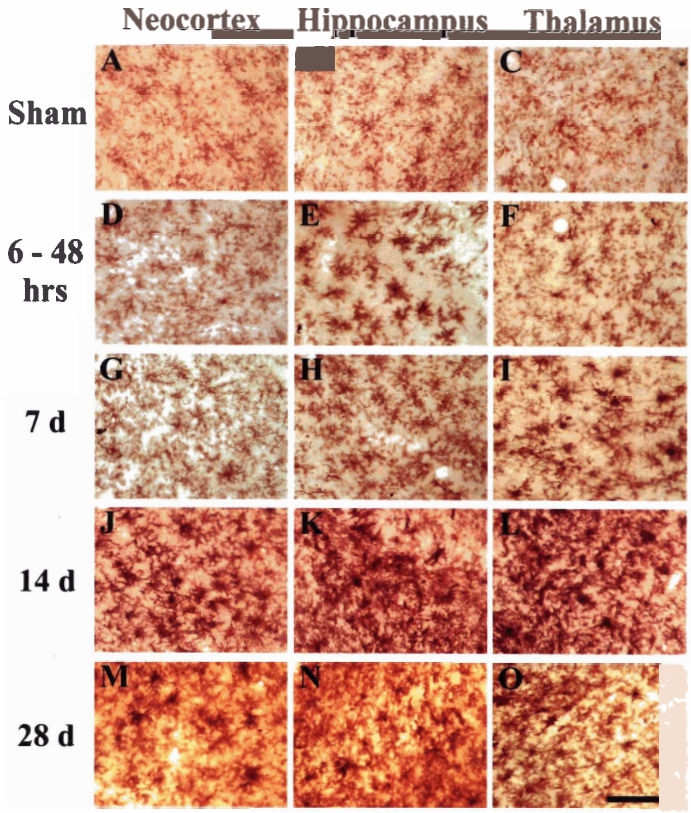
Neocortex
Hippocampus
Thalamus
Sham
6 - 48 hrs
7 d
14 d
28 d
A
C
D
E
F
G
H
I
J
K
L
M
N
O

Figure 3-2

Fig. 3-3. Spatiotemporal evaluation of macrophage localization within DBI loci. Similar to microglial evaluation, antibodies to CD 68, that recognize a macrophage-specific cell surface marker, were used to visualize macrophages within loci known to elicit DBI-mediated TAI. Sham-injury (A-C) reveals limited numbers of immunoreactive cells primarily in perivascular locales. Between 6 – 24 hrs post-injury, parenchymal macrophage immunoreactivity can be observed within the neocortex (D) and hippocampus (E) with minimal thalamic (F) involvement. However, note that by 7 d post-injury, all three regions (G-I) demonstrate robust macrophage immunoreactivity which persists at 14 (J-L) and 28 (M-O) d post-injury. (scale bar = 100 μm)

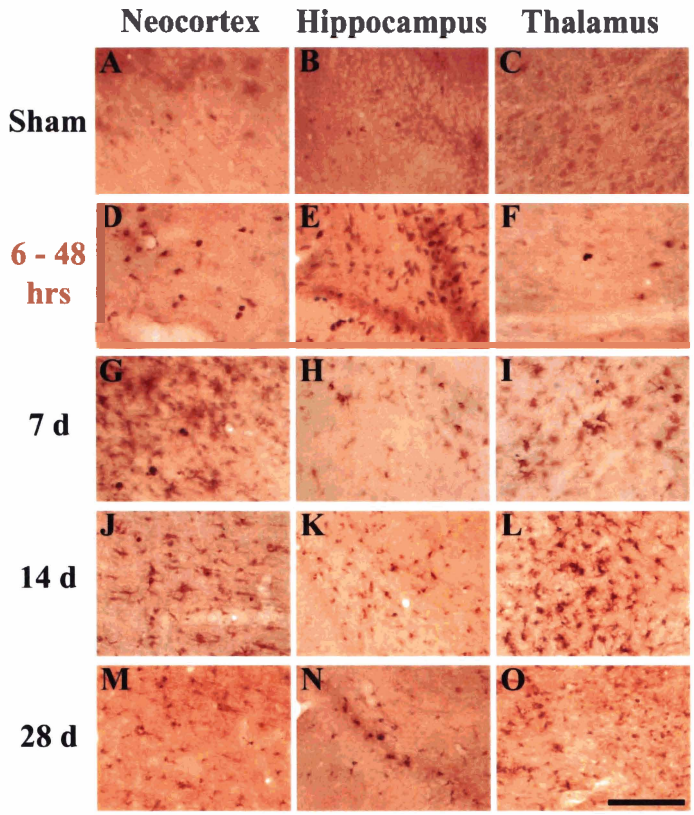
Neocortex
Hippocampus
Thalamus
Sham
6 - 48 hrs
7 d
14 d
28 d
A
B
C
D
E
F
G
H
I
J
K
L
M
N
O

Figure 3-3

Fig. 3-4. These low-magnification brain microphotographs illustrate the spatiotemporal course of albumin immunoreactivity following DBI. Note that with sham-injury, albumin is confined to the vascular walls and lumen with limited immunoreactivity observed in the subcortical white matter. However, at 6 hrs post-injury, diffuse albumin immunoreactivity is observed throughout the interstitium of the brain. By 24 hrs post-injury, scattered immunoreactivity persists within neocortical and hippocampal parenchyma while the thalamic parenchyma now reveals limited immunoreactivity. By 7 d post-injury, only minimal albumin immunoreactivity is present. At all post-injury time points, there was no evidence of contusion, hemorrhage, or overt tissue necrosis.

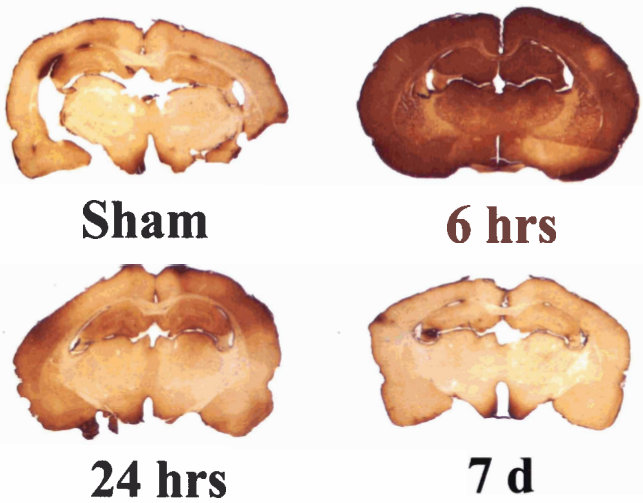

Figure 3-4

back to their somata of origin while others were found in isolation. Focal axonal swellings demonstrated no distal immunoreactivity consistent with axonal disconnection that has been previously characterized in Chapter 2. By 7 d post-injury, these immunoreactive axonal swellings were no longer visible, again consistent with previous observations (Singleton et al., 2002).

Albumin Immunoreactivity as a Marker of BBB Alteration

At 6 hrs post-injury, endogenous albumin immunoreactivity could be identified diffusely distributed throughout the interstices of the neocortex, hippocampus, and thalamus. This blood-brain disruption to the normally intravascularly confined serum albumin occurred without evidence of overt contusion, hemorrhage, or tissue disruption (Fig. 3-4B). By 24 – 48 hrs post-injury, scattered albumin immunoreactivity persisted within the interstices of the neocortex and hippocampus while the thalamus now revealed limited immunoreactivity again confined to the extracellular compartment (Fig. 3-4C). By 7 d post-injury, only minimal albumin immunoreactivity was evident with the tissue now appearing reminiscent of that obtained from sham-injured animals (Fig. 3-4D).

Microglia / Macrophage Responses to DBI

Having evaluated the 6 and 24 h as well as 2 d post-injury time points, observations from these tissue sections revealed comparable findings. These findings, however, differed significantly from findings observed between 7 – 28 d post-injury.

Therefore, observations are grouped as post-acute (6 – 48 h post-injury) and longer-term (7 – 28 d post-injury) to provide clarity and to highlight responses within these post-injury time frames.

Post-acute Neuroinflammatory Responses

At 6 – 24 hrs post-injury, LM and confocal evaluation revealed scattered immunoreactive microglia within the mediodorsal neocortex, hippocampal dentate gyrus, and dorsolateral thalamus that maintained highly ramified processes consistent with a resting phenotype. Other scattered microglia demonstrated reduced immunoreactivity within their processes together with rounding of their cell bodies, all of which were suggestive of the initial stages of activation (Fig. 3-2D-F). Microglia found scattered among diffusely injured axons did not show any consistent spatial relationship to the axonal swellings, their proximal axonal shafts, or their downstream disconnected axonal segments that now revealed early anterograde change. In contrast to those microglia found within these diffusely injured loci, microglia within the adjoining parenchyma wherein no axonal swellings could be found, maintained a resting morphology.

At the EM level, microglia were identified via the presence of an electron-dense CD 11b/c reaction product that outlined their cell membranes. The resting and activated microglial ultrastructural features were similar although the resting cells displayed highly ramified appendages, while activated cells revealed enlarged, amoeboid-like cell membranes. The microglia contained a prominent, round nucleus with heterogeneous

chromatin clumps beneath the nuclear envelope. Their cytoplasm revealed granular endoplasmic reticulum with long, narrow cisternae extending through the cytoplasm. Mitochondria together with electron dense laminar bodies as well as inclusion bodies characteristic of lipofuscin were also distributed throughout the cytoplasm. Despite axonal injury, no specific microglia – axonal associations could be discerned within the above described loci. Activated microglia did not directly approximate either the axonal swellings or their proximal / distal axonal segments (Fig. 3-5).

In the 6 – 24 h time frame, immunoreactive tissue macrophages could also be identified by LM and confocal microscopy. These cells were localized to the neocortical and hippocampal parenchyma at 6 hrs post-injury without thalamic involvement (Fig 3-3D-E). The adjoining, non-TAI containing brain regions revealed no parenchymal macrophage immunoreactivity. In all cases, macrophage morphology was similar to that observed in sham-injured tissue. Within the neocortex, the macrophages displayed a graded parenchymal distribution; heavier macrophage concentrations occurred in the superficial cortex abutting the subarachnoid space, with increasingly reduced concentrations seen in the deeper cortical layers. In contrast, the hippocampal macrophage distribution was more heterogeneous in that cells were found evenly scattered throughout the hippocampal region. While diffusely distributed within these loci, macrophages were not associated with any component of axonal injury. EM evaluation of macrophage ultrastructure, via CD 68 electron-dense reaction product membrane deposition, was comparable to that of activated microglia and confirmed no axonal associations.

Fig. 3-5. Electron micrograph of the dorsolateral thalamus at 6 – 24 hrs post-injury. Dual-label antibody processing for microglia (CD 11b/c) and TAI (APP) was employed although both appear electron dense at the EM level. Note that electron-dense reaction product and distinct ultrastructural morphology allow for identification of both the microglia and reactive axons. Activated microglial ultrastructure (single asterisk) demonstrates an ameboid-like membrane, ringed with an electron-dense CD 11b/c reaction product. Also note the prominent round nucleus with heterogeneous chromatin clumps beneath the nuclear envelope and granular endoplasmic reticulum with long, narrow cisternae extending through the cytoplasm. Electron-dense laminar bodies as well as inclusion bodies characteristic of lipofuscin can also be seen distributed throughout the cytoplasm. TAI (double asterisk) is characterized by axonal swellings containing electron-dense APP reaction product, organelle pooling, neurofilament misalignment, and microtubule loss. Additionally, more advanced axonal pathology (arrow) is found within this field. In this image, the microglia approximates the axonal swelling yet does not directly engage it, confirming LM and confocal impressions. Note that microglia are often separated from sites of axonal injury by glial swellings. (scale bar = 2 μm)

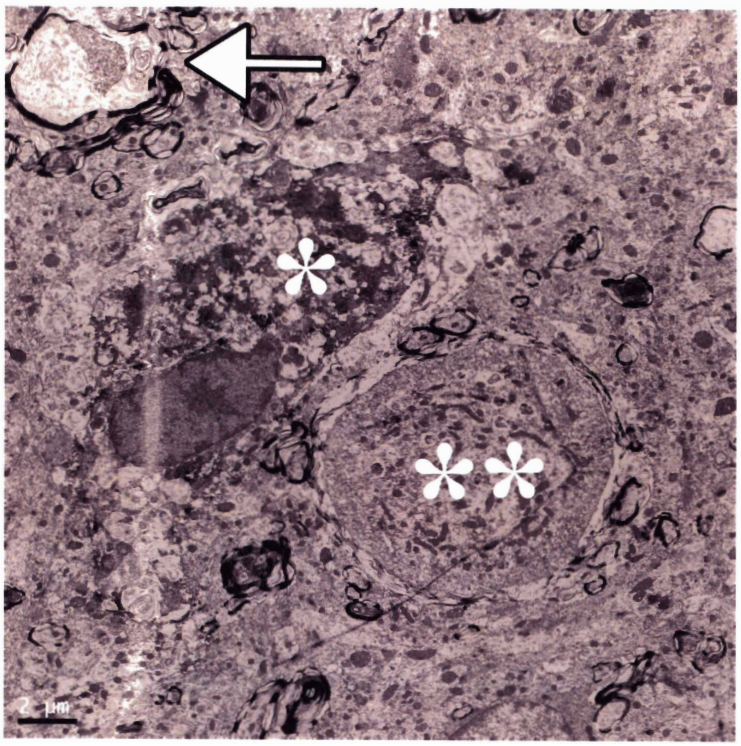

Figure 3-5

By 24 – 48 hrs post-injury, microglial immunoreactivity within the above described loci again revealed resting and activated phenotypes while microglia within adjoining, non-TAI containing parenchyma still maintained a resting morphology.

Within the brain sites revealing diffuse TAI, activated microglia appeared more numerous than previously seen. The activated microglia demonstrated reduced branch ramification and more intense immunoreactive amoeboid-like morphology. Despite enhanced activation, there was still no evidence of direct microglial engagement of the traumatically injured axons, similar to observations made at the earlier post-injury time point (Fig. 3-6). While activated microglial morphology now predominated within injured loci, additional microglia adopted a lengthened morphology. This suggested a redistribution of their processes consistent with potential migration (Fig. 3-7). EM evaluation revealed activated microglia within injured loci scattered among sites of axonal injury characterized by electron-dense APP reaction product, organelle pooling, neurofilament misalignment, and microtubule loss (Fig. 3-5). However, there was no evidence of microglial projections or engulfment of these sites of injury and reactive change. In fact, glial swellings often separated microglia from sites of axonal injury.

LM and confocal microscopy also revealed macrophage immunoreactivity that persisted within neocortical and hippocampal parenchyma, with scattered thalamic immunoreactivity now recognized at 24 – 48 hrs post-injury (Fig. 3-3F). While numerous macrophages were found in isolation scattered throughout these brain loci, occasional macrophages could now be recognized approximating the somata of perisomatically axotomized neurons, particularly those within the neocortex (Fig. 3-8).

Fig. 3-6. This figure is a confocal micrograph of the dorsolateral thalamus at 24 hrs post-injury following double-label antibody processing for microglia and TAI. Microglia (isolectin B4; green - double arrowheads) and TAI (APP; red - single arrowheads) were identified to assess potential interactions between inflammatory cells and TAI, a key characteristic of DBI. Note that while microglial activation and DBI-mediated TAI pathogenesis share a spatiotemporal relationship, there is no evidence of direct microglial association with any component of injured axons at this post-injury time point. Although activated microglia can be seen scattered among traumatically injured axons, no direct engagement of these fibers occurs. (scale bar = 20 μm; Note: Isolectin also binds blood vessels (BV).)

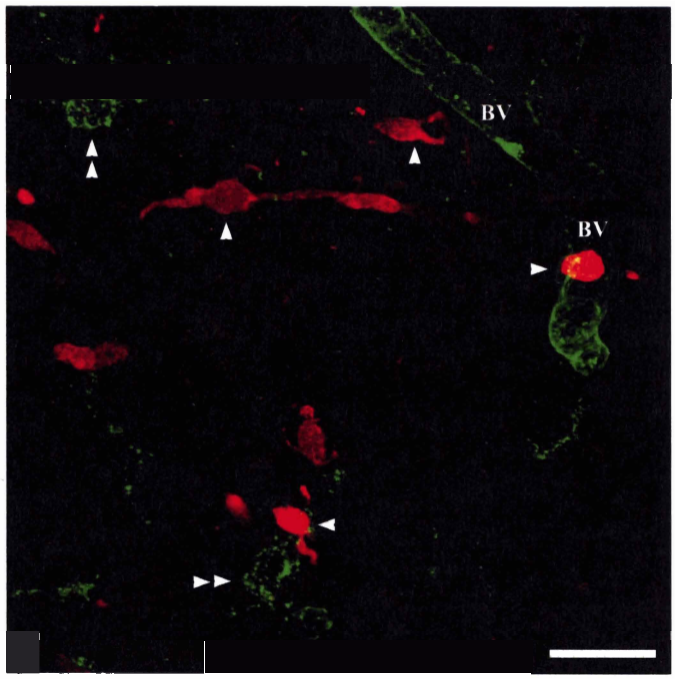

Figure 3-6

Fig. 3-7. This figure reveals a confocal micrograph of microglia processed with Alexa-488 conjugated isolectin B4 antibodies at 24 hrs post-injury. While most microglia within DBI loci adopt activated phenotypes (arrows), select cells now reduce their ramified processes and redistribute them in an elongated fashion (arrowheads). The generation of apparent forward and trailing processes suggests potential migration although fixation of tissue prior to immunocytological processing made definitive evaluation of this migration difficult. (scale bar = 20 μm)

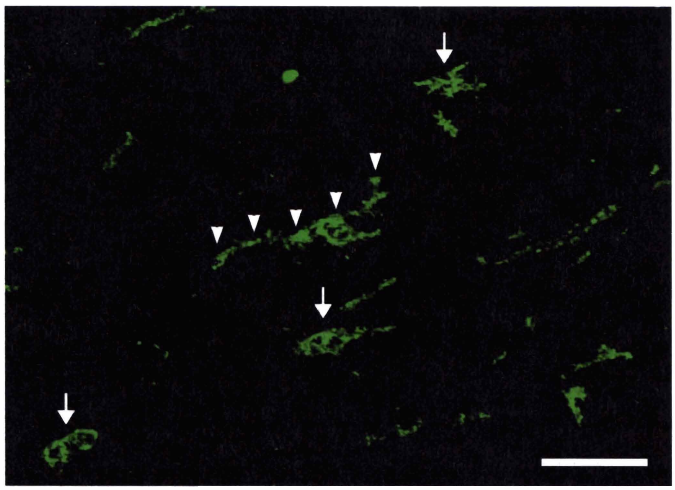

Figure 3-7

Fig. 3-8. Confocal micrograph of the mediodorsal neocortex at 24 hrs post-injury. Double-label antibody processing for macrophages (CD 68 - green) and TAI (APP - red) were used to examine potential immune cell – neuron interactions following DBI. Note that while macrophages can be identified within the parenchyma in isolation (single arrow), select macrophages approximate somata linked to TAI (double arrowhead). Macrophages encompass a significant portion of the somatic membrane via either round or semi-circular morphology. Additionally, semi-circular macrophages appear to partially encircle the soma; however, limited phagocytic activity is observed at later post-injury time points. (scale bar = 8 μm)

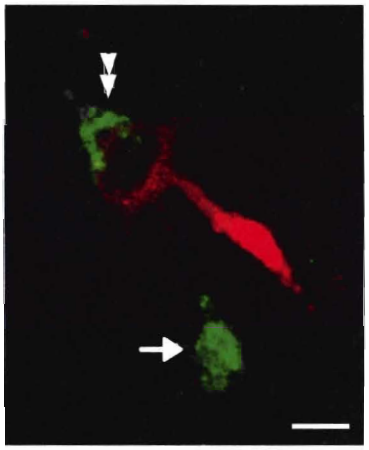

Figure 3-8

Macrophages were observed encompassing significant portions of the neuronal soma, with many now taking on a rounded or semi-circular shape to closely follow the neuron's contour. EM evaluation revealed the macrophages' close adherence to the neuronal somatic membrane (Fig. 3-9). With the approximation of the somatic membrane, there was no evidence of somatic engulfment or phagocytic activity; yet, this macrophage investment was associated with somatic bouton disruption (Fig. 3-9A) and loss (Fig. 3-9B).

Longer-term Neuroinflammatory Responses

By 7 d post-injury, LM and confocal microscopy revealed enhanced microglial / macrophage immunoreactivity within the diffusely injured loci (Figs. 3-2G-I and 3-3G-I) with increased macrophage immunoreactivity recognized within the thalamus (Fig. 3-3I). Once again, only resting microglial morphology and sparse macrophage immunoreactivity could be observed within adjoining, non-TAI containing regions. LM evaluation of TAI-containing loci revealed no evidence of widespread necrotic neuronal cell death or tissue necrosis similar to that typically described following focal brain pathology. Similarly, no related microglial or macrophage clustering was observed in relation to these diffusely injured loci and their damaged axonal segments despite continued microglial activation and the presence of macrophages.

At 14 – 28 d post-injury, activated microglial / macrophage immunoreactivity persisted within the previously identified neocortical, hippocampal, and thalamic loci (Figs. 3-2J-O and 3-3J-O). Limited activated microglia / macrophages were now

Fig. 3-9. These electron micrographs of DBI loci at 24 hrs post-injury were processed following dual-labeling of macrophages (CD 68) and TAI (APP) to identify these components using methodology similar to microglia – TAI evaluation. In these examples, macrophages approximate somata within DBI-mediated TAI loci. While select macrophages (asterisk) maintain their conventional rounded morphology (A), other microglia adopt semi-circular morphology to approximate a significant portion of the somatic membrane (B). Macrophage ultrastructure is similar to that of activated microglia while neuronal somatic ultrastructure (Nu) reveals no significant pathological change. Note that this macrophage investment is associated with apparent bouton disruption (box with enlargement in panel A). Other examples reveal somatic membranes devoid of bouton ultrastructure (B). (scale bar = 1 μm; enlargement scale bar = 250 nm)

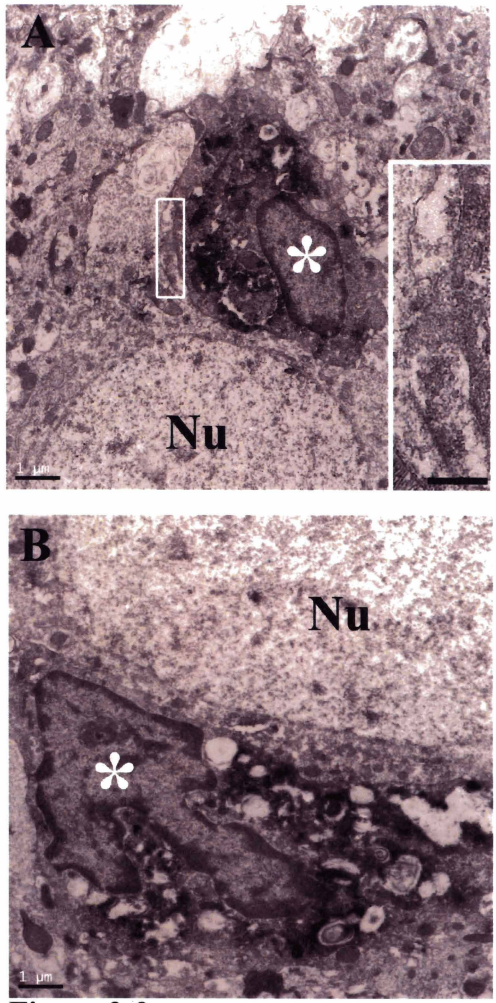

Figure 3-9

identified within tissue immediately adjacent to these loci with more remote sites continuing to maintain resting microglial morphology and sparse macrophage immunoreactivity. In contrast, enhanced macrophage immunoreactivity was recognized along the dentate gyrus granule cell layer (Fig. 3-3N). While not observed at earlier time points, limited activated microglial aggregations were now seen, particularly within the thalamus at 28 d post-injury (Fig. 3-10). However, these aggregations, previously described following focal pathology, were not numerous within injured loci. Comparable to LM observations from earlier time points, there was no evidence of widespread necrotic cell death or tissue necrosis.

While evaluations of immune cell – axonal interactions at earlier time points did not reveal specific spatial associations, EM evaluation of activated microglia / macrophages at all time points beyond 7 d post-injury revealed consistent immune cell interactions with axonal injury foci. These interactions included immune cell projections and/or cell body contact with damaged axons or their related debris as well as phagocytosis, inferred from myelin debris observed within the cytoplasm of immunoreactive cells (Fig. 3-11). Similar to LM findings within this time frame, widespread necrotic cell death or tissue necrosis was not observed. In a related finding, macrophages localized to neuronal somatic membranes still did not show evidence of somatic engulfment or phagocytic activity.

Fig. 3-10. This micrograph reveals the atypical finding of microglial aggregations within the dorsolateral thalamus at 28 d post-injury. Using antibodies to CD 11b/c, the majority of activated microglia within DBI loci do not cluster (arrow). However, limited findings of grouped activated microglia are observed (encircled). This finding is more characteristically observed during histological examination following focal brain injury. (scale bar = 100 μm)

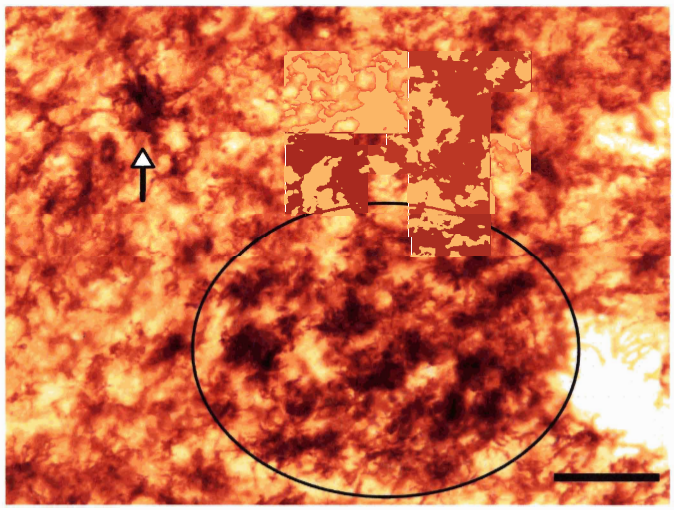

Figure 3-10

Fig. 3-11. These electron micrographs of DBI loci at 7 – 28 d post-injury identified microglia using electron-dense CD 11b/c reaction product deposition on the cell membrane. Although microglia did not engage damaged axons at more acute post-injury time points, these micrographs reveal activated microglial recognition of axonal debris (arrows) by projection formation (A) and direct cell body contact (B). Phagocytosis is inferred from myelin debris observed within the immune cell cytoplasm (box in panel B). Neither widespread immune cell clustering nor somatic engulfment, each suggestive of neuronal cell death, are observed at this time interval. (scale bar = 2 μm)

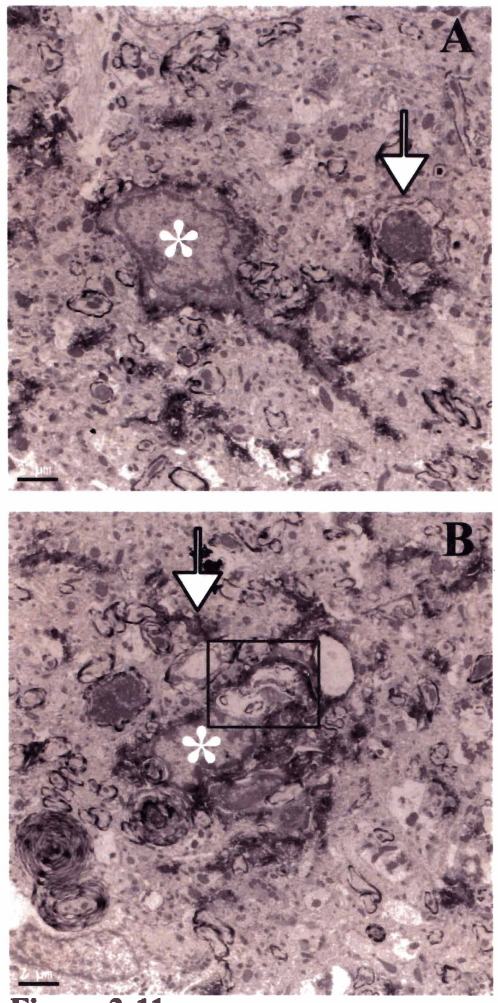

Figure 3-11

Discussion

The inflammatory response to TBI represents a coordinated effort by resident microglia and peripheral blood leukocytes to protect the brain following trauma. Although this protective function is essential to preserving viable tissue and promoting recovery, recent evidence suggests that the neuroinflammation itself may also be responsible for the initiation of delayed / secondary injury cascades (Morganti-Kossmann et al., 2002). Accordingly, a fully comprehensive examination of TBI-mediated neuroinflammation is essential for designing rational approaches to therapeutically modulate pathological aspects of this response. With this rationale in mind, this manuscript provided a spatiotemporal characterization of microglia / macrophage interactions following DBI as assessed by light, confocal, and electron microscopic evaluation of microglial activation and macrophage localization within the diffusely injured brain revealing TAI in the absence of focal contusion or hemorrhage.

As intrinsic primary immune effecter cells of the brain parenchyma, microglia are the first line of defense following traumatic insult (Kreutzberg, 1996). Focal TBI often results in primary axotomy together with other destructive and ischemic neuronal changes while diffuse TBI results primarily in DAI, known as TAI in the experimental setting, that leads to delayed or secondary axotomy without concomitant tissue disruption. Previous studies documenting focal TBI-mediated microglial activation have demonstrated a robust response to primary axotomy generated via either *ex vivo* slice preparation (Dailey and Waite, 1999; Stence et al., 2001; Grossmann et al., 2002), *in vivo* stab wounding (Carbonell et al., 2005), or *in vivo* medial forebrain bundle

transection (Cho et al., 2006), all of which involve direct tissue transection. In comparison, microglial responses to diffuse TBI and its associated axotomy have received little attention. Previous studies of rodent and human microglial activation following TBI have demonstrated no specific associations between microglia and injured axons (Oehmichen et al., 1999; Csuka et al., 2000) despite evidence for traumatically induced microglia – neuronal interactions (Aldskogius and Kozlova, 1998; Bruce-Keller, 1999). In the current communication, microglial activation shared a spatiotemporal relationship with TAI within diffusely injured brain loci that included the mediodorsal neocortex, hippocampal dentate gyrus, and dorsolateral thalamus. However, the activated microglia did not show, via confocal or electron microscopy, any specific and/or consistent relationship to sites of axonal injury in the acute stages following injury. The observed activation persisted until at least 28 d post-injury and in this sense, was consistent with time courses of microglial activation following brain and spinal cord trauma (Aihara et al., 1995; Popovich et al., 1997;Stence et al., 2001; Rodriguez-Paez et al., 2005). However, in the current study, the immune cell recognition of axonal debris at the EM level occurred only between 7 – 28 d post-injury. In contrast to this microglial activation, other microglia within adjoining, non-TAI containing parenchyma maintained a resting morphology. This data suggests an early generalized microglial response to DBI followed by a delayed targeted response to its attendant axotomy, with the microglia in non-TAI containing regions remaining quiescent.

This initial microglial activation without specific axonal targeting suggests that in DBI, microglia are activated within their local microenvironments yet remain stationary despite DBI-mediated axotomy. A recent study by Nimmerjahn and colleagues (2005) supports this observation via documentation that resting microglia, traditionally believed to be dormant during times of homeostasis, actively survey their local microenvironment using projections from ramified processes, sending longer projections to areas of local tissue damage associated with overt tissue disruption and BBB compromise while their cell bodies remain stationary (Nimmerjahn et al., 2005). It seems reasonable that microglia can adopt activated phenotypes and continuously monitor local parenchymal domains yet remain non-migratory, failing to send projections to sites of axonal injury. This finding with diffuse injury may reflect the lack of appropriate chemotactic stimuli that are typically generated following focal brain injury wherein overt BBB and/or tissue disruption occurs (Chen et al., 2003; Carbonell et al., 2005). Further, moving on the premise that rapid axolemmal closure associated with perisomatic TAI and consequent axotomy, as outlined in Chapter 2, most likely preclude the unregulated release of intra-axonal components into the surrounding parenchyma, this also suggests insufficient chemotactic molecule concentrations to stimulate migration and/or projection formation. In the current study, the subtle interstitial albumin immunoreactivity at 6 hrs post-injury, combined with the absence of overt neuronal / tissue damage, supports a scenario in which blood-borne signaling molecule concentrations may be sufficient to achieve microglial activation yet insufficient to stimulate migration and/or projection formation, at least in the early

stages following injury. Our finding of microglia within adjoining, non-TAI containing regions that are also exposed to albumin yet fail to demonstrate an activated phenotype suggests a specific role for TAI pathogenesis in microglial activation. To date, the molecular mechanisms dictating traumatically induced microglial activation and motility are poorly understood. However, studies are presently beginning to elucidate the specific molecules and receptors, including ATP and cysteine-cysteine chemokine receptor 5, involved in microglial activation and chemotaxis following trauma (Polazzi and Contestabile, 2002; Carbonell et al., 2005; Davalos et al., 2005).

Although microglia were not recruited to sites of TAI within the acute phases following injury, motile morphology was observed in select cells. Following DBI-induced activation, select microglia became elongated with the suggestion of forward and trailing processes. Although the majority of activated microglia remained diffusely distributed throughout injured loci, microglial motility is consistent with infrequent observations of microglial aggregations at later time points post-injury. Further assessment of microglial motility was confounded by the acute upregulation of microglial APP following activation (Banati et al., 1993), which made LM distinction between microglial processes and reactive axons difficult in certain instances, and by the inability of APP immunoreactivity to recognize TAI at longer post-injury time points (Singleton et al., 2002). The development of novel TAI markers allowing for long-term labeling of injured axons will allow for more definitive conclusions concerning microglial motility to sites of diffuse axonal pathology.

In addition to microglial activation within injured loci, macrophages were also found within neocortical and hippocampal parenchyma at 6 hrs post-injury, with their recognition in the thalamus by 24 hrs. In all of these loci, the macrophages persisted until at least 28 d post-injury. Csuka and colleagues (2000), using an impact-acceleration model of DBI that did not document immune cell interactions with sites of axonal injury, described macrophage immunoreactivity within the meninges, basal subarachnoid space, Virchow-Robin's space, ventricular choroid plexus, subventricular zone, and perivascular locales suggesting minimal post-injury parenchymal entry (Csuka et al., 2000). In contrast, in the current study macrophages were distributed within the parenchyma of the diffusely injured loci. For example, macrophages were observed within superficial and deep layers of the neocortex, a finding consistent with previous observations of macrophage infiltration following lateral fluid percussion-induced mild brain injury (Aihara et al., 1995). Parenchymal macrophage immunoreactivity at relatively early post-injury time points is strongly suggestive of macrophages originating from the peripheral vasculature although differentiation of resident microglia cannot be definitively excluded. Macrophages found within the parenchyma of diffusely injured loci without overt contusion or related hemorrhage suggests the potential for coordinated movement through an injury-induced, transiently perturbed BBB (Hartl et al., 1997a; Hartl et al., 1997b) as suggested by post-injury interstitial albumin immunoreactivity (Cortez et al., 1989; Schmidt and Grady, 1993; Barzo et al., 1996; Baskaya et al., 1997). Although the precise origins of DBI-mediated parenchymal macrophages cannot be definitively determined from this study, these

findings illustrate the importance of using multiple DBI models in future studies to assess leukocyte localization following trauma. Studies using pre-injury labeled peripheral blood monocytes and/or bone marrow chimeric animals may provide insight into the relative contribution and distribution of exogenous versus endogenous macrophage populations following DBI (Popovich and Hickey, 2001; Ladeby et al., 2005).

While numerous macrophages were observed in isolation, other macrophages approximated somata of perisomatically axotomized neurons, particularly within the neocortex by 24 hrs post-injury. EM evaluation of macrophage – soma interactions revealed macrophages encompassing large components of the somatic membrane, having adopted rounded or semi-circular morphology to approximate the membrane, potentially participating in somatic bouton disruption and loss. This association was reminiscent of the phenomenon in which regenerating neurons undergo inflammatory-mediated deafferentation of synaptic terminals which confers an adaptive advantage for potential synaptic reorganization, known as synaptic stripping (Blinzinger and Kreutzberg, 1968). Using facial nerve primary axotomy, a model quite dissimilar from DBI-mediated secondary axotomy, microglia, macrophages, and peripheral leukocytes all responded to initial neuronal degeneration prior to regeneration. Microglia were specifically implicated in separating boutons from neuronal cell bodies (Kreutzberg, 1995; Graeber et al., 1998; Raivich et al., 1998). Given the suggestion of somatic reorganization and repair following DBI-mediated axotomy (Singleton et al., 2002), macrophage – somatic associations seem plausible. Although microglia were not

recognized approximating somatic membranes following DBI, neuronal mechanisms responsible for immune cell recruitment following trauma may be different given the primary versus secondary nature of axotomy. Perhaps mechanisms stimulated by primary axotomy favor microglial recruitment whereas mechanisms following secondary axotomy preferentially recruit macrophages. However, it is also possible that these macrophages may have differentiated from perineuronal microglia that approximate somata under non-pathologic conditions (Peters et al., 1991).

At this time, it is unclear whether these macrophages originated from the peripheral vasculature or differentiated from prepositioned microglia. Nonetheless, close approximation of the macrophage to the somatic membrane is strongly suggestive of immune cell – neuron crosstalk mechanisms. To date, several molecules released by neurons following trauma have been implicated in immune cell activation and recruitment (Polazzi and Contestabile, 2002). The severity of neuronal injury may dictate the nature of these signals with reversible injury leading to immune cell-mediated trophic support while irreversible injury may enhance immune cell-derived neurotoxic-mediated cell death (Streit et al., 1999). Given the suggestion of neuronal somatic reorganization and repair as well as the absence of widespread necrotic neuronal cell death following moderate DBI (Singleton et al., 2002), these observations support potential immune cell – neuron trophic interactions. Studies in our laboratory are currently examining the long-term fate of neurons to provide additional insight into neuronal signaling responses and outcomes following DBI.

Following TBI, immune cell activation is driven primarily by neuronal degeneration (Kreutzberg, 1996; Streit, 2000). However, the lack of DBI-mediated cell death in the cFPI model (Singleton et al., 2002) suggests that ongoing microglial / macrophage activation (up to 28 d in the current communication) may be supported by DBI-mediated secondary pathologies such as cellular membrane perturbation and/or Wallerian degeneration leading to synaptic disruption. Membrane perturbation may stimulate cytokine / chemokine release by injured neurons and/or surrounding glia (Aloisi, 2001; Hansson and Ronnback, 2003). The post-injury release of these molecules may then contribute to sustained immune cell activation long after the initial injury stimulus has dissipated (Bajetto et al., 2002; Babcock et al., 2003; Gentleman et al., 2004; Kim and de Vellis, 2005). Similarly, Wallerian change and related deafferentation are known stimuli for immune cell activation. Given the rapid Wallerian degeneration that takes place following DBI-mediated perisomatic TAI outlined in Chapter 2, the presence of axonal breakdown products may also contribute to prolonged activation. Studies by Dong and colleagues, using a dissimilar entorhinal cortex lesion paradigm involving transection of afferent fibers to the hippocampus, noted microglial activation within denervated portions of the hippocampus as late as fifteen days post-injury (Dong et al., 2004; Dong et al., 2005; Dong et al., 2006). In the current communication, sustained macrophage activation was observed along the hippocampal dentate gyrus granule cell layer, corresponding to sites of synaptic input and consistent with previous findings following experimental DBI (Carbonell and Grady, 1999). As such, deafferentation may trigger supplemental neuronal injury response mechanisms

that continue to signal immune cells originally activated by stimulatory molecules released during the initial traumatic episode (Aldskogius et al., 1999; Bruce-Keller, 1999). Although precise identification of secondary injury mechanisms leading to prolonged immune cell activation remains elusive, persistent post-traumatic microglial / macrophage activation has implications for understanding neuronal plasticity and potential recovery following trauma (Banati, 2002; Banati, 2003).

The current communication's findings may also have implications for neuropathological evaluation of TBI. Microglial clustering in post-mortem histological neuropathology is currently used as a diagnostic indicator of TBI-related pathobiology that includes axotomy (Adams et al., 1989). These clusters or nodules have been documented with survival times of at least seven weeks post-injury (Povlishock and Becker, 1985) with more recent evidence of clustering between ten and fifteen days post-injury (Geddes et al., 1997; Oehmichen et al., 1999). In the current communication, only isolated microglial aggregations occurred at 28 d post-injury. Further, LM morphology of these aggregations revealed dissimilarities between these aggregations and those clusters / nodules involved in microglial-mediated neuronophagia. Given the absence of focal pathology within DBI-mediated TAI-containing loci, previous descriptions of microglial clusters may be indicative of focal pathology, in which necrotic cell death and/or hemorrhagic tissue damage triggers microglial recruitment via chemotactic signaling molecules. In contrast, the lack of neuronal cell death and the absence of overt tissue damage associated with moderate DBI may explain why microglial clustering does not take place, at least within the time

frame of the current communication. Our findings suggest that histopathological and forensic identifications of TBI that rely on surrogate markers of neuronal injury, such as microglial clustering, may overlook and thus underestimate more subtle forms of diffuse pathology. Accordingly, TBI histopathological evaluation may be expanded to address microglial / macrophage immunoreactive findings indicative of DBI, namely early and persistent microglial activation and macrophage localization within diffuse brain regions without requisite cluster / nodule formation.

Chapter 4

GENERAL DISCUSSION

The purpose of this section is not to reiterate material provided in the previous discussions related to Chapters 2 and 3. Rather the goal here is to explore general concepts pertinent to the findings of this dissertation as a whole. A brief synopsis is provided to review the most prominent findings related to the study of DBI-mediated perisomatic TAI and the related neuroinflammatory response thereby providing a foundation for future investigation.

SYNOPSIS

To complete this dissertation on TAI pathogenesis within the perisomatic domain and the related microglia / macrophage responses to DBI, a midline/central FPI model of moderate severity was utilized. This model provided a reliable and reproducible axonal pathology that was localized to a specific distance from the soma of origin and was found within specific anatomical loci. Additionally, diffuse TAI was observed without evidence of overt focal contusions and/or hemorrhagic-mediated tissue damage. Using immunohistochemical techniques, antibodies to the anterogradely transported β-APP were used to mark the site of focally impaired axonal transport

following injury, a key characteristic of TAI pathology. The spatiotemporal progression, ultrastructural pathology, and permeability alteration of this injury site as well as findings related to the soma and proximal / distal segments were characterized in Chapter 2 while microglia / macrophage responses to DBI and its associated pathology were explored in Chapter 3.

As detailed in Chapter 2, TAI within the perisomatic domain resulted in an ultra-rapid secondary axotomy and Wallerian degeneration. Investigation of perisomatic TAI was prompted by an initial study of the related somatic response to secondary perisomatic axotomy. Despite axonal disconnection within 40 – 60 μm of the sustaining soma, DBI-mediated traumatically injured neurons did not progress to rapid cell death (Singleton et al., 2002). This observation, which contrasted previous studies of neuronal death following axonal transection within a similar distance from the soma, suggested that the manner in which perisomatic axotomy took place afforded some form of somatic protection following axonal trauma. It was speculated that the time frame over which secondary axotomy evolved (i.e. within several hours following DBI) was an important factor. However, as reported in this dissertation, as early as 15 – 30 min following DBI, perisomatically injured axons had lost continuity with their downstream segments while the related soma and proximal axonal segment showed no overt signs of pathology. Ultrastructural analysis of the site of axonal injury revealed neurofilament disorganization, microtubule loss, mitochondrial pathology, and pooling of intra-axonal organelles. These observations were comparable to those documented in previous studies of TAI within long tract axons of the brainstem (Pettus et al., 1994; Pettus and

Povlishock, 1996). The related distal axonal segment ultrastructure was persevered at this time point; however, by 60 – 180 min post-injury, the initial stages of Wallerian degeneration were apparent. The site of axonal swelling and disconnection was independent of overt alterations in axolemmal permeability. Taken together, these observations suggest that maintenance of axonal integrity rather than speed of disconnection is more important in providing somatic protection following TAI.

The neuroinflammatory response to DBI and its related pathological sequelae as outlined in Chapter 2 was the focus of Chapter 3. The immune response to TBI involves both resident microglia as well as peripheral blood monocytes recruited from the surrounding vasculature. Microglia / macrophage responses to DBI were characterized using antibodies to immune cell surface proteins in conjunction with TAI labeling to visualize diffusely injured brain loci uncomplicated by focal pathology. Given the rapidity of TAI pathology, it was assumed that immune cells would rapidly target sites of axotomy. At 6 – 24 hrs following DBI, scattered LM microglial activation was observed within injured loci while other scattered microglia within adjoining non-TAI containing regions maintained a resting phenotype. DBI-mediated activated microglia phenotype included a rounded cell body, decreased process ramification, and enhanced immunoreactivity that persisted until at least 28 d post-injury. Comprehensive EM evaluation did not reveal specific microglia – neuron associations within the first seven days post-injury, rather simply an initial generalized activation response to trauma. Microglial-mediated phagocytosis of axonal debris followed at subsequent post-injury time points without evidence of clustering / nodule formation. Macrophages were also

observed within injured neocortical and hippocampal loci at 6 hrs post-injury with recognition in the thalamus at 24 hrs post-injury, again with little to no immunoreactivity within adjoining non-TAI containing regions. These cells appeared within the parenchyma despite no evidence of focal contusion, hemorrhage, or tissue disruption. EM evaluation revealed a spatiotemporal relationship to TAI comparable to microglial findings. However, select macrophages approximated somata of perisomatically axotomized neurons within 24 hrs post-injury although their origin from either peripheral blood monocyte or microglial differentiation could not be definitively determined. Despite this association, there was no evidence of somatic engulfment or phagocytic activity. Macrophage immunoreactivity within injured loci persisted at 28 d post-injury while adjoining regions remained devoid of immunoreactivity. These findings suggest that neuroinflammatory responses to DBI are distinct from those related to focal TBI and that TBI histological evaluation that relies on markers such as microglial clustering may inadvertently overlook and thus underestimate the extent of DBI-mediated axonal pathology.

INHERENT DIFFICULTIES IN STUDYING DBI-MEDIATED TAI

As the work detailed in this dissertation indicates, TAI in the perisomatic domain is characterized by ultra-rapid secondary axotomy and Wallerian degeneration and is accompanied by reactive microglia / macrophage responses. To study TAI and its resultant consequences within the context of DBI, a reliable and reproducible injury model is necessary. Rodent FPI (Dixon et al., 1987) provides a clinically relevant model

of human diffuse TBI. Descriptive characterizations of brain pathology generated by the central and lateral / parasagittal versions of this model include physiological, metabolic, and cytological pathology as well as hemorrhagic and related ischemic damage, BBB disruption, and alterations of behavioral and cognitive outcome measures (McIntosh et al., 1987; Dixon et al., 1988; McIntosh et al., 1989; Hicks et al., 1996; Thomas et al., 2000; Thompson et al., 2005). Focusing on axonal pathology, the nature of DBI is such that traumatically injured axons are found among other CNS constituents that demonstrate little or no pathology. Given that midline/central FPI of moderate severity generates TAI within diffuse brain regions, among other fibers and cells exhibiting no distinct pathological alterations, and without evidence of overt focal pathology, this injury model mimics comparable pathologies described in mild to moderate human DBI (Adams, 1992; Graham, 1996).

Although DBI-mediated TAI can be generated in specific anatomical loci using FPI, study of its cellular and molecular pathologies is confounded by the nature of this injury. TAI is found scattered throughout the brain as well as interspersed within normal CNS constituents making examination of injured axons difficult. Although identification of microscopic diffuse TAI has been facilitated through the use of antibodies targeting specific axonal pathological cascades or end-products, isolation of injured axons for molecular analysis is a daunting task given the likelihood of the concomitant collection of axons and brain tissue immediately adjacent to the pathology. In contrast to diffuse injury, the highly concentrated and homogenous nature of focal brain injury lends itself to a variety of experimental techniques to examine the cellular

response to injury. In focal injury, an injury nidus may be reliably located and isolated from related tissue allowing for numerous analyses to study cellular responses.

Despite these inherent limitations, the study of DAI, and its experimental equivalent TAI, remains an important scientific objective. With DAI as the predominant mechanism of injury for 40 – 50 percent of TBI hospital admissions and, as such, a major contributor to the morbidity and mortality associated with TBI (Meythaler et al., 2001), continued basic science research into TAI pathobiology is needed to provide insights into mechanisms of axonal damage and to discern potential targets for therapeutic treatment options. Thus, translational research between basic science and clinical arenas is vital; however, the application of basic science knowledge to the clinical realm must be carefully measured. Inevitably, it is the collective brain response to diffuse injury that ultimately dictates axonal pathology and the related inflammatory responses.

MECHANISMS OF ULTRA-RAPID TAI PATHOLOGY

Given the precise anatomical localization of injury as well as the related secondary axotomy and Wallerian degeneration, DBI-mediated perisomatic TAI pathology offers a unique opportunity to study axonal injury mechanisms and to explore pathobiological consequences of neuron – glial cell interactions and neuronal pathway deafferentation within the context of TBI. As DBI relates to axonal injury mechanisms, previous studies from our laboratory and others implicate calpain and caspase-mediated cytoskeletal proteolysis within minutes to hours following TAI (Saatman et al., 1996;

Buki et al., 1999; Buki et al., 2000; Saatman et al., 2003) with others reporting similar cytoskeletal pathology within this time frame (Gennarelli et al., 1993; Jafari et al., 1997; Maxwell and Graham, 1997; Jafari et al., 1998). The spatiotemporal progression of thalamic perisomatic TAI is comparable to studies of experimental diffuse neuronal injury using fluid percussion which include thalamic neuronal damage as early as 10 min following injury (Dixon et al., 1987; Hicks et al., 1996; Bramlett et al., 1997; Sato et al., 2001). However, despite the abundance of information regarding TAI pathogenesis, the precise subcellular mechanisms of perisomatic TAI pathology remain elusive.

A variety of antibodies to proteolytic proteins and degradation products implicated in TAI pathobiology have been used to attempt to describe mechanisms of injury within the perisomatic domain. However, markers of calpain and caspase activation as well as spectrin proteolytic products have met with little success in this region (unpublished observations). These same antibodies have been successful in determining mechanisms of brainstem TAI pathology suggesting that axonal size may be a factor not only in antibody binding affinity but also in potential mechanisms of pathology. Large caliber axons found within ascending and descending white matter tracts of the brainstem offer a larger target for antibody binding than the smaller caliber axons of the thalamus. Brainstem axons are also myelinated. Given that myelination confers additional strength to the axon, more severe diffuse injury forces stimulating the above mentioned mechanisms may be required to generate pathology within this region. These ideas are contrasted by the unmyelinated initial segment and thinly myelinated

internodal segment in which perisomatic TAI pathology is observed, perhaps making these segments preferentially vulnerable to lower magnitude injury forces. As outlined in Chapter 2, perisomatic injury is localized to the grey – white matter interface, an area that is selectively vulnerable to shear and tensile forces (Smith et al., 1997; Meythaler et al., 2001). It is possible that potentially less severe forces are needed to generate perisomatic TAI and may result in a more rapid initiation of pathological cascades following injury. Similarly, lack of tracer flooding at the site of perisomatic secondary axotomy suggests either minimal or no pathological influx of extracellular ions at this site. Perhaps influx at this site is more insidious and stimulates the afore mentioned pathological cascades albeit at levels insufficiently recognized by antibody affinity.

Although the acute mechanisms of perisomatic TAI pathogenesis remain elusive, we continue to evaluate the long-term implications of perisomatic TAI and related axotomy. Ongoing stereological studies from our laboratory suggest neuronal somatic shrinkage at 7 d following moderate cFPI without evidence of widespread neuronal cell death with similar observations out to 28 d post-injury (article in preparation). While mechanisms for neuronal shrinkage are currently being evaluated, previous studies of perisomatic TAI indicate that injured neurons are terminal deoxynucleotidyl transferase-mediated biotinylated dUTP nick end labeling (TUNEL) negative and demonstrate multiple independent injury phenotypes (Singleton et al., 2002; Singleton and Povlishock, 2004). Recently, our laboratory has studied DBI-mediated neuronal mechanoporation (Farkas et al., 2006). Perhaps non-lethal disruption of the neuronal membrane leads to ionic dysregulation creating fluid shifts which

ultimately lead to cellular shrinkage. Taken together, these observations have important clinical implications for head injured patients in that the initiation of DAI pathology may take place more rapidly than currently believed.

RAPIDITY OF AXOTOMY

The rapidity at which perisomatically injured neurons undergo secondary axotomy and consequent Wallerian change is disturbing given the relevance of DAI to human head injury and therapeutic modalities aimed at prevention / attenuation of axonal damage following TBI. Studies of human DAI suggest secondary axotomy pathogenesis evolves over approximately 12 hrs (Grady et al., 1993; Christman et al., 1994; Povlishock and Christman, 1995) while experimental paradigms indicate a more accelerated time frame, approximately 4 – 6 hrs (Pettus et al., 1994; Pettus and Povlishock, 1996). However, as outlined in Chapter 2, secondary axotomy following DBI-mediated perisomatic TAI was observed as early as 15 – 30 min post-injury with consequent Wallerian degeneration noted soon thereafter. Given that the time delay between initial trauma and axonal disconnection within the perisomatic domain is shorter than times observed within previous studies of TAI-mediated secondary axotomy, study of rapid and therapeutically relevant interventions becomes even more significant.

The phenomenon of DBI-mediated perisomatic TAI remains novel with only limited study of this unique pathobiology to date (Singleton et al., 2002; Singleton and Povlishock, 2004). Although ultra-rapid secondary axotomy, as discussed in Chapter 2,

was also noted within the neocortex and hippocampus, observations for this dissertation were confined to thalamic nuclei with the inference that these findings could be extended to neocortical and hippocampal pathology. However, confirmation of identical neocortical and hippocampal secondary axotomy pathology requires further investigation. The clinical relevance of these thalamic studies is supported by documentation of TBI-mediated thalamic neuronal damage in a variety of patients whose outcomes range from moderately disabled to vegetative (Anderson et al., 1996; Adams et al., 2000; Uzan et al., 2003; Maxwell et al., 2004) as well as studies of post-injury cognitive function in humans and experimental animals (Terayama et al., 1991; Pierce et al., 1998; Ding et al., 2001).

In a related fashion, relatively little information exists concerning anterograde / Wallerian degeneration following TBI. Studies of CNS Wallerian change come mainly from spinal cord injury (Becerra et al., 1995; Buss et al., 2004) or from experimental *in vitro* transection of dorsal root ganglia (Sievers et al., 2003). Classic descriptions of Wallerian degeneration in humans suggest a pathology that evolves over months and persists for years following injury (Strich, 1968; Becerra et al., 1995; Buss et al., 2004) while experimental models accelerate the time frame for pathological change (Maxwell et al., 2003). The discovery of a mutant mouse strain with slow Wallerian degeneration has helped to provide additional insight into this pathological process by allowing for examination of Wallerian change over longer post-injury time periods (Perry et al., 1991). A more recent study by Maxwell and colleagues reported ultrastructural findings of Wallerian change at 24 hrs post-injury using an optic nerve stretch injury model of

TAI (Maxwell et al., 2003). However, as outlined in Chapter 2, DBI-mediated Wallerian degeneration within 60 – 180 min post-injury and its relationship to ultra-rapid secondary axotomy are unique observations in that the speed at which these events take place is significantly faster than previously recognized.

The speed of these events has important implications for therapeutic interventions aimed at attenuation / elimination of their pathogenesis. To date, numerous studies attenuating TAI in animal models have met with limited results in clinical trials (Narayan et al., 2002). Although TAI pathogenesis is accelerated in animals relative to the human condition, our findings suggest that despite early intervention following injury (~ 15 min) there will be irreversible axonal damage leading to neuronal pathway degeneration. Providing complete neuroprotection following TBI may be an unrealistic expectation; nonetheless, therapeutic intervention remains an important component of attenuating more vigorous neuronal pathology. Apparently "uninjured" axons may have a delayed response to trauma given the progressive increase in injured axon and reactive swelling numbers over time. Recognition of injured axons with apparent normal morphology remains an important TBI research objective in that these axons appear amenable to therapeutic intervention and may be rescued from their impending demise.

NEURONAL SIGNALING MODULATING MICROGLIAL ACTIVITY FOLLOWING TRAUMATIC BRAIN INJURY

It would seem reasonable and rational that neurons communicate with surrounding microglia to promote a homeostatic environment during periods of rest

while at the same time possessing the capacity to stimulate microglial activation following traumatic insult. Several lines of evidence supporting microglia – neuron crosstalk are provided by both *in vivo* and *in vitro* studies (Aldskogius and Kozlova, 1998; Polazzi and Contestabile, 2002). During periods of inactivity, microglia demonstrate a heterogeneous distribution among different regions of the adult rat brain (Savchenko et al., 2000). Given observations that microglia within different brain regions demonstrate slightly differing morphologies, this suggests that microglial activation may be affected by localization and interactions with various cell types throughout the brain (Polazzi and Contestabile, 2002). For example, when CD200, a membrane glycoprotein expressed by neurons and whose receptor is found on microglia, was absent, microglia showed an activated phenotype and formed aggregates expressing inflammatory molecules (Hoek et al., 2000). This suggests a neuronal mechanism of microglial downregulation of immune function. Similarly, when microglial cultures were exposed to neuron-conditioned media, differentiating neurons released factor(s) capable of inducing apoptosis of activated, but not unstimulated, microglia suggesting a neuronal-mediated regulation of microglial activation which serves as a protective mechanism against an overactive inflammatory response (Polazzi and Contestabile, 2003).

Evidence also exists for neuronal-mediated mechanisms of microglial activation following traumatic injury. When neurons die, independent of the specific cause of death, the microglial reaction is stereotyped and consists of quick transformation into an activated phenotype (Streit et al., 1999; Streit, 2000). Several studies have documented

the release of pro-inflammatory agents (e.g. TNF-α, IL-1, IL-6) and trophic factors by activated microglia in response to neuronal death (Bartholdi and Schwab, 1997; Toku et al., 1998; Batchelor et al., 1999; Pearson et al., 1999; Stoll et al., 2002). The scripted microglial response to neuronal cell death is one of motility to the injury site followed by alterations in morphology including retraction of processes, proliferation, and increased membrane expression of surface molecules such as complement type 3 receptor (CR3) and major histocompatibility complex class II (MHC Class II) antigen. Microglia then differentiate into macrophages only in the presence of extensive neuronal degeneration (Kreutzberg, 1996). In a related response, microglia are also capable of recruiting monocytes and lymphocytes from the blood stream (Aloisi, 2001). Although these findings suggest that microglial activation may aggravate ongoing inflammatory responses, microglia have also been shown to secrete anti-inflammatory molecules such as TGF-β and IL-10 (Aloisi, 2001) suggesting a dichotomy of both microglial-mediated neuropathological and neuroprotective functions. Therefore, the promotion of neuronal survival or exacerbation of neuronal death may depend primarily on the nature of the neuronal signals responsible for microglial activation which are released following trauma (Streit et al., 1999; Polazzi and Contestabile, 2002).

Although cytokines responsible for microglial activation have been recognized, their mechanisms of action and the long-term consequences for microglial activation remain poorly understood. Emerging literature on the subject of microglial activation suggests candidate genes and unique morphological characteristics may also be responsible. One such gene is microglia response factor (mrf-1) which encodes a

calcium binding protein that does not appear to play a role in phagocytic activity and is upregulated following neuronal injury (Tanaka et al., 1998). Given that mrf-1 is not upregulated by phagocytosis, induction may require cell-cell contact between microglia and degenerating neurons and/or the release by damaged neurons of signals capable of altering gene expression (Polazzi and Contestabile, 2002). Similarly, microglial cells have a unique pattern of potassium channels and the possibility of increased extracellular potassium levels around injured neurons inducing their activation is supported by an *in vivo* spreading depression model of potassium chloride that induced microglial activation (Gehrmann et al., 1993).

Injured neurons may also regulate microglial activation through coordinated release or leakage of stimulatory molecules such as ATP (Walz et al., 1993). Several studies have shown that ATP stimulates microglia to release biologically active substances such as IL-1β (Sanz and Di Virgilio, 2000), TNF-α (Hide et al., 2000), nitric oxide (Ohtani et al., 2000), and IL-6 (Shigemoto-Mogami et al., 2001) as well as induce microglial chemotaxis (Honda et al., 2001). More recent *in vivo* studies have shown microglial processes to autonomously converge on focal injury sites induced by laser ablation with ATP release from damaged tissue implicated as a key mediator of this response (Davalos et al., 2005; Nimmerjahn et al., 2005). Additionally, matrix metalloproteinase-3 released by apoptotic neuronal cells has recently been shown to activate microglia *in vitro* (Kim et al., 2005). Additional mediator candidates include platelet-activating factor (PAF), a phospholipid that plays various roles in neuronal function and whose receptor is expressed in microglial cells (Mori et al., 1996; Aihara

et al., 2000) as well as neurotransmitters (e.g. glutamate) released by neurons which may signal adjacent microglia via receptor-based interactions (Noda et al., 2000). Finally, a recently identified chemokine, fractalkine, appears to function as an important signaling molecule between neurons and microglia (Mizuno et al., 2003). The specific receptor, CX3CR1, is found primarily on microglia suggesting an important signaling role for this molecule (Nishiyori et al., 1998). Similarly, the cysteine-cysteine chemokine receptor 5, which may be stimulated by a number of biologically active molecules, has recently been shown to play a role in microglial activation and motility following focal stab wounding (Carbonell et al., 2005).

Taken together, these studies strongly suggest neuronal injury-mediated microglial signaling within the context of normal brain function and during the period immediately following traumatic insult. The list of microglial activators is sure to grow as our understanding of the neuronal response to injury continues to evolve. Additionally, associated glial responses from cells such as astrocytes are also involved in microglial activation via the release of various stimulatory molecules and thus contribute to neuroinflammatory responses (Aldskogius and Kozlova, 1998; Shih et al., 2006). Along these lines, our ability to manipulate these signaling molecules individually or in combination may offer an opportunity to intervene therapeutically with the hope that regulation of neuroinflammatory responses may promote neuroprotective strategies while limiting unintended neuropathological consequences.

CYTOKINES FOLLOWING TRAUMATIC BRAIN INJURY

Continued studies are needed to discern the chemotactic factors involved in leukocyte recruitment to DBI loci although cytokines and chemokines generated by glial cells have been implicated in this process (Bajetto et al., 2002; Babcock et al., 2003). Cytokines are usually released within minutes after an appropriate stimulus because they are stored intracellularly as precursor molecules and eventually modified into active molecules. Following activation, microglia may secrete pro-inflammatory cytokines, most notably interleukin 1 (IL-1) (Gentleman et al., 2004). IL-1 is synthesized by microglia following experimental brain injury and can be found in microglia close to APP immunoreactive cells and neurites in head-injured patients (Fagan and Gage, 1990; Taupin et al., 1993; Griffin et al., 1994). Other cytokines elevated in the brain following traumatic injury are IL-6 and tumor necrosis factor alpha (TNF-α) (Goodman et al., 1990; McClain et al., 1991; Shohami et al., 1999). Both IL-1 and TNF-α are capable of altering vascular permeability and could facilitate macrophage entry into parenchymal areas from which microglia secrete these molecules thus facilitating macrophage interactions with injured neurons (Beynon et al., 1993; Burke-Gaffney and Keenan, 1993). However, Soares and colleagues suggest that inflammatory leukocyte recruitment and diffuse neuronal degeneration are separate pathological processes resulting from TBI. Following lateral FPI, neuronal degeneration took place within deep diencephalic structures in the absence of IgG extravasation and neutrophil infiltration (Soares et al., 1995). Taken together, these data illustrate a discrepancy as to the importance of leukocyte recruitment in response to neuronal

degeneration following trauma and highlight the importance of continued research into cytokine / chemokine mechanisms of action.

Similar discrepancies exists concerning activation of intracellular adhesion molecule 1 (ICAM-1), which is pivotal in mediating the extravasation of leukocytes across cerebral vessels, as well as with chemokines associated with leukocyte recruitment within the context of TBI (Morganti-Kossmann et al., 2002). ICAM-1 expression is increased in the cerebral vessels of rats with diffuse axonal injury, despite the absence of neutrophils in the brain parenchyma. Similarly, monocyte chemotactive protein 1 (MCP-1; acting on macrophages) but not macrophage inflammatory protein 2 (MIP-2; acting on neutrophils) was elevated in these animals further supporting these findings (Rancan et al., 2001). However, both chemokines were elevated following focal brain injury, corroborating the finding of neutrophil and macrophage accumulation within cortical contusions (Otto et al., 2001). These data highlight heterogeneous inflammatory responses within the contexts of focal and diffuse TBI and illustrate the complexity of molecular interactions taking place during the secondary phases of injury. The roles of cytokines and chemotactic factors in leukocyte recruitment as well as in glial activation following DBI remain the focus of ongoing studies.

NEUROINFLAMMATORY CONCLUSIONS

While dissimilar from DBI pathology which leads to secondary axotomy, studies of inflammatory responses to primary axotomy provide a starting point to

examine immune cell reactivity to traumatic injury. Facial nerve axotomy via transection leads to microglial activation within hours after injury with microglia remaining in the area for at least two weeks. Transection leads to perineuronal ensheathment of neurons by microglia which accomplishes two neuroprotective actions: removal of excitatory input through displacement of afferent synapses known as synaptic stripping (Blinzinger and Kreutzberg, 1968) and close physical proximity of axotomized neurons to microglial cells which may facilitate targeted delivery of growth and/or neurotrophic factors promoting regeneration (Streit, 2002). Microglia are thought to be essential components of the neuronal regenerative response, a response which is blunted within the CNS by a variety of factors, based on the fact that transection-mediated axotomy of rubrospinal tract neurons in the cervical spinal cord, that does not result in regeneration, elicits only minimal microglial activation (Barron et al., 1990; Tseng et al., 1996). Given the diffuse nature of TAI which leads to comparatively less pathology than is seen following focal brain injury and/or axonal transection paradigms, both of which elicit cell death, lack of specific DBI-mediated microglia – axonal interactions during the acute post-injury phases appears reasonable. It is not surprising that DBI-mediated perisomatic TAI, which demonstrates rapid axolemmal closure as discussed in Chapter 2, does not elicit robust microglial / macrophage activation targeting the site of injury. On the other hand, our data do indicate macrophage localization to somata of injured neurons with evidence of bouton disruption. However, the lack of cell death does not allow for a massive inflammatory response given that the primary trigger for such a response (i.e. cell death) is absent.

Ultimately, the balance between neuroprotection and neuropathology within the context of TBI-induced neuroinflammation is delicate. Inflammatory cell recruitment, activation, and repair mechanisms are important components to preserve remaining neuronal structure and function and to protect the brain from potentially more serious consequences. However, the neuroprotective response must be tightly regulated to prevent unintended and deleterious consequences resulting in damage to adjacent uninjured tissue. Appropriate responses to injury must be tapered by mechanisms of downregulation following completion of repair processes. These mechanisms may include migration of inflammatory cells away from injury sites and/or immune cell apoptosis (Vela et al., 2002). Otherwise, an unregulated inflammatory response will ultimately promote increased neuronal injury that will stimulate continued and/or *de novo* inflammatory responses creating vicious cycles of neuronal injury followed by further neuroinflammation leading to even greater neuronal injury. Unfortunately, our current understanding of these regulatory mechanisms is incomplete and merits continued investigation. Through future studies, our comprehension of the basic science mechanisms behind neuroinflammation will lead to therapeutic interventions targeting various steps in the inflammatory cascade, ultimately creating a process that may be manipulated and hence regulated to enhance neuroprotection while limiting unwanted neuropathological consequences.

FUTURE STUDIES

While this dissertation offers new insights into DBI and its associated pathologies, much work still remains to fully comprehend this pathological condition. The anatomical reproducibility of perisomatic TAI within the mediodorsal neocortex, hippocampal dentate gyrus, and dorsolateral thalamus using the midline/central FPI model of moderate severity combined with an established timeline for perisomatic TAI and subsequent secondary axotomy within this cytoarchitectural region provides several possibilities for future investigations. First, regional specificity of perisomatic TAI allows for thorough examination of the consequent deafferentation associated with axotomy, Wallerian change, and synaptic disruption. By focusing on the anatomical endpoints to which injured axons project, the impact of DBI-mediated secondary axotomy on downstream synaptic terminals may be examined. Through collaborative efforts with investigators at other university, we are beginning to examine regional neuronal injury responses to diffuse TBI via Western blot analyses of antibodies targeting pre (e.g. synaptophysin, synaptotagmin) and post-synaptic (e.g. PSD-95, PSD-93) elements as well as axonal constituents (e.g. myelin breakdown products). Following characterization of these injured loci, the anatomical areas to which these injured axons project will then be examined by Western blot and LM / EM immunohistochemistry to determine the mechanisms and consequences of DBI-mediated deafferentation. Although this effort is in its early stages, initial results indicate a coordinated temporal response to diffuse TAI with elevations in myelin

breakdown products followed by synaptic breakdown products (unpublished observations).

In addition to the synaptic fate associated with secondary axotomy, characterization of the axonal disconnection site also requires continued investigation. As reported in Chapter 2, sites of perisomatic axotomy were impermeable to pre-injury administered 10 kDa dextran. While this finding was unexpected and suggested either axolemmal sealing prior to disconnection or ultra-rapid axolemmal closure following axotomy, these hypotheses require additional testing to provide more substantive evidence supporting mechanisms of membrane resealing / repair. Use of a smaller molecular weight dextran molecule may provide insight into potential size disruptions within the axolemma. Perhaps disruption sizes are such that they exclude the 10 kDa dextran but may be permeable to smaller molecular weight species. Similarly, more refined EM studies may provide insight into membranous cytoskeleton structural dynamics at the point of disconnection. Understanding neuronal membrane disruption and resealing is important to designing rational therapeutic strategies aimed at either repairing the membrane itself or targeting ongoing pathologies via intra-neuronal delivery of pharmacological agents during the post-traumatic period.

From the standpoint of DBI-mediated neuroinflammatory responses, initial characterization was offered in Chapter 3 although these findings are only preliminary descriptions of this complex biological process. The midline/central FPI model elicits diffuse TAI within specific anatomical loci that are uncomplicated by elements of focal injury. This offers a unique opportunity to model DBI without underlying focal injury

components that may confound inflammatory cell analyses. One question that arose during evaluation of macrophage immunoreactivity is from where do these cells originate? To date, the precise origin(s) for brain macrophages following trauma remains elusive although the nature of the injury may dictate the relative contributions of endogenous and exogenous cells. Macrophages may differentiate from endogenous microglia following activation, may be recruited from the peripheral blood as monocytes and then differentiate upon arrival at the injury site, or both of these mechanisms may be at work simultaneously. Two experimental strategies could be used to study this question. First, bone marrow chimeric animals may be utilized based on their unique cellular properties. While microglia enter the brain during embryonic development and self-renew, monocytes originate from bone marrow throughout life. Monocytes derived from chimeric bone marrow will have unique protein characteristics distinguishing them from endogenous brain cell populations. Following DBI and macrophage differentiation, antibodies targeting the unique chimeric phenotype could provide evidence of either immunopositive bone marrow-derived monocyte entry, immunonegative microglial differentiation, or a combination of exogenous and endogenous cells. If both macrophage lineages are present, these studies will still provide valuable information as to the relative contributions made by each lineage as well as lineage-dependent localization following injury. In a related approach, pre-injury labeling of circulating blood monocytes with a fluorescent marker could also allow for brain identification and localization of these cells following injury.

In sum, this dissertation provides further characterization of DBI-mediated TAI pathology and neuroinflammatory responses. TAI within the perisomatic domain results in ultra-rapid secondary axotomy with consequent Wallerian change and is highlighted by apparent axolemmal impermeability. The neuroinflammatory response accompanying this pathology is characterized by early, yet initially uncoordinated, and persistent activated microglial / macrophage reactivity which fails to target sites of axonal injury during the acute post-injury stages and does not reveal evidence of immune cell clustering / nodule formation. However, macrophages approximated somata of injured neurons but did not reveal somatic engulfment or phagocytic activity. These immunological findings are distinct from those observed following focal brain injury and further illustrate the heterogeneous responses to DBI. Taken together, these studies provide the impetus for future examinations of the mechanisms of DBI-related pathologies, namely DAI pathogenesis and secondary neuroinflammatory responses.

From a clinical standpoint, the overall number of TBI cases has fallen in recent years; however, one must be careful when interpreting this statistic. If TBI incidents are stratified by their level of severity, severe cases have decreased while mild to moderate cases have remain constant or increased. Improvements in highway safety, vehicle construction, and personal protective equipment have greatly contributed to the decline in severe incidents. However, individuals suffering mild to moderate injury often do not seek medical treatment due to the relative paucity of symptoms only to later present with physical and/or cognitive issues requiring medical attention. In that mild to moderate TBI often includes significant DBI, it is hoped that this work will further

stimulate research into the mechanisms of DBI pathology with the goals of ameliorating or eliminating DAI via targeted therapeutic interventions and manipulating neuroinflammation to maximize neuroprotective effects while minimizing neuropathological consequences.

LIST OF REFERENCES

List of References

Traumatic Brain Injury In the United States: A Report to Congress. 1999. Division of Acute Care, Rehabilitation Research, and Disability Prevention, National Center for Injury Prevention and Control, Centers for Disease Control and Prevention, U.S. Department of Health and Human Services.

Traumatic Brain Injury. Injury Fact Book, 2000-2001. 110-113. 2002. Atlanta, GA, Division of Acute Care, Rehabilitation Research, and Injury Prevention, National Center for Injury Prevention and Control, Centers for Disease Control, U.S. Department of Health and Human Services.

Abou-Hamden A, Blumbergs PC, Scott G, Manavis J, Wainwright H, Jones N, McLean J (1997) Axonal injury in falls. J Neurotrauma 14: 699-713.

Adams JH (1992) Head Injury. In: Greenfield's Neuropathology (Adams JH, Duchen LW, eds), pp 106-152. New York: Oxford University Press.

Adams JH, Doyle D, Ford I, Gennarelli TA, Graham DI, McLellan DR (1989) Diffuse axonal injury in head injury: definition, diagnosis and grading. Histopathology 15: 49-59.

Adams JH, Graham DI, Jennett B (2000) The neuropathology of the vegetative state after an acute brain insult. Brain 123: 1327-1338.

Adams JH, Graham DI, Murray LS, Scott G (1982) Diffuse axonal injury due to nonmissile head injury in humans: an analysis of 45 cases. Ann Neurol 12: 557-563.

Adams JH, Mitchell DE, Graham DI, Doyle D (1977) Diffuse brain damage of immediate impact type. Its relationship to 'primary brain-stem damage' in head injury. Brain 100: 489-502.

Adelson PD, Jenkins LW, Hamilton RL, Robichaud P, Tran MP, Kochanek PM (2001) Histopathologic response of the immature rat to diffuse traumatic brain injury. J Neurotrauma 18: 967-976.

Ahlgren S, Li GL, Olsson Y (1996) Accumulation of beta-amyloid precursor protein and ubiquitin in axons after spinal cord trauma in humans: immunohistochemical observations on autopsy material. Acta Neuropathol (Berl) 92: 49-55.

Ahmed FA, Ingoglia NA, Sharma SC (2001) Axon resealing following transection takes longer in central axons than in peripheral axons: implications for axonal regeneration. Exp Neurol 167: 451-455.

12. Aihara M, Ishii S, Kume K, Shimizu T (2000) Interaction between neurone and microglia mediated by platelet-activating factor. Genes Cells 5: 397-406.

13. Aihara N, Hall JJ, Pitts LH, Fukuda K, Noble LJ (1995) Altered immunoexpression of microglia and macrophages after mild head injury. J Neurotrauma 12: 53-63.

14. Aldskogius H, Kozlova EN (1998) Central neuron-glial and glial-glial interactions following axon injury. Prog Neurobiol 55: 1-26.

15. Aldskogius H, Liu L, Svensson M (1999) Glial responses to synaptic damage and plasticity. J Neurosci Res 58: 33-41.

16. Alexander MP (1995) Mild traumatic brain injury: pathophysiology, natural history, and clinical management. Neurology 45: 1253-1260.

17. Aloisi F (2001) Immune function of microglia. Glia 36: 165-179.

18. Anderson CV, Wood DM, Bigler ED, Blatter DD (1996) Lesion volume, injury severity, and thalamic integrity following head injury. J Neurotrauma 13: 59-65.

19. Babcock AA, Kuziel WA, Rivest S, Owens T (2003) Chemokine expression by glial cells directs leukocytes to sites of axonal injury in the CNS. J Neurosci 23: 7922-7930.

20. Bajetto A, Bonavia R, Barbero S, Schettini G (2002) Characterization of chemokines and their receptors in the central nervous system: physiopathological implications. J Neurochem 82: 1311-1329.

Banati RB (2002) Brain plasticity and microglia: is transsynaptic glial activation in the thalamus after limb denervation linked to cortical plasticity and central sensitisation? J Physiol Paris 96: 289-299.

22. Banati RB (2003) Neuropathological imaging: in vivo detection of glial activation as a measure of disease and adaptive change in the brain. Br Med Bull 65: 121-131.

46. Bruce-Keller AJ (1999) Microglial-neuronal interactions in synaptic damage and recovery. J Neurosci Res 58: 191-201.

47. Buki A, Okonkwo DO, Wang KK, Povlishock JT (2000) Cytochrome c release and caspase activation in traumatic axonal injury. J Neurosci 20: 2825-2834.

48. Buki A, Siman R, Trojanowski JQ, Povlishock JT (1999) The role of calpain-mediated spectrin proteolysis in traumatically induced axonal injury. J Neuropathol Exp Neurol 58: 365-375.

49. Burke-Gaffney A, Keenan AK (1993) Modulation of human endothelial cell permeability by combinations of the cytokines interleukin-1 alpha/beta, tumor necrosis factor-alpha and interferon-gamma. Immunopharmacology 25: 1-9.

50. Buss A, Brook GA, Kakulas B, Martin D, Franzen R, Schoenen J, Noth J, Schmitt AB (2004) Gradual loss of myelin and formation of an astrocytic scar during Wallerian degeneration in the human spinal cord. Brain 127: 34-44.

51. Buss A, Schwab ME (2003) Sequential loss of myelin proteins during Wallerian degeneration in the rat spinal cord. Glia 42: 424-432.

52. Cajal SR (1914) Degeneration and regeneration of the nervous system (English Translation). London: Oxford University Press-1928.

53. Cammermeyer J (1970) The life history of the microglial cell: a light microscopic study. In: Neurosciences Research (Ehrenpreis S, Solnitzky OC, eds), pp 44-130. New York: Academic Press.

54. Carbonell WS, Grady MS (1999) Regional and temporal characterization of neuronal, glial, and axonal response after traumatic brain injury in the mouse. Acta Neuropathol (Berl) 98: 396-406.

55. Carbonell WS, Murase S, Horwitz AF, Mandell JW (2005) Migration of perilesional microglia after focal brain injury and modulation by CC chemokine receptor 5: an in situ time-lapse confocal imaging study. J Neurosci 25: 7040-7047.

56. Chen S, Pickard JD, Harris NG (2003) Time course of cellular pathology after controlled cortical impact injury. Exp Neurol 182: 87-102.

57. Cho BP, Song DY, Sugama S, Shin DH, Shimizu Y, Kim SS, Kim YS, Joh TH (2006) Pathological dynamics of activated microglia following medial forebrain bundle transection. Glia 53: 92-102.

58. Christman CW, Grady MS, Walker SA, Holloway KL, Povlishock JT (1994) Ultrastructural studies of diffuse axonal injury in humans. J Neurotrauma 11: 173-186.

59. Clark RS, Kochanek PM, Chen M, Watkins SC, Marion DW, Chen J, Hamilton RL, Loeffert JE, Graham SH (1999) Increases in Bcl-2 and cleavage of caspase-1 and caspase-3 in human brain after head injury. FASEB J 13: 813-821.

60. Clark RS, Schiding JK, Kaczorowski SL, Marion DW, Kochanek PM (1994) Neutrophil accumulation after traumatic brain injury in rats: comparison of weight drop and controlled cortical impact models. J Neurotrauma 11: 499-506.

61. Clifton GL, Choi SC, Miller ER, Levin HS, Smith KR, Jr., Muizelaar JP, Wagner FC, Jr., Marion DW, Luerssen TG (2001) Intercenter variance in clinical trials of head trauma--experience of the National Acute Brain Injury Study: Hypothermia. J Neurosurg 95: 751-755.

62. Compston A, Zajicek J, Sussman J, Webb A, Hall G, Muir D, Shaw C, Wood A, Scolding N (1997) Glial lineages and myelination in the central nervous system. J Anat 190 (Pt 2): 161-200.

63. Conradi S (1969) Observations on the ultrastructure of the axon hillock and initial axon segment of lumbosacral motoneurons in the cat. Acta Physiol Scand Suppl 332:65-84.: 65-84.

64. Cooper GM (2000) The Cell - A Molecular Approach. Sunderland, MA: Sinauer Associates, Inc.

65. Cortez SC, McIntosh TK, Noble LJ (1989) Experimental fluid percussion brain injury: vascular disruption and neuronal and glial alterations. Brain Res 482: 271-282.

66. Csuka E, Hans VH, Ammann E, Trentz O, Kossmann T, Morganti-Kossmann MC (2000) Cell activation and inflammatory response following traumatic axonal injury in the rat. Neuroreport 11: 2587-2590.

67. Dailey ME, Waite M (1999) Confocal imaging of microglial cell dynamics in hippocampal slice cultures. Methods 18: 222-30, 177.

68. Davalos D, Grutzendler J, Yang G, Kim JV, Zuo Y, Jung S, Littman DR, Dustin ML, Gan WB (2005) ATP mediates rapid microglial response to local brain injury in vivo. Nat Neurosci 8: 752-758.

69. del Rio Hortega P (1932) Microglia. In: Cytology and Cellular Pathology of the Nervous System (Penfield W, ed), pp 483-534. New York: Hoeber.

70. Ding Y, Yao B, Lai Q, McAllister JP (2001) Impaired motor learning and diffuse axonal damage in motor and visual systems of the rat following traumatic brain injury. Neurol Res 23: 193-202.

71. Dixon CE, Lighthall JW, Anderson TE (1988) Physiologic, histopathologic, and cineradiographic characterization of a new fluid-percussion model of experimental brain injury in the rat. J Neurotrauma 5: 91-104.

72. Dixon CE, Lyeth BG, Povlishock JT, Findling RL, Hamm RJ, Marmarou A, Young HF, Hayes RL (1987) A fluid percussion model of experimental brain injury in the rat. J Neurosurg 67: 110-119.

73. Dong JH, Ying GX, Liu X, Wang WY, Wang Y, Ni ZM, Zhou CF (2005) Expression of thymosin beta4 mRNA by activated microglia in the denervated hippocampus. Neuroreport 16: 1629-1633.

74. Dong JH, Ying GX, Liu X, Wang WY, Wang Y, Ni ZM, Zhou CF (2006) Lesion-induced gelsolin upregulation in the hippocampus following entorhinal deafferentation. Hippocampus 16: 91-100.

75. Dong JH, Ying GX, Zhou CF (2004) Entorhinal deafferentation induces the expression of profilin mRNA in the reactive microglial cells in the hippocampus. Glia 47: 102-108.

76. Egan DA, Flumerfelt BA, Gwyn DG (1977) Axon reaction in the red nucleus of the rat. Perikaryal volume changes and the time course of chromatolysis following cervical and thoracic lesions. Acta Neuropathol (Berl) 37: 13-19.

77. Elder GA, Friedrich VL, Jr., Kang C, Bosco P, Gourov A, Tu PH, Zhang B, Lee VM, Lazzarini RA (1998) Requirement of heavy neurofilament subunit in the development of axons with large calibers. J Cell Biol 143: 195-205.

78. Fagan AM, Gage FH (1990) Cholinergic sprouting in the hippocampus: a proposed role for IL-1. Exp Neurol 110: 105-120.

79. Farkas O, Lifshitz J, Povlishock JT (2006) Mechanoporation induced by diffuse traumatic brain injury: an irreversible or reversible response to injury? J Neurosci 26: 3130-3140.

80. Finnie JW, Blumbergs PC, Manavis J, Summersides GE, Davies RA (2000) Evaluation of brain damage resulting from penetrating and non-penetrating captive bolt stunning using lambs. Aust Vet J 78: 775-778.

81. Finnie JW, Manavis J, Blumbergs PC, Summersides GE (2002) Brain damage in sheep from penetrating captive bolt stunning. Aust Vet J 80: 67-69.

82. Fitzpatrick MO, Maxwell WL, Graham DI (1998) The role of the axolemma in the initiation of traumatically induced axonal injury. J Neurol Neurosurg Psychiatry 64: 285-287.

83. Gallyas F, Farkas O, Mazlo M (2002) Traumatic compaction of the axonal cytoskeleton induces argyrophilia: histological and theoretical importance. Acta Neuropathol (Berl) 103: 36-42.

84. Geddes JF, Vowles GH, Beer TW, Ellison DW (1997) The diagnosis of diffuse axonal injury: implications for forensic practice. Neuropathol Appl Neurobiol 23: 339-347.

85. Gehrmann J, Mies G, Bonnekoh P, Banati R, Iijima T, Kreutzberg GW, Hossmann KA (1993) Microglial reaction in the rat cerebral cortex induced by cortical spreading depression. Brain Pathol 3: 11-17.

86. Gennarelli TA, Thibault LE, Adams JH, Graham DI, Thompson CJ, Marcincin RP (1982) Diffuse axonal injury and traumatic coma in the primate. Ann Neurol 12: 564-574.

87. Gennarelli TA, Tipperman R, Maxwell WL, Graham DI, Adams JH, Irvine A (1993) Traumatic damage to the nodal axolemma: an early, secondary injury. Acta Neurochir Suppl (Wien) 57: 49-52.

88. Gentleman SM, Leclercq PD, Moyes L, Graham DI, Smith C, Griffin WS, Nicoll JA (2004) Long-term intracerebral inflammatory response after traumatic brain injury. Forensic Sci Int 146: 97-104.

89. Gentleman SM, Nash MJ, Sweeting CJ, Graham DI, Roberts GW (1993) Beta-amyloid precursor protein (beta APP) as a marker for axonal injury after head injury. Neurosci Lett 160: 139-144.

90. Gentleman SM, Roberts GW, Gennarelli TA, Maxwell WL, Adams JH, Kerr S, Graham DI (1995) Axonal injury: a universal consequence of fatal closed head injury? Acta Neuropathol (Berl) 89: 537-543.

91. George R, Griffin JW (1994) Delayed macrophage responses and myelin clearance during Wallerian degeneration in the central nervous system: the dorsal radiculotomy model. Exp Neurol 129: 225-236.

92. Giehl KM, Tetzlaff W (1996) BDNF and NT-3, but not NGF, prevent axotomy-induced death of rat corticospinal neurons in vivo. Eur J Neurosci 8: 1167-1175.

93. Giulian D, Chen J, Ingeman JE, George JK, Noponen M (1989) The role of mononuclear phagocytes in wound healing after traumatic injury to adult mammalian brain. J Neurosci 9: 4416-4429.

94. Gleckman AM, Bell MD, Evans RJ, Smith TW (1999) Diffuse axonal injury in infants with nonaccidental craniocerebral trauma: enhanced detection by beta-amyloid precursor protein immunohistochemical staining. Arch Pathol Lab Med 123: 146-151.

95. Goldstein LS, Yang Z (2000) Microtubule-based transport systems in neurons: the roles of kinesins and dyneins. Annu Rev Neurosci 23:39-71.: 39-71.

96. Goodman JC, Robertson CS, Grossman RG, Narayan RK (1990) Elevation of tumor necrosis factor in head injury. J Neuroimmunol 30: 213-217.

97. Gotow T, Tanaka T, Nakamura Y, Takeda M (1994) Dephosphorylation of the largest neurofilament subunit protein influences the structure of crossbridges in reassembled neurofilaments. J Cell Sci 107: 1949-1957.

98. Grady MS, McLaughlin MR, Christman CW, Valadka AB, Fligner CL, Povlishock JT (1993) The use of antibodies targeted against the neurofilament subunits for the detection of diffuse axonal injury in humans. J Neuropathol Exp Neurol 52: 143-152.

99. Graeber MB, Lopez-Redondo F, Ikoma E, Ishikawa M, Imai Y, Nakajima K, Kreutzberg GW, Kohsaka S (1998) The microglia/macrophage response in the neonatal rat facial nucleus following axotomy. Brain Res 813: 241-253.

100. Graham DI (1996) Neuropathology of Head Injury. In: Neurotrauma (Narayan RK, Wilberger JE, Povlishock JT, eds), pp 43-59. New York: McGraw-Hill.

101. Graham DI, Gennarelli T, McIntosh T (2002) Trauma. In: Greenfield's Neuropathology (Graham DI, Lantos PL, eds), pp 823-898. London: Arnold.

102. Griffin JW, George EB, Hsieh S, Glass JD (1995) Axonal degeneration and disorders of the axonal cytoskeleton. In: The Axon: Structure, Function, and Pathophysiology (Waxman SG, Kocsis JD, Stys PK, eds), pp 375-390. New York: Oxford University Press.

103. Griffin WS, Sheng JG, Gentleman SM, Graham DI, Mrak RE, Roberts GW (1994) Microglial interleukin-1 alpha expression in human head injury: correlations with neuronal and neuritic beta-amyloid precursor protein expression. Neurosci Lett 176: 133-136.

104. Grossmann R, Stence N, Carr J, Fuller L, Waite M, Dailey ME (2002) Juxtavascular microglia migrate along brain microvessels following activation during early postnatal development. Glia 37: 229-240.

105. Guerrero JL, Thurman DJ, Sniezek JE (2000) Emergency department visits associated with traumatic brain injury: United States, 1995-1996. Brain Inj 14: 181-186.

106. Hall ED, Gibson TR, Pavel KM (2005a) Lack of a gender difference in post-traumatic neurodegeneration in the mouse controlled cortical impact injury model. J Neurotrauma 22: 669-679.

107. Hall ED, Sullivan PG, Gibson TR, Pavel KM, Thompson BM, Scheff SW (2005b) Spatial and temporal characteristics of neurodegeneration after controlled cortical impact in mice: more than a focal brain injury. J Neurotrauma 22: 252-265.

108. Hansson E, Ronnback L (2003) Glial neuronal signaling in the central nervous system. FASEB J 17: 341-348.

109. Hardman JM, Manoukian A (2002) Pathology of head trauma. Neuroimaging Clin N Am 12: 175-87, vii.

110. Hartl R, Medary M, Ruge M, Arfors KE, Ghajar J (1997a) Blood-brain barrier breakdown occurs early after traumatic brain injury and is not related to white blood cell adherence. Acta Neurochir Suppl 70: 240-242.

111. Hartl R, Medary MB, Ruge M, Arfors KE, Ghajar J (1997b) Early white blood cell dynamics after traumatic brain injury: effects on the cerebral microcirculation. J Cereb Blood Flow Metab 17: 1210-1220.

112. He MH, Cheung ZH, Yu EH, Tay DK, So KF (2004) Cytochrome c release and caspase-3 activation in retinal ganglion cells following different distance of axotomy of the optic nerve in adult hamsters. Neurochem Res 29: 2153-2161.

113. Heidemann SR, Hamborg MA, Thomas SJ, Song B, Lindley S, Chu D (1985) Spatial organization of axonal microtubules. j CELL BIOL 99: 1289-1295.

114. Hermann DM, Mies G, Hata R, Hossmann KA (2000) Microglial and astrocytic reactions prior to onset of thalamic cell death after traumatic lesion of the rat sensorimotor cortex. Acta Neuropathol (Berl) 99: 147-153.

115. Hicks R, Soares H, Smith D, McIntosh T (1996) Temporal and spatial characterization of neuronal injury following lateral fluid-percussion brain injury in the rat. Acta Neuropathol (Berl) 91: 236-246.

116. Hide I, Tanaka M, Inoue A, Nakajima K, Kohsaka S, Inoue K, Nakata Y (2000) Extracellular ATP triggers tumor necrosis factor-alpha release from rat microglia. J Neurochem 75: 965-972.

117. Hirokawa N (1991) Molecular architecture and dynamics of the neuronal cytoskeleton. In: The Neuronal Cytoskeleton (R.D.Burgoyne, ed), pp 5-75. New York: Wiley-Liss.

118. Hitt AL, Luna EJ (1994) Membrane interactions with the actin cytoskeleton. Curr Opin Cell Biol 6: 120-130.

119. Hoek RM, Ruuls SR, Murphy CA, Wright GJ, Goddard R, Zurawski SM, Blom B, Homola ME, Streit WJ, Brown MH, Barclay AN, Sedgwick JD (2000) Down-regulation of the macrophage lineage through interaction with OX2 (CD200). Science 290: 1768-1771.

120. Honda S, Sasaki Y, Ohsawa K, Imai Y, Nakamura Y, Inoue K, Kohsaka S (2001) Extracellular ATP or ADP induce chemotaxis of cultured microglia through Gi/o-coupled P2Y receptors. J Neurosci 21: 1975-1982.

121. Jafari SS, Maxwell WL, Neilson M, Graham DI (1997) Axonal cytoskeletal changes after non-disruptive axonal injury. J Neurocytol 26: 207-221.

122. Jafari SS, Nielson M, Graham DI, Maxwell WL (1998) Axonal cytoskeletal changes after nondisruptive axonal injury. II. Intermediate sized axons. J Neurotrauma 15: 955-966.

123. Julien JP, Mushynski WE (1998) Neurofilaments in health and disease. Prog Nucleic Acid Res Mol Biol 61: 1-23.

124. Kampfl A, Posmantur RM, Zhao X, Schmutzhard E, Clifton GL, Hayes RL (1997) Mechanisms of calpain proteolysis following traumatic brain injury: implications for pathology and therapy: implications for pathology and therapy: a review and update. J Neurotrauma 14: 121-134.

125. Katz DI, Alexander MP (1994) Traumatic brain injury. Predicting course of recovery and outcome for patients admitted to rehabilitation. Arch Neurol 51: 661-670.

126. Kim SU, de Vellis J (2005) Microglia in health and disease. J Neurosci Res 81: 302-313.

127. Kim YS, Kim SS, Cho JJ, Choi DH, Hwang O, Shin DH, Chun HS, Beal MF, Joh TH (2005) Matrix metalloproteinase-3: a novel signaling proteinase from apoptotic neuronal cells that activates microglia. J Neurosci 25: 3701-3711.

128. Kirkpatrick LL, Brady ST (1999) Basic Neurochemistry: Molecular, Cellular, and Medical Aspects. Philadelphia: Lippincott-Raven.

129. Kraus JF, McArthur DL, Silverman TA, Jayaraman M (1996) Epidemiology of Head Injury. In: Neurotrauma (Narayan RK, Wilberger JE, Povlishock JT, eds), pp 13-30. New York: McGraw Hill.

130. Kreutzberg GW (1995) Reaction of the neuronal cell body to axonal damage. In: The Axon (Waxman SG, Kocsis JD, Stys PK, eds), pp 355-374. New York: Oxford University Press.

131. Kreutzberg GW (1996) Microglia: a sensor for pathological events in the CNS Trends Neurosci 19: 312-318.

132. Ladeby R, Wirenfeldt M, Garcia-Ovejero D, Fenger C, Dissing-Olesen L, Dalmau I, Finsen B (2005) Microglial cell population dynamics in the injured adult central nervous system. Brain Res Brain Res Rev 48: 196-206.

133. Langlois, J. A., Rutland-Brown W, and Thomas K.E. Truamatic Brain Injury in the United States: Emergency Department Visits, Hospitalizations, and Deaths. 2004. Atlanta, GA, Centers for Disease Control and Prevention, National Center for Injury Prevention and Control.

134. Lee MK, Cleveland DW (1996) Neuronal intermediate filaments. Annu Rev Neurosci 19:187-217.: 187-217.

135. Levin HS (1989) Neurobehavioral outcome of mild to moderate head injury. In: Mild to Moderate Head Injury (Hoff JT, Anderson TE, Cole TM, eds), pp 153-195. Boston: Blackwell Scientific.

136. Lewen A, Li GL, Nilsson P, Olsson Y, Hillered L (1995) Traumatic brain injury in rat produces changes of beta-amyloid precursor protein immunoreactivity. Neuroreport 6: 357-360.

137. Lewis SB, Finnie JW, Blumbergs PC, Scott G, Manavis J, Brown C, Reilly PL, Jones NR, McLean AJ (1996) A head impact model of early axonal injury in the sheep. J Neurotrauma 13: 505-514.

138. Li GL, Farooque M, Holtz A, Olsson Y (1995) Changes of beta-amyloid precursor protein after compression trauma to the spinal cord: an experimental study in the rat using immunohistochemistry. J Neurotrauma 12: 269-277.

139. Lieberman AR (1971) The axon reaction: a review of the principal features of perikaryal responses to axon injury. Int Rev Neurobiol 14:49-124.: 49-124.

140. Liu PH, Wang YJ, Tseng GF (2003) Close axonal injury of rubrospinal neurons induced transient perineuronal astrocytic and microglial reaction that coincided with their massive degeneration. Exp Neurol 179: 111-126.

141. Lodish H, Berk A, Zipursky SL, Matsudaira P, Baltimore D, Darnell JE (1999) Molecular Cell Biology. W.H. Freeman & Co.

142. LoPachin RM, Lehning EJ (1997) Mechanism of calcium entry during axon injury and degeneration. Toxicol Appl Pharmacol 143: 233-244.

143. Lubinska L (1977) Early course of Wallerian degeneration in myelinated fibres of the rat phrenic nerve. Brain Res 130: 47-63.

144. Ludwin SK (1997) The pathobiology of the oligodendrocyte. J Neuropathol Exp Neurol 56: 111-124.

145. Lunn ER, Perry VH, Brown MC, Rosen H, Gordon S (1989) Absence of Wallerian Degeneration does not Hinder Regeneration in Peripheral Nerve. Eur J Neurosci 1: 27-33.

146. Margulies SS, Thibault LE (1989) An analytical model of traumatic diffuse brain injury. J Biomech Eng 111: 241-249.

147. Margulies SS, Thibault LE, Gennarelli TA (1990) Physical model simulations of brain injury in the primate. J Biomech 23: 823-836.

148. Markgraf CG, Clifton GL, Moody MR (2001) Treatment window for hypothermia in brain injury. J Neurosurg 95: 979-983.

149. Marmarou CR, Walker SA, Davis CL, Povlishock JT (2005) Quantitative analysis of the relationship between intra- axonal neurofilament compaction and impaired axonal transport following diffuse traumatic brain injury. J Neurotrauma 22: 1066-1080.

150. Masumura M, Hata R, Uramoto H, Murayama N, Ohno T, Sawada T (2000) Altered expression of amyloid precursors proteins after traumatic brain injury in rats: in situ hybridization and immunohistochemical study. J Neurotrauma 17: 123-134.

151. Mathew P, Graham DI, Bullock R, Maxwell W, McCulloch J, Teasdale G (1994) Focal brain injury: histological evidence of delayed inflammatory response in a new rodent model of focal cortical injury. Acta Neurochir Suppl (Wien) 60: 428-430.

152. Maxwell WL, Domleo A, McColl G, Jafari SS, Graham DI (2003) Post-acute alterations in the axonal cytoskeleton after traumatic axonal injury. J Neurotrauma 20: 151-168.

153. Maxwell WL, Graham DI (1997) Loss of axonal microtubules and neurofilaments after stretch-injury to guinea pig optic nerve fibers. J Neurotrauma 14: 603-614.

154. Maxwell WL, Irvine A, Graham, Adams JH, Gennarelli TA, Tipperman R, Sturatis M (1991) Focal axonal injury: the early axonal response to stretch. J Neurocytol 20: 157-164.

155. Maxwell WL, Kosanlavit R, McCreath BJ, Reid O, Graham DI (1999) Freeze-fracture and cytochemical evidence for structural and functional alteration in the axolemma and myelin sheath of adult guinea pig optic nerve fibers after stretch injury. J Neurotrauma 16: 273-284.

156. Maxwell WL, McCreath BJ, Graham DI, Gennarelli TA (1995) Cytochemical evidence for redistribution of membrane pump calcium- ATPase and ecto-Ca-ATPase activity, and calcium influx in myelinated nerve fibres of the optic nerve after stretch injury. J Neurocytol 24: 925-942.

157. Maxwell WL, Pennington K, MacKinnon MA, Smith DH, McIntosh TK, Wilson JT, Graham DI (2004) Differential responses in three thalamic nuclei in moderately disabled, severely disabled and vegetative patients after blunt head injury. Brain 127: 2470-2478.

158. Maxwell WL, Povlishock JT, Graham DL (1997) A mechanistic analysis of nondisruptive axonal injury: a review [published erratum appears in J Neurotrauma 1997 Oct;14(10):755]. J Neurotrauma 14: 419-440.

159. McBride RL, Feringa ER, Garver MK, Williams JK, Jr. (1989) Prelabeled red nucleus and sensorimotor cortex neurons of the rat survive 10 and 20 weeks after spinal cord transection. J Neuropathol Exp Neurol 48: 568-576.

160. McClain C, Cohen D, Phillips R, Ott L, Young B (1991) Increased plasma and ventricular fluid interleukin-6 levels in patients with head injury. J Lab Clin Med 118: 225-231.

161. McIntosh TK, Noble L, Andrews B, Faden AI (1987) Traumatic brain injury in the rat: characterization of a midline fluid-percussion model. Cent Nerv Syst Trauma 4: 119-134.

162. McIntosh TK, Vink R, Noble L, Yamakami I, Fernyak S, Soares H, Faden AI (1989) Traumatic brain injury in the rat: characterization of a lateral fluid-percussion model. Neuroscience 28: 233-244.

163. McKenzie JE, Gentleman SM, Roberts GW, Graham DI, Royston MC (1994) Increased numbers of beta APP-immunoreactive neurones in the entorhinal cortex after head injury. Neuroreport 6: 161-164.

164. McKenzie KJ, McLellan DR, Gentleman SM, Maxwell WL, Gennarelli TA, Graham DI (1996) Is beta-APP a marker of axonal damage in short-surviving head injury? Acta Neuropathol (Berl) 92: 608-613.

165. McNeil PL, Baker MM (2001) Cell surface events during resealing visualized by scanning-electron microscopy. Cell Tissue Res 304: 141-146.

166. Meaney DF, Smith DH, Shreiber DI, Bain AC, Miller RT, Ross DT, Gennarelli TA (1995) Biomechanical analysis of experimental diffuse axonal injury. J Neurotrauma 12: 689-694.

167. Merline M, Kalil K (1990) Cell death of corticospinal neurons is induced by axotomy before but not after innervation of spinal targets. J Comp Neurol 296: 506-516.

168. Meythaler JM, Peduzzi JD, Eleftheriou E, Novack TA (2001) Current concepts: diffuse axonal injury-associated traumatic brain injury. Arch Phys Med Rehabil 82: 1461-1471.

169. Mitchison T, Kirschner M (1984) Dynamic instability of microtubule growth. Nature 312: 237-242.

170. Mizuno T, Kawanokuchi J, Numata K, Suzumura A (2003) Production and neuroprotective functions of fractalkine in the central nervous system. Brain Res 979: 65-70.

171. Morganti-Kossmann MC, Rancan M, Stahel PF, Kossmann T (2002) Inflammatory response in acute traumatic brain injury: a double-edged sword. Curr Opin Crit Care 8: 101-105.

172. Mori M, Aihara M, Kume K, Hamanoue M, Kohsaka S, Shimizu T (1996) Predominant expression of platelet-activating factor receptor in the rat brain microglia. J Neurosci 16: 3590-3600.

173. Murakami N, Yamaki T, Iwamoto Y, Sakakibara T, Kobori N, Fushiki S, Ueda S (1998) Experimental brain injury induces expression of amyloid precursor protein, which may be related to neuronal loss in the hippocampus. J Neurotrauma 15: 993-1003.

174. Narayan RK, Michel ME, Ansell B, Baethmann A, Biegon A, Bracken MB, Bullock MR, Choi SC, Clifton GL, Contant CF, Coplin WM, Dietrich WD, Ghajar J, Grady SM, Grossman RG, Hall ED, Heetderks W, Hovda DA, Jallo J, Katz RL, Knoller N, Kochanek PM, Maas AI, Majde J, Marion DW, Marmarou A, Marshall LF, McIntosh TK, Miller E, Mohberg N, Muizelaar JP, Pitts LH, Quinn P, Riesenfeld G, Robertson CS, Strauss KI, Teasdale G, Temkin N, Tuma R, Wade C, Walker MD, Weinrich M, Whyte J, Wilberger J, Young AB, Yurkewicz L (2002) Clinical trials in head injury. J Neurotrauma 19: 503-557.

175. NIH Consensus Development Panel on Rehabilitation of Persons With Traumatic Brain Injury (1999) Rehabilitation of persons with traumatic brain injury. JAMA 282: 974-983.

176. Nimmerjahn A, Kirchhoff F, Helmchen F (2005) Resting microglial cells are highly dynamic surveillants of brain parenchyma in vivo. Science 308: 1314-1318.

177. Nishiyori A, Minami M, Ohtani Y, Takami S, Yamamoto J, Kawaguchi N, Kume T, Akaike A, Satoh M (1998) Localization of fractalkine and CX3CR1 mRNAs in rat brain: does fractalkine play a role in signaling from neuron to microglia? FEBS Lett 429: 167-172.

178. Nixon RA, Lewis SE, Dahl D, Marotta CA, Drager UC (1989) Early posttranslational modifications of the three neurofilament subunits in mouse retinal ganglion cells: neuronal sites and time course in relation to subunit polymerization and axonal transport. Brain Res Mol Brain Res 5: 93-108.

179. Noda M, Nakanishi H, Nabekura J, Akaike N (2000) AMPA-kainate subtypes of glutamate receptor in rat cerebral microglia. J Neurosci 20: 251-258.

180. Oehmichen M, Meissner C, Schmidt V, Pedal I, Konig HG, Saternus KS (1998) Axonal injury--a diagnostic tool in forensic neuropathology? A review. Forensic Sci Int 95: 67-83.

181. Oehmichen M, Theuerkauf I, Meissner C (1999) Is traumatic axonal injury (AI) associated with an early microglial activation? Application of a double-labeling technique for simultaneous detection of microglia and AI. Acta Neuropathol (Berl) 97: 491-494.

182. Ohtani Y, Minami M, Satoh M (2000) Expression of inducible nitric oxide synthase mRNA and production of nitric oxide are induced by adenosine triphosphate in cultured rat microglia. Neurosci Lett 293: 72-74.

183. Okonkwo DO, Pettus EH, Moroi J, Povlishock JT (1998) Alteration of the neurofilament sidearm and its relation to neurofilament compaction occurring with traumatic axonal injury. Brain Res 784: 1-6.

184. Otto VI, Stahel PF, Rancan M, Kariya K, Shohami E, Yatsiv I, Eugster HP, Kossmann T, Trentz O, Morganti-Kossmann MC (2001) Regulation of chemokines and chemokine receptors after experimental closed head injury. Neuroreport 12: 2059-2064.

185. Palacios G (1990) A double immunocytochemical and histochemical technique for demonstration of cholinergic neurons and microglial cells in basal forebrain and neostriatum of the rat. Neurosci Lett 115: 13-18.

186. Paxinos G, Watson C (1986) The Rat Brain in Stereotaxic Coordinates. New York: Academic Press.

187. Pearson VL, Rothwell NJ, Toulmond S (1999) Excitotoxic brain damage in the rat induces interleukin-1beta protein in microglia and astrocytes: correlation with the progression of cell death. Glia 25: 311-323.

188. Perry VH, Brown MC, Lunn ER (1991) Very Slow Retrograde and Wallerian Degeneration in the CNS of C57BL/Ola Mice. Eur J Neurosci 3: 102-105.

189. Perry VH, Brown MC, Lunn ER, Tree P, Gordon S (1990) Evidence that Very Slow Wallerian Degeneration in C57BL/Ola Mice is an Intrinsic Property of the Peripheral Nerve. Eur J Neurosci 2: 802-808.

190. Persson L (1976) Cellular reactions to small cerebral stab wounds in the rat frontal lobe. An ultrastructural study. Virchows Arch B Cell Pathol 22: 21-37.

191. Pesini P, Kopp J, Wong H, Walsh JH, Grant G, Hokfelt T (1999) An immunohistochemical marker for Wallerian degeneration of fibers in the central and peripheral nervous system. Brain Res 828: 41-59.

192. Peters A, Palay S, Webster H (1991) The Fine Structure of the Nervous System. New York: Oxford University Press.

193. Pettus EH, Christman CW, Giebel ML, Povlishock JT (1994) Traumatically induced altered membrane permeability: its relationship to traumatically induced reactive axonal change. J Neurotrauma 11: 507-522.

194. Pettus EH, Povlishock JT (1996) Characterization of a distinct set of intra-axonal ultrastructural changes associated with traumatically induced alteration in axolemmal permeability. Brain Res 722: 1-11.

195. Pierce JE, Smith DH, Trojanowski JQ, McIntosh TK (1998) Enduring cognitive, neurobehavioral and histopathological changes persist for up to one year following severe experimental brain injury in rats. Neuroscience 87: 359-369.

196. Pierce JE, Trojanowski JQ, Graham DI, Smith DH, McIntosh TK (1996) Immunohistochemical characterization of alterations in the distribution of amyloid precursor proteins and beta-amyloid peptide after experimental brain injury in the rat. J Neurosci 16: 1083-1090.

197. Pijak DS, Hall GF, Tenicki PJ, Boulos AS, Lurie DI, Selzer ME (1996) Neurofilament spacing, phosphorylation, and axon diameter in regenerating and uninjured lamprey axons. J Comp Neurol 368: 569-581.

198. Polazzi E, Contestabile A (2002) Reciprocal interactions between microglia and neurons: from survival to neuropathology. Rev Neurosci 13: 221-242.

199. Polazzi E, Contestabile A (2003) Neuron-conditioned media differentially affect the survival of activated or unstimulated microglia: evidence for neuronal control on apoptotic elimination of activated microglia. J Neuropathol Exp Neurol 62: 351-362.

200. Popovich PG, Hickey WF (2001) Bone marrow chimeric rats reveal the unique distribution of resident and recruited macrophages in the contused rat spinal cord. J Neuropathol Exp Neurol 60: 676-685.

201. Popovich PG, Wei P, Stokes BT (1997) Cellular inflammatory response after spinal cord injury in Sprague-Dawley and Lewis rats. J Comp Neurol 377: 443-464.

202. Povlishock JT (1992) Traumatically induced axonal injury: pathogenesis and pathobiological implications. Brain Pathol 2: 1-12.

203. Povlishock JT, Becker DP (1985) Fate of reactive axonal swellings induced by head injury. Lab Invest 52: 540-552.

204. Povlishock JT, Becker DP, Cheng CL, Vaughan GW (1983) Axonal change in minor head injury. J Neuropathol Exp Neurol 42: 225-242.

205. Povlishock JT, Christman CW (1995) The pathobiology of traumatically induced axonal injury in animals and humans: a review of current thoughts. J Neurotrauma 12: 555-564.

206. Povlishock JT, Marmarou A, McIntosh T, Trojanowski JQ, Moroi J (1997) Impact acceleration injury in the rat: evidence for focal axolemmal change and related neurofilament sidearm alteration. J Neuropathol Exp Neurol 56: 347-359.

207. Povlishock JT, Pettus EH (1996) Traumatically induced axonal damage: evidence for enduring changes in axolemmal permeability with associated cytoskeletal change. Acta Neurochir Suppl (Wien) 66:81-6: 81-86.

208. Raghupathi R, Graham DI, McIntosh TK (2000) Apoptosis after traumatic brain injury. J Neurotrauma 17: 927-938.

209. Raine CS (1999) Neurocellular Anatomy. In: Basic Neurochemistry (Siegel GJ, Agranoff BW, Albers RW, Fisher SK, Uhler MD, eds), pp 3-30. Philadelphia: Lippencott - Raven.

210. Raivich G, Bohatschek M, Kloss CU, Werner A, Jones LL, Kreutzberg GW (1999) Neuroglial activation repertoire in the injured brain: graded response, molecular mechanisms and cues to physiological function. Brain Res Brain Res Rev 30: 77-105.

211. Raivich G, Jones LL, Kloss CU, Werner A, Neumann H, Kreutzberg GW (1998) Immune surveillance in the injured nervous system: T-lymphocytes invade the axotomized mouse facial motor nucleus and aggregate around sites of neuronal degeneration. J Neurosci 18: 5804-5816.

212. Rancan M, Otto VI, Hans VH, Gerlach I, Jork R, Trentz O, Kossmann T, Morganti-Kossmann MC (2001) Upregulation of ICAM-1 and MCP-1 but not of MIP-2 and sensorimotor deficit in response to traumatic axonal injury in rats. J Neurosci Res 63: 438-446.

213. Rodriguez-Paez AC, Brunschwig JP, Bramlett HM (2005) Light and electron microscopic assessment of progressive atrophy following moderate traumatic brain injury in the rat. Acta Neuropathol (Berl) 109: 603-616.

214. Saatman KE, Abai B, Grosvenor A, Vorwerk CK, Smith DH, Meaney DF (2003) Traumatic axonal injury results in biphasic calpain activation and retrograde transport impairment in mice. J Cereb Blood Flow Metab 23: 34-42.

215. Saatman KE, Bozyczko-Coyne D, Marcy V, Siman R, McIntosh TK (1996) Prolonged calpain-mediated spectrin breakdown occurs regionally following experimental brain injury in the rat. J Neuropathol Exp Neurol 55: 850-860.

216. Sanz JM, Di Virgilio F (2000) Kinetics and mechanism of ATP-dependent IL-1 beta release from microglial cells. J Immunol 164: 4893-4898.

217. Sato M, Chang E, Igarashi T, Noble LJ (2001) Neuronal injury and loss after traumatic brain injury: time course and regional variability. Brain Res 917: 45-54.

218. Savchenko VL, McKanna JA, Nikonenko IR, Skibo GG (2000) Microglia and astrocytes in the adult rat brain: comparative immunocytochemical analysis demonstrates the efficacy of lipocortin 1 immunoreactivity. Neuroscience 96: 195-203.

219. Schmidt RH, Grady MS (1993) Regional patterns of blood-brain barrier breakdown following central and lateral fluid percussion injury in rodents. J Neurotrauma 10: 415-430.

220. Schwartz JH, Westbrook GL (2000) Principles of Neural Science. New York: McGraw-Hill.

221. Shaw G (1991) Neurofilament Proteins. In: The Neuronal Cytoskeleton (R.D.Burgoyne, ed), pp 185-214. New York: Wiley-Liss, Inc.

222. Sherriff FE, Bridges LR, Gentleman SM, Sivaloganathan S, Wilson S (1994a) Markers of axonal injury in post mortem human brain. Acta Neuropathol (Berl) 88: 433-439.

223. Sherriff FE, Bridges LR, Sivaloganathan S (1994b) Early detection of axonal injury after human head trauma using immunocytochemistry for beta-amyloid precursor protein. Acta Neuropathol (Berl) 87: 55-62.

224. Shigematsu K, McGeer PL (1992) Accumulation of amyloid precursor protein in neurons after intraventricular injection of colchicine. Am J Pathol 140: 787-794.

225. Shigemoto-Mogami Y, Koizumi S, Tsuda M, Ohsawa K, Kohsaka S, Inoue K (2001) Mechanisms underlying extracellular ATP-evoked interleukin-6 release in mouse microglial cell line, MG-5. J Neurochem 78: 1339-1349.

226. Shih AY, Fernandes HB, Choi FY, Kozoriz MG, Liu Y, Li P, Cowan CM, Klegeris A (2006) Policing the police: astrocytes modulate microglial activation. J Neurosci 26: 3887-3888.

227. Shohami E, Ginis I, Hallenbeck JM (1999) Dual role of tumor necrosis factor alpha in brain injury. Cytokine Growth Factor Rev 10: 119-130.

228. Siegel SE, Agranoff BW, Albers RW, Fisher SK, Uhler MD (1999) Basic Neurochemistry: Molecular, Cellular and Medical Aspects. Philadelphia: Lippincott-Raven.

229. Sievers C, Platt N, Perry VH, Coleman MP, Conforti L (2003) Neurites undergoing Wallerian degeneration show an apoptotic-like process with Annexin V positive staining and loss of mitochondrial membrane potential. Neurosci Res 46: 161-169.

230. Sihag RK, Nixon RA (1989) In vivo phosphorylation of distinct domains of the 70-kilodalton neurofilament subunit involves different protein kinases. J Biol Chem 264: 457-464.

231. Sihag RK, Nixon RA (1990) Phosphorylation of the amino-terminal head domain of the middle molecular mass 145-kDa subunit of neurofilaments. Evidence for regulation by second messenger-dependent protein kinases. J Biol Chem 265: 4166-4171.

232. Singleton RH, Povlishock JT (2004) Identification and characterization of heterogeneous neuronal injury and death in regions of diffuse brain injury: evidence for multiple independent injury phenotypes. J Neurosci 24: 3543-3553.

233. Singleton RH, Zhu J, Stone JR, Povlishock JT (2002) Traumatically induced axotomy adjacent to the soma does not result in acute neuronal death. J Neurosci 22: 791-802.

234. Smith DH, Chen XH, Xu BN, McIntosh TK, Gennarelli TA, Meaney DF (1997) Characterization of diffuse axonal pathology and selective hippocampal damage following inertial brain trauma in the pig. J Neuropathol Exp Neurol 56: 822-834.

235. Smith DH, Wolf JA, Lusardi TA, Lee VM, Meaney DF (1999) High tolerance and delayed elastic response of cultured axons to dynamic stretch injury. J Neurosci 19: 4263-4269.

236. Soares HD, Hicks RR, Smith D, McIntosh TK (1995) Inflammatory leukocytic recruitment and diffuse neuronal degeneration are separate pathological processes resulting from traumatic brain injury. J Neurosci 15: 8223-8233.

237. Sosin DM, Sniezek JE, Waxweiler RJ (1995) Trends in death associated with traumatic brain injury, 1979 through 1992. Success and failure. JAMA 273: 1778-1780.

238. Stence N, Waite M, Dailey ME (2001) Dynamics of microglial activation: a confocal time-lapse analysis in hippocampal slices. Glia 33: 256-266.

239. Stoll G, Jander S, Schroeter M (2002) Detrimental and beneficial effects of injury-induced inflammation and cytokine expression in the nervous system. Adv Exp Med Biol 513: 87-113.

240. Stone JR, Okonkwo DO, Dialo AO, Rubin DG, Mutlu LK, Povlishock JT, Helm GA (2004) Impaired axonal transport and altered axolemmal permeability occur in distinct populations of damaged axons following traumatic brain injury. Exp Neurol 190: 59-69.

241. Stone JR, Singleton RH, Povlishock JT (2000) Antibodies to the C-terminus of the beta-amyloid precursor protein (APP): a site specific marker for the detection of traumatic axonal injury. Brain Res 871: 288-302.

242. Stone JR, Walker SA, Povlishock JT (1999) The visualization of a new class of traumatically injured axons through the use of a modified method of microwave antigen retrieval. Acta Neuropathol (Berl) 97: 335-345.

243. Streit WJ (2000) Microglial response to brain injury: a brief synopsis. Toxicol Pathol 28: 28-30.

244. Streit WJ (2002) Microglia as neuroprotective, immunocompetent cells of the CNS. Glia 40: 133-139.

245. Streit WJ, Walter SA, Pennell NA (1999) Reactive microgliosis. Prog Neurobiol 57: 563-581.

246. Strich SJ (1956) Diffuse degeneration of the cerebral white matter in severe dementia following head injury. J Neurol Neurosurg Psychiatry 19: 163-185.

247. Strich SJ (1961) Shearing of nerve fibers as a cause of brain damage due to head injury: A pathological study of twenty cases. Lancet 2: 443-448.

248. Strich SJ (1968) Notes on the Marchi method for staining degenerating myelin in the peripheral and central nervous system. J Neurol Neurosurg Psychiatry 31: 110-114.

249. Sullivan HG, Martinez J, Becker DP, Miller JD, Griffith R, Wist AO (1976) Fluid-percussion model of mechanical brain injury in the cat. J Neurosurg 45: 521-534.

250. Tanaka S, Suzuki K, Watanabe M, Matsuda A, Tone S, Koike T (1998) Upregulation of a new microglial gene, mrf-1, in response to programmed neuronal cell death and degeneration. J Neurosci 18: 6358-6369.

251. Taupin V, Toulmond S, Serrano A, Benavides J, Zavala F (1993) Increase in IL-6, IL-1 and TNF levels in rat brain following traumatic lesion. Influence of pre- and post-traumatic treatment with Ro5 4864, a peripheral-type (p site) benzodiazepine ligand. J Neuroimmunol 42: 177-185.

252. Terasaki M, Miyake K, McNeil PL (1997) Large plasma membrane disruptions are rapidly resealed by Ca2+-dependent vesicle-vesicle fusion events. J Cell Biol 139: 63-74.

253. Terayama Y, Meyer JS, Kawamura J, Weathers S (1991) Role of thalamus and white matter in cognitive outcome after head injury. J Cereb Blood Flow Metab 11: 852-860.

254. Thomas S, Prins ML, Samii M, Hovda DA (2000) Cerebral metabolic response to traumatic brain injury sustained early in development: a 2-deoxy-D-glucose autoradiographic study. J Neurotrauma 17: 649-665.

255. Thompson HJ, Lifshitz J, Marklund N, Grady MS, Graham DI, Hovda DA, McIntosh TK (2005) Lateral fluid percussion brain injury: a 15-year review and evaluation. J Neurotrauma 22: 42-75.

256. Thurman D (2001) The epidemiology and economics of head trauma. In: Head Trauma: Basic, Preclinical, and Clinical Directions (Miller L, Hayes R, eds), New York: Wiley and Sons.

257. Thurman DJ, Alverson C, Dunn KA, Guerrero J, Sniezek JE (1999) Traumatic brain injury in the United States: A public health perspective. J Head Trauma Rehabil 14: 602-615.

258. Toku K, Tanaka J, Yano H, Desaki J, Zhang B, Yang L, Ishihara K, Sakanaka M, Maeda N (1998) Microglial cells prevent nitric oxide-induced neuronal apoptosis in vitro. J Neurosci Res 53: 415-425.

259. Tseng GF, Wang YJ, Lai QC (1996) Perineuronal microglial reactivity following proximal and distal axotomy of rat rubrospinal neurons. Brain Res 715: 32-43.

260. Uzan M, Albayram S, Dashti SG, Aydin S, Hanci M, Kuday C (2003) Thalamic proton magnetic resonance spectroscopy in vegetative state induced by traumatic brain injury. J Neurol Neurosurg Psychiatry 74: 33-38.

261. Vallee RB, Bloom GS (1991) Mechanisms of fast and slow axonal transport. Annu Rev Neurosci 14: 59-92.

262. Vallee RB, Bloom GS, Theurkauf WE (1984) Microtubule-associated proteins: subunits of the cytomatrix. j CELL BIOL 99: 38s-44s.

263. Van den Heuvel C., Lewis S, Wong M, Manavis J, Finnie J, Blumbergs PC, Jones N, Reilly P (1998) Diffuse neuronal perikaryon amyloid precursor protein immunoreactivity in a focal head impact model. Acta Neurochir Suppl (Wien) 71:209-11.: 209-211.

264. Vandekerckhove J, Vancompernolle K (1992) Structural relationships of actin-binding proteins. Curr Opin Cell Biol 4: 36-42.

265. Vela JM, Yanez A, Gonzalez B, Castellano B (2002) Time course of proliferation and elimination of microglia/macrophages in different neurodegenerative conditions. J Neurotrauma 19: 1503-1520.

266. Villegas-Perez MP, Vidal-Sanz M, Rasminsky M, Bray GM, Aguayo AJ (1993) Rapid and protracted phases of retinal ganglion cell loss follow axotomy in the optic nerve of adult rats. J Neurobiol 24: 23-36.

267. Waller A (1850) Experiments on the section of glossopharyngeal and hypoglossal nerves of the frog and observations of the alternatives produced thereby in the structures of their primitive fibres. Philos Trans R Soc Lond 140: 423.

268. Walz W, Ilschner S, Ohlemeyer C, Banati R, Kettenmann H (1993) Extracellular ATP activates a cation conductance and a K+ conductance in cultured microglial cells from mouse brain. J Neurosci 13: 4403-4411.

269. Wolf JA, Stys PK, Lusardi T, Meaney DF, Smith DH (2001) Traumatic axonal injury induces calcium influx modulated by tetrodotoxin-sensitive sodium channels. J Neurosci 21: 1923-1930.

270. Yakovlev AG, Faden AI (2001) Caspase-dependent apoptotic pathways in CNS injury. Mol Neurobiol 24: 131-144.

271. Yakovlev AG, Knoblach SM, Fan L, Fox GB, Goodnight R, Faden AI (1997) Activation of CPP32-like caspases contributes to neuronal apoptosis and neurological dysfunction after traumatic brain injury. J Neurosci 17: 7415-7424.

272. Young W (1996) Death by Calcium: A Way of Life. In: Neurotrauma (Narayan RK, Wilberger J, Povlishock J, eds), pp 1421-1431. New York: McGraw-Hill.

Vita

Brian Joseph Kelley was born on December 15, 1976 in Washington, District of Columbia and is an American citizen. He graduated from Gonzaga College High School, Washington, District of Columbia in 1995. He received a Bachelor of Science degree in Chemistry with a concentration in Biochemistry and a Bachelor of Arts degree in Biology from the University of Virginia, Charlottesville, Virginia in 1999. He entered the M.D./Ph.D. program at the Medical College of Virginia / Virginia Commonwealth University, Richmond, Virginia in 2000 and received his doctorate from the Department of Anatomy and Neurobiology in the fall of 2006.